ISSN 0869-5938, Stratigraphy and Geological Correlation, 2019, Vol. 27, No. 7, pp. 729–782. © Pleiades Publishing, Ltd., 2019.

The Key Section for the Upper Palaeozoic of the New Siberian Islands (Tas-Ary Peninsula, Kotel'ny Island)

M. K. Danukalova[a, *], A. B. Kuzmichev[a], V. G. Ganelin[a], Yu. A. Gatovsky[b], O. L. Kossovaya[c, d], T. N. Isakova[a], D. Weyer[e], N. G. Astashkin[a], and V. V. Eriklintsev[a]

[a] *Geological Institute, Russian Academy of Sciences, Moscow, 119017 Russia*
[b] *Faculty of Geology, Lomonosov Moscow State University, Moscow, 119991 Russia*
[c] *Karpinsky Russian Geological Research Institute, St. Petersburg, 199106 Russia*
[d] *Kazan Federal University, Kazan, 420008 Republic of Tatarstan, Russia*
[e] *Natural History Museum, Berlin, Germany*
**e-mail: danukalovamk@yandex.ru*

Received March 1, 2018; revised October 20, 2018; accepted October 25, 2018

Abstract—The information on the Late Palaeozoic deposits of the New Siberian Islands is essential to clarify the palaeogeography of the surrounding Arctic Region and to quest the original location of the New Siberian continental block prior to the Amerasian ocean opening. The best Upper Palaeozoic section of the islands, located in the western part of the Kotel'ny Island (Tas-Ary Peninsula), was examined in detail. The studied rocks characterize a transitional facial zone between the northeastern shallow-water (central areas of the Kotel'ny Island) and the southwestern deep-water ones (Bel'kov Island). The stratigraphy of the Carboniferous and partly Permian strata was specified by the study of four fauna groups, detrital zircon dating, and structure interpretation. The section demonstrates a gradual change of depositional environments from shallow-marine in the Lower Carboniferous to deep-water in the middle Carboniferous and Permian. The Tournaisian and Visean rocks (Tas-Ary Formation, not less than 950 m) were formed on the open shelf or ramp with predominant carbonate sedimentation. They were deposited above the storm-wave base during the early Tournaisian and at greater depth later. The Serpukhovian–Middle (?) Permian rocks (Bel'kov Formation, not less than 300 m) were accumulated on the deep-water subaqueous slope and, possibly, at its base. Black shales and turbidite sandstones compose a significant part of the Bel'kov Formation. Sandstones have a siliciclastic–carbonate composition in the upper Lower Carboniferous and are carbonate-free up the section. The boundary between Tas-Ary and Bel'kov formations corresponds to a change in the shelf-to-basin profile and depositional style. At this time (the beginning of the Serpukhovian), the subsidence rate increased, a pronounced slope was formed, and a new source of clastics appeared on land. This reorganization was probably related to the Northern Taimyr orogen rise. The lithological similarity of the Lower Carboniferous deposits of the Tas-Ary Peninsula and Southern Taimyr, the synchronous shift in sedimentation from carbonate to terrigenous rocks, and the same source of clastic material for the Upper Carboniferous–Permian sandstones in both regions indicate their belonging to the same sedimentary basin in the Late Palaeozoic. We believe that the western part of the New Siberian Islands represented a continental margin in Late Devonian, Carboniferous and Permian times, and that it was a continuation of the Verkhoyansk margin. The latter is possible, taking into account rotation of the New Siberian Islands block according to the two-pole rotational model of the Amerasian basin opening.

Keywords: Arctic, New Siberian Islands, stratigraphy, Carboniferous, Permian, conodonts, brachiopods, corals, foraminifera

DOI: 10.1134/S0869593819070013

INTRODUCTION

The Carboniferous–Permian deposits within the New Siberian Islands archipelago are exposed in two islands: Bel'kov and Kotel'ny (Fig. 1). They are characterized by a rapid change of facies in the western (in modern coordinates) direction: from thin shallow-marine limestone in the central part of Kotel'ny Island to deep-water shales and turbidites on Bel'kov Island (Kos'ko et al., 1985; Kuzmichev, 2009; Pease et al., 2015). The only complete section of the Carboniferous and a large part of the Permian, well exposed in the cliff and enriched in diverse fauna, is located on the Tas-Ary Peninsula (west of Kotel'ny Island). Here a stratotype of the Lower Carboniferous Tas-Ary Formation was described and the best exposures of the overlying Bel'kov Formation are situated. The age of the latter was estimated as the Middle Carboniferous

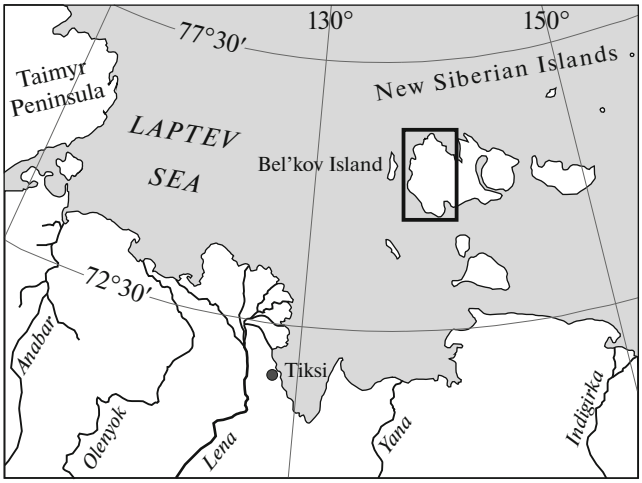

Fig. 1. Location of the studied region. Kotel'ny Island is shown with a rectangle.

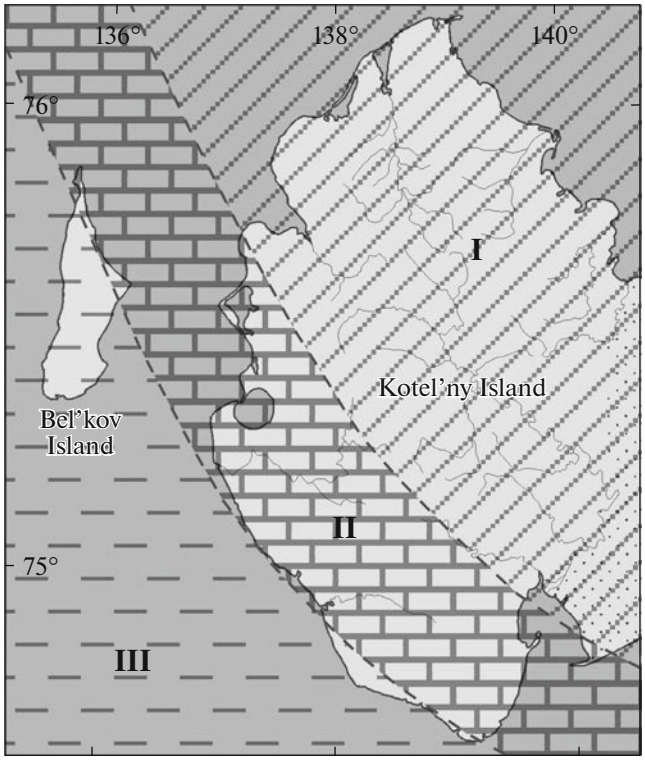

Fig. 2. Facies zoning of the Visean deposits within Kotel'ny and Bel'kov islands according to the authors' data, with additions from (Kos'ko et al., 1985; Kos'ko and Korago, 2009). The position of boundaries of the facies zones can be somewhat different for other intervals of the Carboniferous–Permian history, but the general trend of basin deepening to the southwest remains unchanged. (I) Land (?), in the southern part, shallow shelf: thin fine-grained and clayey limestone, bioclastic interlayers (Kos'ko et al., 1985). At later stages of the geological history (Middle Carboniferous–Permian), this zone mostly corresponds to shallow-marine settings. (II) Transitional zone, open deep shelf: fine-grained spiculite limestone, including clayey varieties, with chert (this work). (III) Deep-water zone, the underwater slope facies: mudstone, siltstone, turbidite sandstone, slump structures, carbonate concretions (it is general description of the Lower Carboniferous–Permian deposits on Bel'kov Island (according to the authors' observations); it is impossible to identify the Visean deposits there on the basis of the available data).

(Kos'ko et al., 1985). The structure of this area is relatively complicated, but it is still possible to understand it and to confidently reconstruct the rock sequence. The Tas-Ary section belongs to the transitional facies zone and is a link between coeval deposits of shallow and deep-water settings (Fig. 2). It should be studied to justify correlations with the sections in the northern Siberian Platform and Eastern Taimyr region and to find a key to understanding the palaeogeography of the basin which occupied the recent Laptev Sea shelf area. In the north of the Siberian Platform, the Upper Palaeozoic strata contain oil-bearing rocks.

This paper reports new data on the Carboniferous–Permian deposits on the Tas-Ary Peninsula obtained by M.K. Danukalova, A.B. Kuzmichev, and V.V. Eriklintsev in 2009 and 2014. The study of our big collection of macro- and microfauna made it possible to substantially clarify the stratigraphy and to supplement the conclusions on depositional settings and palaeogeography. Brachiopods were studied by V.G. Ganelin and N.G. Astashkin, corals were studied by O.L. Kossovaya and D. Weyer, and conodonts were investigated by Yu.A. Gatovsky. For the highest carbonate horizons of the section, foraminifera were also studied (T.N. Isakova). Dating of detrital zircons was carried out to justify the maximum age of the upper barren part of the sequence.

GENERAL GEOLOGY OF THE TAS-ARY PENINSULA

Tas-Ary is designated on the maps as an island; however, taking into account the fact that its northwestern end is connected by a wide pebble spit to the Kotel'ny Island shore (Fig. 3), it is more correct to call it a peninsula. The main part of this peninsula has a length of 7 km at a width of 1.5–2 km; from the southwestern and northwestern "sea" sides, it is surrounded by a cliff interrupted by river valleys. Almost all cliffs are accessible from the beach. The Carboniferous–Permian section is exposed in this very area; its uppermost horizons crop out on the southeastern coast. The Upper Devonian and Palaeogene rocks are occasionally exposed along the lowland northeastern coast facing the Durnaya Lagoon (Fig. 3). Exposed rocks are almost absent in the central part of the peninsula, except for rare outcrops in the river valleys.

The Palaeozoic rocks making up the Tas-Ary Peninsula are mapped within four subdivisions (Kos'ko et al., 1985): Nerpalakh Formation (Frasnian), Chekur Formation (Famennian–lower Tournaisian), Tas-Ary Formation (Tournaisian–Serpukhovian),

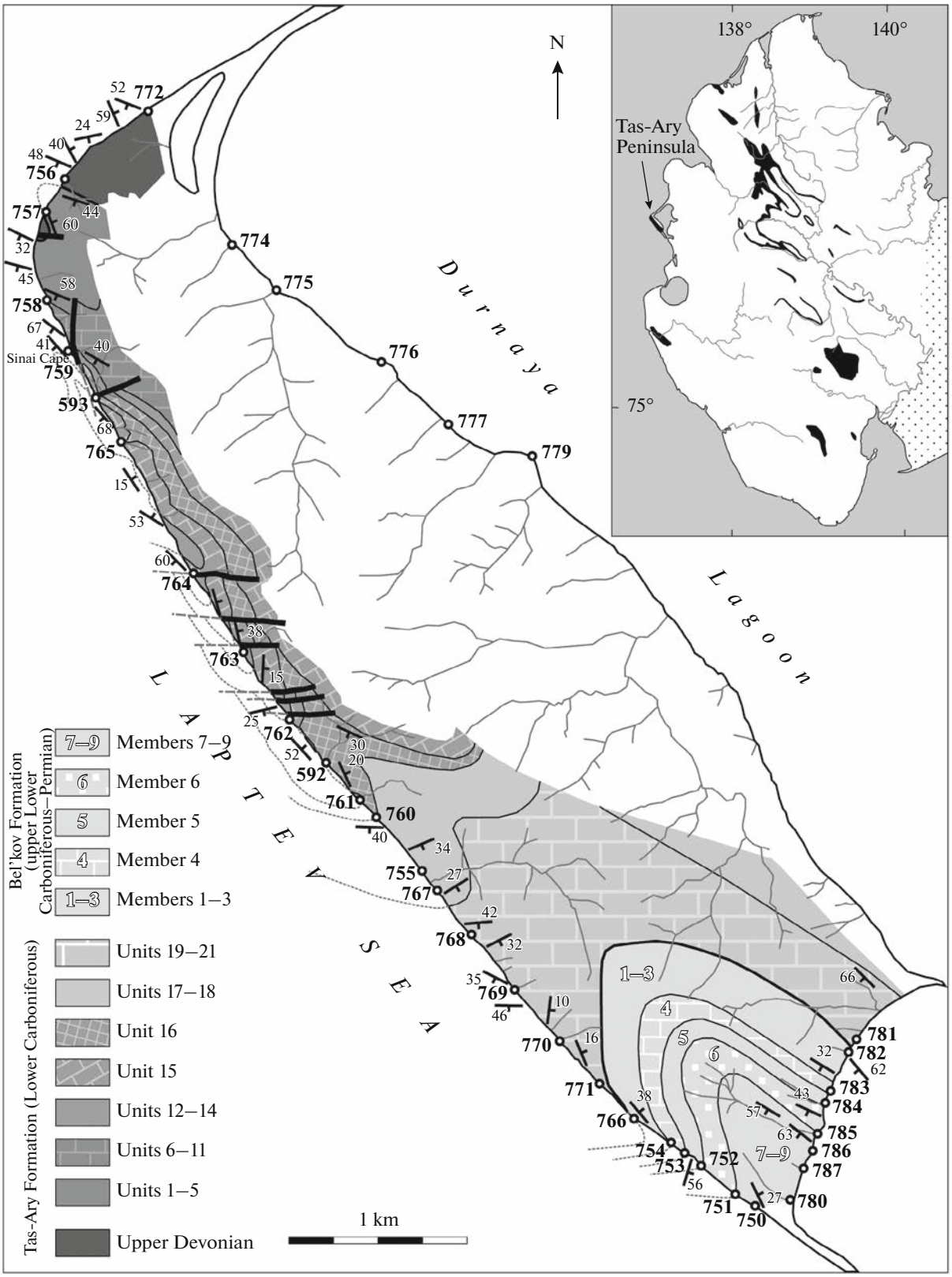

Fig. 3. Generalized geological map of the southern and western parts of the Tas-Ary Peninsula with a removed cover of the Quaternary deposits (by A.B. Kuzmichev and M.K. Danukalova). The Upper Devonian and Neogene rock outcrops on the eastern coast are not shown. Bold black lines indicate the faults, while pale dotted lines indicate the boundaries of some subdivisions and faults traced over the sea. Inset: the Carboniferous and Permian rock outcrops (black filling) on Kotel'ny Island and location of the Tas-Ary Peninsula. Bunge Land is shown with dotted pattern.

and Bel'kov Formation (Bashkirian). The *Nerpalakh Formation* is composed of a complex of shallow marine deposits with a visible thickness of at least 150 m: calcareous shale and limestone, often with abundant benthic fauna, siltstone, mudstone, and sandstone of siliciclastic–carbonate composition. The latter are minor and occur as interlayers deposited by bottom currents (only at the top of the formation). The *Chekur Formation* is made mainly of medium- to coarse-grained siliciclastic sandstone with a large-scale cross-stratification, likely of delta or bar nature. The formation, according to our observations, is at least 120 m in thickness. There is no macrofauna in the Tas-Ary section, except for rare crinoid fragments. The *Tas-Ary Formation*, as reported by the previous researchers, is composed largely of limestone and mudstone with a rich complex of benthic fauna; this formation is about 1.1 km in thickness. Its description including 28 units is given in (Kos'ko et al., 1985). Calcareous sandstones 40 m thick with slump structures and mudstone interbeds containing phosphatic concretions were mentioned at the top of the formation. The age of the formation was based on foraminifera and brachiopods. The *Bel'kov Formation*, according to (Kos'ko et al., 1985) is dominated by mudstone, siltstone, and sandstone. The latter contain volcanic rock fragments. Bioclastic limestone and limestone conglomerate-breccia are minor. The visible thickness of this formation on the Tas-Ary Peninsula is estimated at 145 m. Fauna was found only in this section and only in its lower part; basing on it, the age of the whole formation is estimated as the Bashkirian. By analogy with the Bel'kov Formation on the Bel'kov Island (Pease et al., 2015), before the start of fieldwork, we assumed that its stratigraphic interval on the Tas-Ary Peninsula could be wider than indicated in the published literature. It should be noted that the Bashkirian age of the stratigraphic subdivisions, with which the Bel'kov Formation was correlated in terms of fauna, was later revised (Chapter 5.1).

We managed to photograph the cliffs of the northwestern and southwestern coasts of the studied peninsula with a continuous panorama from the fast ice in June, which greatly facilitated the correlation of lithological units. It turned out that the same units of the Tas-Ary Formation were repeated many times in the cliff, which explained the inconsistencies between the previously published description of the section (Kos'ko et al., 1985) and our observations. The structure of the key section in the peninsula's southwestern coast is not quite convenient for a stratigraphic description, because rocks crop out for a considerable distance along the core of the anticline whose axis submerged southeastward at an angle of 14°–23°. The strike of the axis approximately coincides with the orientation of the coast, and in the coastal cliff both the anticline core and adjacent limbs can be exposed, which causes frequent changes in the beds orientation (Fig. 3). The folded structure is complicated by faults of several generations. Two fault systems are characterized by mappable displacements which significantly disrupt the sequence observed in the cliff. EW-trending and ENE faults with an amplitude of a few meters or a few tens of meters are the most numerous (Fig. 3). Fault planes are inclined in different directions and at different angles, from subvertical to 40°; in some cases, they flatten out significantly from the upper edge of the cliff to its base. In most cases, the rock correlation in the limbs was not complicated. Some of these faults have a negligible strike-slip component. The second system is represented by rare NS-trending faults with unclear kinematics. The map (Fig. 3) shows only one of such faults which intersects with the coast south of the Sinai Cape. The rock correlation around this fault is detailed in the description of the unit 11 of the Tas-Ary Formation.

TAS-ARY FORMATION

The transition from siliciclastic siltstone and sandstone of the Chekur Formation to clayey–carbonate rocks of the Tas-Ary Formation is gradual. During the medium-scale geological survey, a forty-meter limestone unit with benthic fauna was assigned to the Tas-Ary section base (Kos'ko et al., 1985). Meanwhile, the cited publication does not contain a description of underlying deposits on the Tas-Ary Peninsula; the descripion of the Chekur Formation is given for the section located to the south (Khos-Terryutyakh River), where it is more carbonate. During the field works, we were guided by noticeable ("mappable") changes in the rock composition (and, accordingly, depositional environments), so the base of Tas-Ary Formation was placed at a different level, at which noticeable reddish lenticular beds of cross-stratified lime-free sandstone disappear. The position of this boundary is relatively tentative. Sandstone also occurs higher in the section, but there it contains carbonate (mainly calcitic) cement and many carbonate clasts, owing to which the rock is more similar in its appearance to limestone than to sandstone. An evidently carbonate section starts from the level which was taken as a boundary between the considered formations. Its lowermost part with a thickness of 220 m, which is devoid of macrofauna, was likely attributed by the survey geologists to the top of the Chekur Formation.

The contact of the formations was observed at three points in the northwest of the studied peninsula (Fig. 3). This is due to a folded structure of this area. The southern point is the most convenient for exploration: the anticline core showing the uppermost part of the Chekur Formation crops out 143 m southwest of site 757, and a monoclinal section of the Tas-Ary Formation, which is interrupted by rare low-amplitude faults, begins in the southern limb. The monocline of 0.7 km in length demonstrates a continuous sequence of the lower third of this formation (330 m). We subdivided the Tas-Ary Formation with a total thickness of

950–980 m into 21 lithological units (Fig. 4) and named some of them. A bottom to top description of the section is given below. Some rock varieties are illustrated with photographic images of thin sections, which are placed in the ESM_1 file in Supp. Data. Microphotographs of the Bel'kov Formation rocks are also given there. Fossil characteristics of the section is reported in the ESM_6 file (Chapter 5).

The Lower Part of the Tas-Ary Formation

Unit 1 (transitional; 50 m in thickness). It is composed of alternation of three rock types. (1) Gray clastic limestones (in fact, medium- to fine-grained sandstones and silty sandstones; ESM_1, fig. S1a). They contain up to 50% silicate grains as quartz and chert. Carbonate occurs as both clasts and cement. Grains are characterized by a variable degree of roundness. The unit bottom occasionally contains gravel and coarse chert (less commonly, quartz) sand particles. (2) Dark gray limy mudstone. (3) Poorly sorted clay–carbonate rocks with a "speckled" texture. The latter are predominant in the section and represent an intensely bioturbated mixture of clay, carbonate mud, silt- and sand-sized particles; they occasionally contain fragments of ostracod (?) shells.

The thickness of the layers is stable along the strike and varies from a few centimeters to about half a meter (Fig. 5a). Bedding from a distance looks clear, but on closer examination, boundaries between the beds often turn out to be vague owing to bioturbation (Fig. 5b). Some clayey intervals are characterized by filamentary interlayers of clastic limestone. Many rock varieties in unit 1 react with hydrochloric acid; in the rest, carbonate is represented by dolostone. The clay content is higher at the top of the unit. Some silty sandstone beds demonstrate molds of wave ripples on their soles. The abundant siliciclastic material in the rocks of this unit is indicative of gradual change of the depositional settings at the boundary between the Chekur and Tas-Ary formations. Bioturbated clay–sand layers also appear for the first time at the top of the Chekur Formation, but they are calc-free there.

Unit 2 (laminated limestone; 18 m in thickness). It resembles an underlying unit, but unit 2 is characterized by a more regular and pronounced stratification, and the rocks are higher calcareous and light-colored. In the lower and middle parts of this unit, carbonate beds are thicker (0.3–0.5 m on average) than down the section; noticeable mudstone interlayers appear closer to the top. The bioturbation is somewhat less intense than in unit 1. Unit 2 is composed of relatively hard, very fine-grained limestone and clayey limestone; there are also clastic limestones with silicate grains which are similar to those observed in the underlying unit. Fine-grained limestones (wackestone) are depleted in siliciclastic material, rare bioclasts (up to a few millimeters in size) are present. Their lamination is expressed as fine parallel horizons enriched in a silicate material. It is represented mostly by quartz silt. Lamination is often confined to lower parts of the layers.

Unit 3 (24 m in thickness). The lower half of the unit is composed of dolomitized gray medium-grained limestones and dark gray fine-grained ones, both rust-colored on surface. Rocks are likely bioturbated. They form mainly thick layers with indistinct boundaries; a parallel stratification is clearly visible from afar, but it is hardly noticeable at closer examination (an implicit hint of thin lamination is observed only at the bottom of the beds). It can be seen under a microscope that the rocks are siliciclastic–carbonate siltstones and silty sandstones which are occasionally enriched in a clay-sized material. Up the section, rocks become similar to those in unit 2. The upper part of the unit contains a silty sandstone bed of 1 m thick with a vague cross-stratification. The assumed top of unit 3 is visible only at the upper part of the cliff and then is cut off by a normal fault. Some part of the overlying unit appears to be lost in the fault zone.

Unit 4 (20 m in visible thickness). Fine alternation of rocks which are similar to those composing unit 1. Near the top, there is a thick (1.5–2 m) layer of fine-grained nonlaminated clayey limestone which underwent bioturbation (visible on the fresh cut and resembles "speckled" rocks of unit 1). A thin section shows clayey siltstone with silicate and carbonate fragments. A fine fraction occurs as both clay and carbonate mud.

Unit 5 (111 m in thickness). This thick unit is characterized by interlayers of "normal" granular limestone, forming massive plates (Fig. 6), commonly with a microfauna visible through a magnifying glass (ostracods, occasionally foraminifera) and rare small fragments of crinoid stems. This limestone is the first in the section to boil actively in hydrochloric acid and to contain an obvious (sometimes numerous) fossils. Meanwhile, it is still enriched in siliciclastic silt and fine sand (up to 30–40% of rock volume in the lower part of the unit and up to 10–15% in its upper part). This unit is subdivided into three subunits (5a, 5b, and 5c).

Subunit 5a (interval with the first limestone plates; 19 m in thickness). Its lower part (1.5–2 m) is composed of fissile dark-colored limestone with distinct interlayers of gray granular limestone (interlayers are 1–20 cm thick; ESM_1 figs. S1b, S1c). They are overlain by siliciclastic–carbonate sandstone and gritstone (Fig. 7a) with black chert and quartz grains (at least 1 m in thickness). Sandstones are overlain by indistinctly laminated fine-grained limestones forming layers a few decimeters thick. The boundaries between them are unclear, and tops of the beds contain more clay and are obviously bioturbated. Some layers are bioturbated throughout their thickness. These limestones also form massive plates. In addition to them, there are calcareous shale and clayey limestone packages and hard granular limestone interlayers (as at the unit bottom). Wave ripple marks were observed on the top of one of the limestone beds (Fig. 7b). Carbonate sand-

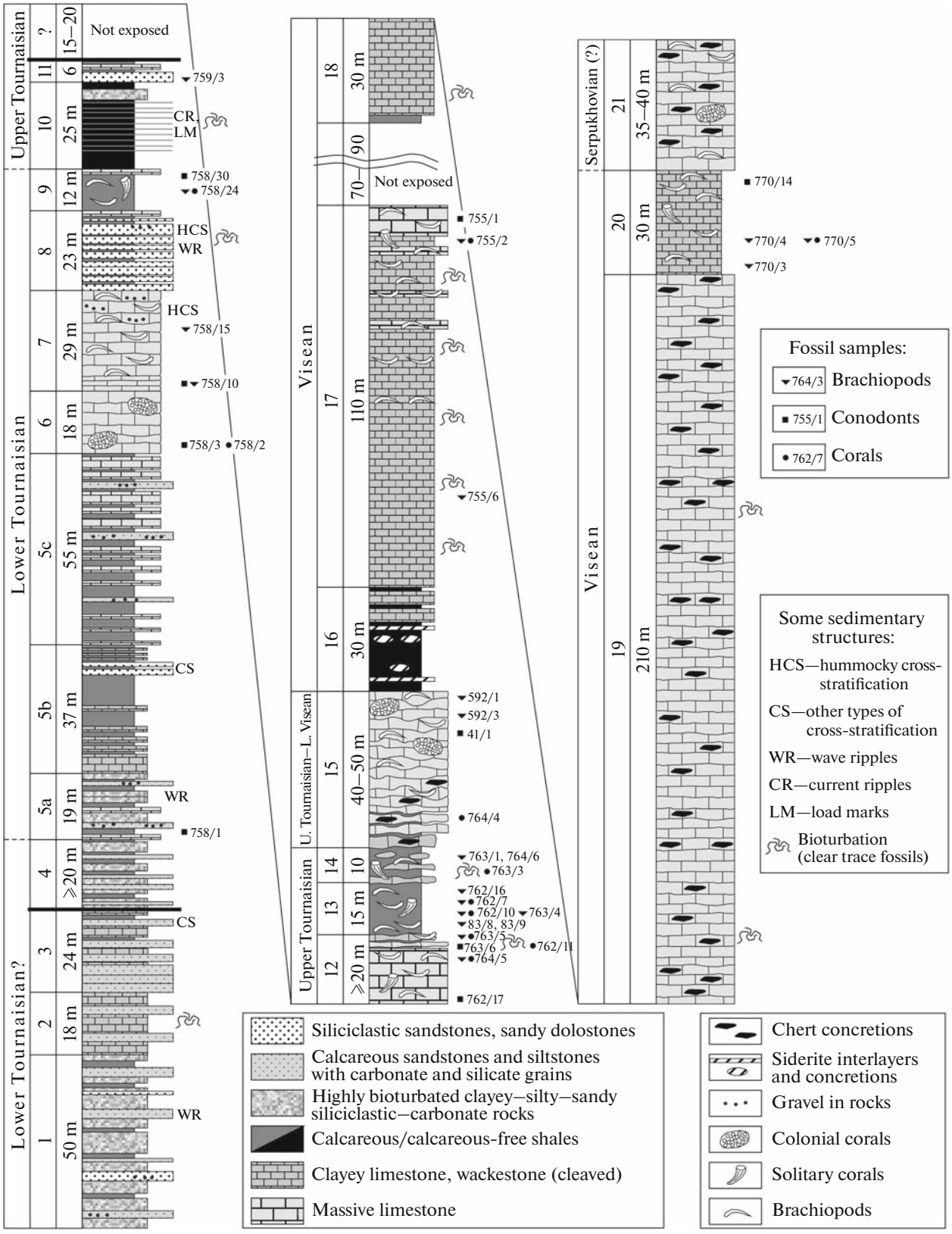

Fig. 4. Composite geological section of the Tas-Ary Formation. Thin interlayers of siliciclastic siltstone and sandstone in unit 10 are shown with gray lines. Bold black lines indicate the faults. Left of this geological section: substages/stages, numbers of lithological units and thickness in meters. The exact position of the samples 84/5, 6, 8, and 9 (brachiopods) is not defined and, therefore, these samples are not shown. They originate from the interval of unit 14–lower part of unit 15. Abbreviations: U. Tournaisian—Upper Tournaisian; L. Visean—Lower Visean.

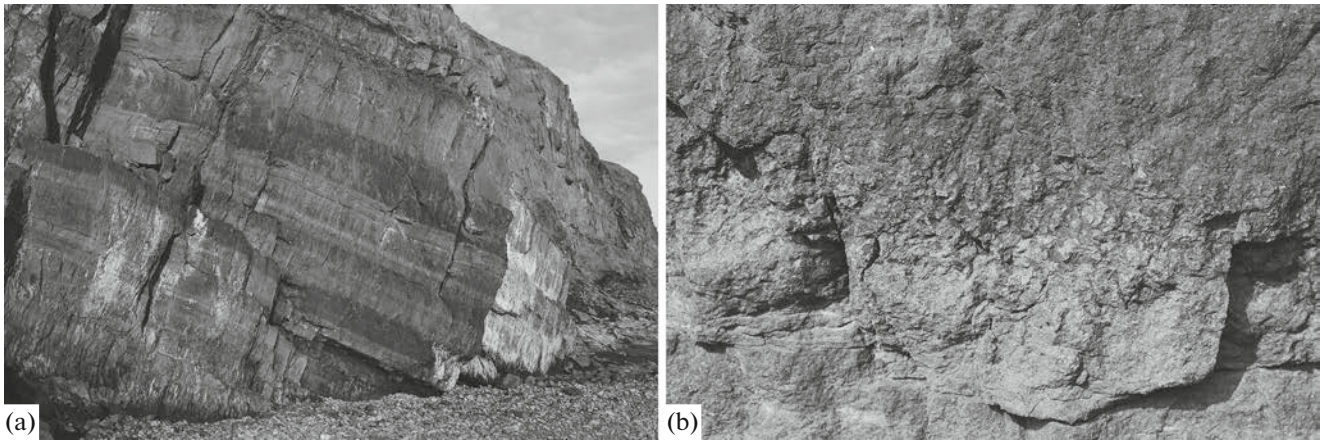

Fig. 5. Deposits of the lower, transitional, unit of the Tas-Ary Formation. (a) General view of the layered section; (b) intense bioturbation at the boundary of the layers; the photograph is 20 cm wide.

Fig. 6. General view of unit 5 with fossil-bearing granular limestone plates, the first in the section.

stones appear in the upper part of subunit 5a once more; chert grains and a fine gently undulating lamination can be noted on its weathering surfaces.

Subunit 5b (clayey; 37 m in thickness). It is composed of cleaved black shale and dark clayey limestone (Fig. 6, middle part), often bioturbated; clayey limestone prevails at its bottom. Unclear horizontal lamination and few thin layers of granular limestone can be noted in the rocks. The upper part consists of a range of contiguous layers (up to 10–15 cm in thickness) of highly weathered carbonate-free sandstone with a low-angle cross-stratification, bright yellow from the surface. Black mudstone with thin clayey limestone interlayers occurs at the top.

Subunit 5c (55 m in thickness). Dark fissile mudstone and clayey limestone with interlayers (plates) of strong granular (mostly fine-grained) gray limestone. The number and thickness of the latter increase up the section; they prevail near the top and form layers up to 0.5 m in thickness. Carbonate sandstone and gritstone beds with chert and quartz gravel, ooids, intraclasts, and bioclasts occur in the unit; the matrix is micritic. At the upper part of the subunit, some limestones demonstrate fine parallel wavy lamination (Fig. 7c) repeating irregular soles of the layers; onlap of laminae was sporadically observed. Some textures resemble small-scale slump folds. There are also layers with an "even" horizontal lamination.

Unit 6 (unit of Coral Cape; 18 m in thickness). Clastic rather dark gray limestones looking macroscopically fine- to very fine-grained with larger fossils fragments. They form layers with a thickness from a few to 20–30 cm (Fig. 8a). Beds are separated by thin (millimeters to a few centimeters) clayey interlayers. It is seen in thin sections that such limestones consist of rounded peloids and intraclasts, bioclasts (sometimes

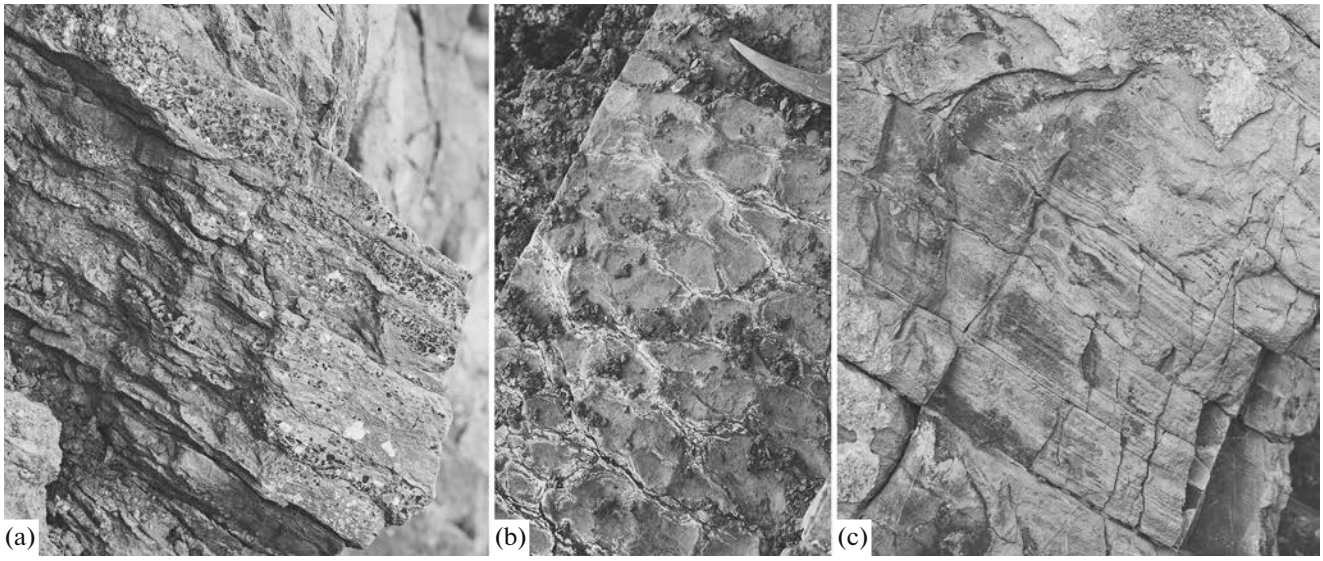

Fig. 7. Some rock varieties in unit 5. (a) Thin interlayering of siliciclastic–carbonate sandstones and gritstones. Gravel is represented by fragments of chert, less often, quartz, sandstone (similar to host rocks), and limestone with a siliciclastic admixture. The photograph is 15 cm high. (b) Wave ripples on the limestone top; (c) thin undulating lamination in limestones in the upper part of unit 5, allegedly resulting from the vital activity of microbial communities (photograph is 25 cm high).

in large quantities), an insignificant (a few percent) admixture of small silicate grains, and sporadic chert gravel; cement is sparite (ESM_1 fig. S1d). These rocks can be attributed to grainstones according to the R. Dunham's classification (Dunham, 1962; cited in Stow, 2012). The macrofauna in limestone is commonly represented by small crinoid stem segments. Sporadic colonial and solitary corals, and brachiopods are also present and are relatively numerous in some layers. The lower boundary of the unit was drawn along a thick bed with coral colonies, clearly visible on its top. This layer forms a plate protruding into the sea, which we called Coral Cape (Fig. 3, site 758). Clayey interlayers are more noticeable in the upper part of the unit; there are a few "sets" with a thickness of up to 0.5 m composed of fissile clayey limestone–calcareous shale with thin horizons (a few centimeters) of fine-grained limestone. At the top of the unit, limestone is coarse-grained bioclastic.

Unit 7 (brachiopod limestones; 29 m in thickness). Limestones which form the base of the unit (2–3 m) differ from rocks at the top of unit 6 in a finer grained matrix and a slightly darker color, and they contain more fauna, dominated by brachiopods. They are more thin-bedded (10–15 cm) and are divided by well-defined shale horizons. Up the section, limestone beds (plates) are thicker, and clayey interlayers are thinner. In this unit, limestones are gray (reddish yellow on the weathered surface), bioclastic (macroscopically coarse-grained, variably grained in thin sections, with clasts ranging in size from silt to gravel), with numerous brachiopod shells and fragments of crinoids and other fauna. They contain siliciclastic grains (from a few percent to 10%) and intraclasts (ESM_1 fig. S1e). The surface of the layers is uneven, the same as down the section. At the top of some layers, there are trace fossils which are similar to *Chondrites*. In the upper part of the unit, there are sandy limestone interbeds with low-angle (hummocky?) cross-stratification, bioclasts, and quartz and chert gravel (Fig. 8b). Sometimes, judging from debris in scree, such rock turns into siliciclastic–carbonate gritstone. It is curious that gritstones are composed of peloids and intraclasts containing small (about 0.1 mm) euhedral crystals of authigenic albite (?) (ESM_1 fig. S1f, S1h). Similar crystals were also found at higher levels of the Tas-Ary Formation (in allohems and scattered in the rock).

Unit 8 (sandy dolostones; 23 m in thickness). We subdivided this unit into three parts (not shown in the column).

Subunit 8a (highly weathered section; maximum of 10 m in thickness). The bottom of unit 8 is transformed in the weathering crust into bleached, pink or reddish porous sandstone and sand with mudstone and siltstone interlayers. Fine-grained rocks sometimes retain a dark (to black) color. Sand and sandstone are fine-grained oligomictic (quartz and rarer chert). Sandstone is characterized by quartz overgrowth cement.

Subunit 8b (middle thick-bedded part of the unit; 9.3 m in thickness). Gray sandy dolostone and dolomitic silicate sandstone with yellow and rusty weathering crusts alternating with clayey shale (Fig. 8c). The thickness of the former is from 5 to 30 cm (rarely, up to 0.5 m) and the thickness of the latter is from a few millimeters to 20–40 cm. Sandstone is usually poorly sorted, with quartz overgrowth (ESM_1 fig. S1g).

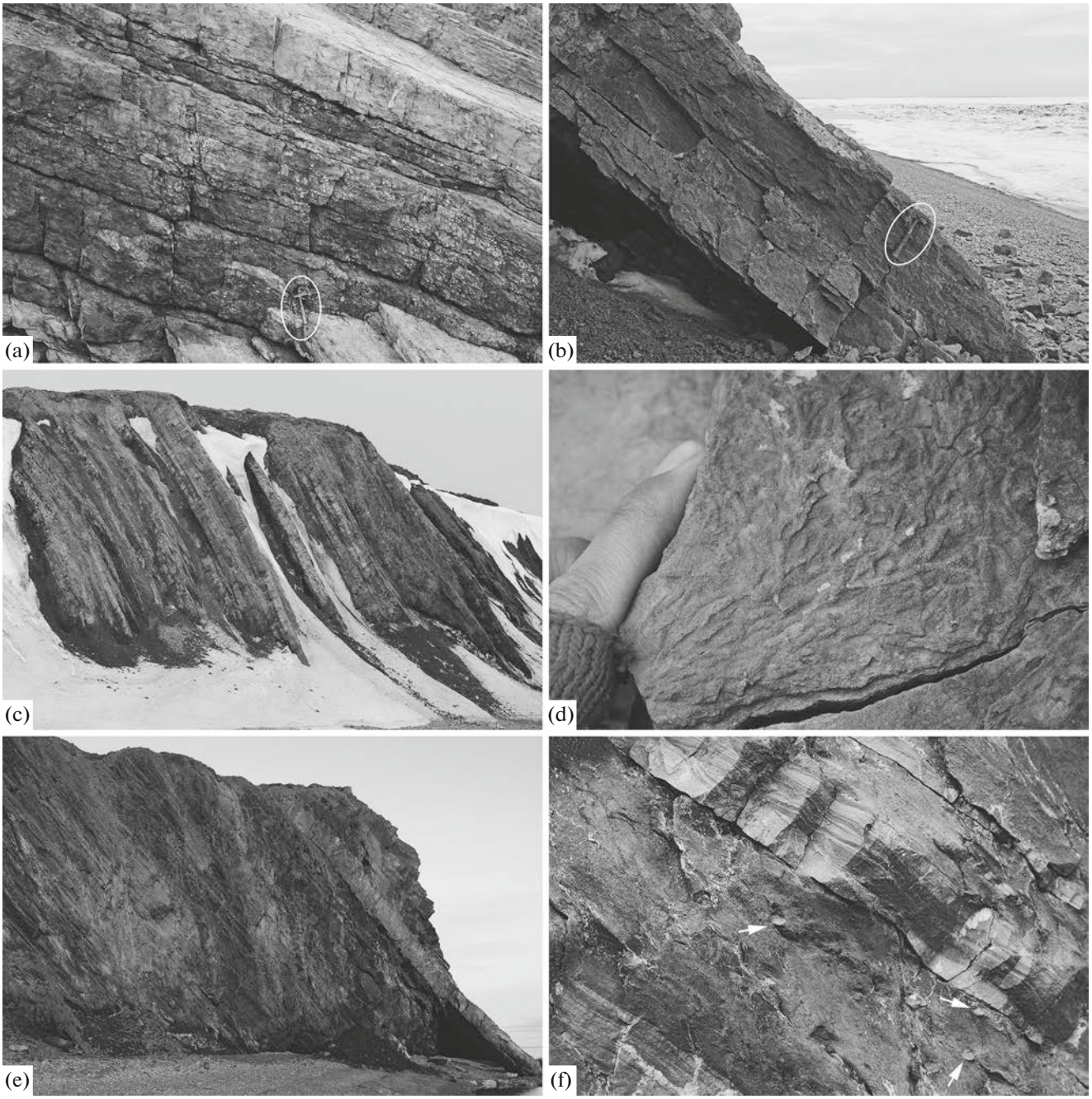

Fig. 8. Characteristic rocks and sedimentary structures of units 6–10. (a) Limestones of the Coral Cape (unit 6; a hammer is encircled); (b) low-angle (storm-generated (?)) cross-stratification in sandy limestone (upper part of unit 7; hammer is encircled); (c) sandy dolostones unit (unit 8, middle and upper parts); in the background to the right, there are dark gray shales of the overlying unit 9; (d) branching burrows on top of the bed, similar in shape to *Chondrites*, but likely resulting from surface (rather than underground) feeding; (e) thin interlayering of mudstone, clayey siltstone, and sandstone (upper part of unit 10). In the right part of the outcrop, "Sinai sandstone": a massive plate forming the Sinai Cape (Fig. 3, site 759). Under it, at the top of unit 10, there are black oolitic shales. (f) Unit 10 sandstones divided by mudstone with molds of tunnels made by burrowing animals (arrows). Cross-lamination in sandstone is visible; the chain of bright lenses in its foot is interpreted as ripples. In many beds, cross-lamination is replaced by horizontal one near the top (lower left part of the photo). The photograph is 15 cm wide. The rhythmicity of the section is indicative of the pulsed input of sand. Apparently, the laminated sandstone horizons can be interpreted as tempestites.

Pyrite grains are observed. During weathering, some layers turn into sand. On the bedding surfaces, there is a coarse coalified plant debris. The upper two meters of the subunit are composed of cross-stratified sandstone–sandy dolostone. Other levels of the section are also marked by a low-angle cross-stratification resembling a storm-generated one; steeply dipping cross laminae are rare. Wave ripples were noted. At the top

and near the top of some layers there are trace fossils represented by a system of small thin tunnels oriented both along the bedding plane and obliquely. Large (up to 15–20 cm long) straight tunnels, some of which branch out, were found at the sole of one layer. Rare beds were bioturbated from bottom to top.

Subunit 8c (upper thin-bedded part of the unit; 3.7 m in thickness). The lower two meters are composed of thinly intercalated sandy and silty dolostone with mudstone (Fig. 8c). Near the base of the subunit, there is a very coarse-grained sandstone (10–15 cm) with carbonate cement containing bioclasts and gravel and small pebbles of chert, quartz, carbonate–quartz siltstone, and sandstone. Up the section, the bedding becomes coarser, and clay interlayers are less frequent in occurrence; then silty dolostones prevail. Dolostones from the lower half of subunit 8c demonstrate sedimentary structures resembling small-scale hummocky cross-stratification and contain small load casts (?) on the soles. Trace fossils are occasionally observed on bedding planes (Fig. 8d). The upper part of the subunit is represented by a range of uneven layers of fine-grained gray limestone with signs of bioturbation and a significant admixture of silicate silt and sand. Limestone at the top is slightly fissile, with numerous brachiopods and corals.

Unit 9 (gray fossiliferous shale; about 11–12 m in thickness). Gray calcareous shales containing numerous randomly oriented fossils (solitary corals and brachiopods, including those with two valves) and imprints of dissolved shells. At some levels, the rock is harder (but also fissile), granular, and more similar to clayey limestone. The upper half of the unit contains a dark gray bioclastic limestone interlayer (10 cm; crinoid fragments are predominant) with a siliciclastic admixture and fine grains of pyrite. Similar limestones form a range of layers (1.5 m) at the top of the unit. There are many fragments and unbroken brachiopod shells in the upper layer. The total thickness of the shale unit is hard to estimate, because it is exposed approximately along the strike.

Unit 10 (unit with sandstones deposited by bottom currents and oolitic shales; 20–25 m in thickness). The bottom quarter of the unit is composed of dark gray shales. In contrast to underlying shales, they do not react with hydrochloric acid, but still contain shell imprints. Apparently, calcite was leached during diagenesis. The overlying part of this unit is is characterized by rhythmic intercalation (Fig. 8e) of shale (clayey in the lower part and silty up the section) with hard light-colored sandstone and siltstone. The number of the latter increases from bottom to top; their thickness is from 0.5 to 15 cm. Sandstone and siltstone consist mainly of quartz and appear "quartzite-like" (sutured contacts between grains are visible under a microscope). Some sandstone layers often demonstrate the following sequence of sedimentary structures (Fig. 8f): cross lamination in the lower part (current ripples) and horizontal lamination above (sometimes with chains of small current ripples). In addition, sandstone and siltstone are marked by small-scale intralayer slump structures and load marks on the sole. Multidirectional tunnels filled with sand were noted in shales (Fig. 8f).

The uppermost part of unit 10 is composed of hard bioturbated clayey–sandy quartz siltstones (3–4 m), which are replaced upsection by black shales (about 1.5 m). Shales contain more competent interlayers. The latter include a variable number of black flattened ooids (up to 2 mm); their concentric structure can be seen in thin sections (ESM_1 fig. S2). Near the top, some layers are entirely composed of ooids and look like Mesozoic tasmanite shales.

Unit 11 ("Sinai sandstone"; apparent thickness is about 6 m). The name of this unit comes from Sinai Cape, which it makes up. It is possible to study only a lower layer of this unit, which as a massive steeply dipping plate with a thickness of about 1.2 m protrudes into the sea (Fig. 8e). This layer is sandy dolostone containing fine siliciclastic material (up to 50% of rock volume, mainly quartz), as well as brachiopods and corals. The rock is overfilled with small "plaques" resembling flattened ooids, similar to those found in underlying shales. Overlying layers are similar in appearance, but form thinner and more irregularly shaped plates. Judging from debris in scree, this part of the unit contains limestone, including bioclastic one. The whole unit is characterized by a reddish yellow color on the weathered surface. Massive layers are divided by loose black clayey sandstone with abundant fauna.

This unit with a small visible thickness completes a continuous section of the Tas-Ary Formation in the northwestern part of the Tas-Ary Peninsula. To the south of Sinai Cape, the sequence is interrupted by a high-amplitude fault, beyond which substantially younger part of the Carboniferous section is exposed (we assigned it to the upper part of unit 13). The rocks of unit 11 are not repeated anywhere else, and we do not know reliably the thickness of unexposed fragment of the section. Supposedly, it is 15–20 m, and "Sinai sandstones" gradually transit up the section to the limestones of unit 12. The middle part of the Tas-Ary Formation (Fig. 4, units 12–16) makes up a significant segment of the western coast of the peninsula (just over 3 km, from site 759 to site 760) (Fig. 3), where the same fragments crop out repeatedly disrupted by normal faults. The description of these units is given below. Their thickness was calculated on the basis of panoramic photographs.

Middle Part of the Tas-Ary Formation

Unit 12 (20 m in visible thickness). Bioclastic limestones that are often recrystallized (ESM_1 fig. S3a). The color varies from dark to light gray; sometimes, the color is mottled. Limestones form flat layers with

a thickness from 10 cm to 1.3 m (usually decimeters) divided by thin horizons of dark clayey limestone (Fig. 9a). Clayey interlayers are thicker in the visible lower part of this unit. The rocks are somewhat different at the northernmost outcrop of the fragment of unit 12: limestones are slightly lumpy, yellow from the surface, with uneven boundaries. Unit 12 is distinguished by large (up to 8 cm) brachiopod shells. Highly convex *Palaeochoristites* are the first to call attention to themselves. Occasionally, they overfill the rock. In addition, this unit contains rare corals; thin sections show ostracods (?) and crinoids. In general, the number of fossils increases up the section. Brachiopod shells commonly lie flat on the bedding surfaces; some corals lie horizontally.

Near the visible base and at the top of the unit, limestone contains a considerable admixture of quartz silt. A thin discontinuous horizontal lamination can be noted at some levels of the section. The upper several meters of the unit are composed of clayey limestones (dark gray fine-grained) with concretion-like interlayers (from 1 to 40 cm) and nodules of bioturbated fine-grained limestones (Fig. 9b). The latter are more light-colored, yellowish on the weathered surface. The thickest layer is located in the top of this unit.

Unit 13 (upper fossiliferous shale; 13–15 m in thickness). Gray calcareous shales (Fig. 10; ESM_2 file in Supp. Data) enriched in solitary corals and various brachiopods, including those with two valves. Fossils are randomly oriented, occasionally pyritized. At the bottom of the unit, shales are only slightly calcareous; they contain rare small (up to a few centimeters in diameter) clayey–carbonate concretions of spherical and irregular shape. In the very bottom (lowermost 0.7 m of the unit), there are thin (up to 10 cm) concretion-shaped interlayers of bioturbated limestones (as in the top of the underlying unit) with numerous fossil fragments. Similar sporadic interlayers, but slightly finer-grained and more clayey, are also present in the upper part of the unit (Figs. 9c, 9d). The thickness of the interlayers is from 1 to 15 cm; they are lenticular and hardly visible from afar.

Unit 14 (alternation of shale and limestone; 7–10 m in thickness; Fig. 10). This unit is similar to the upper portion of unit 12, but its rocks are more contrast and, apparently, more clayey. It is composed of dark gray calcareous shales with gray fine-grained limestone interlayers (a few decimeters), including concretion-like ones and nodules (up to 10 cm). Up the section, the interlayers become more frequent; they can contain clay and be bioturbated. In both shale and limestone, fauna is frequent in occurrence, but it is rarer relative to the underlying unit. Thin sections demonstrate quite numerous sponge spicules. The rocks show faint thin parallel lamination disrupted by bioturbation.

The boundary with limestones of unit 15 is drawn to some extent arbitrarily, because the transition is gradual. In some outcrops, the limestone predominance level is clearly visible in the section, while in others, the boundary is less obvious. Some shale intervals in the upper part of unit 14 contain thin discontinuous (bioturbated) limestone horizons (a few millimeters to a few centimeters). Similar interlayers can also be found in the lower part of unit 15.

Unit 15 ("bumpy" limestones; 40–50 m in thickness). It is composed of gray, granular, irregular platy limestones with very characteristic "bumpy" bedding planes (Fig. 9e), which gives them in places a nodular appearance. In the lower part of the unit, limestones on the fresh cut are darker, with more noticeable clayey interlayers (Fig. 9f); some of them form isolated nodules. Two adjacent thick (40–70 cm) shale beds are located 6–7 m above the bottom. The number of fossils (both unbroken macrofossils, such as brachiopods and corals, and small bioclasts) increases up the section. The bedding surfaces are marked by rare trace fossils resembling *Zoophycos*. In both the lower part of the unit and the top, limestones contain an admixture of clay and siliciclastic silt (up to 15%), and they are finer grained than in the middle part of the section. In addition, silicification developed in the lower part of the unit and at the top. In the first case, it is observed as chert nodules, while in the second case, it is observed as areas of siliceous cement in limestone (visible in thin sections; ESM_1 fig. S3b, S3d) and is caused by redistribution of matter under diagenesis. The outcrops of the whole unit 15 are absent in the coastal cliff, and the maximum apparent thickness is 35 m. Comparison of the studied fragments of the section makes it possible to estimate a true thickness of the unit at 40–50 m.

Rocks of units 13–15 can be considered as a single regressive rhythm. Apparently, the same rhythm is also formed by deposits of units 16–17 (see below); however, their depositional environments differ, only the general trend (regressive) is similar. Units 12 and 15, at first glance, are alike: both are composed of biosparites according to Folk's classification (Folk, 1962) with an abundant macrofauna; in addition, both are overlaid by shale units, and they can be confused in the disrupted section. Meanwhile, limestones of unit 15 are distinguished by "bumpy" bedding planes, silicification, and other fossil assemblages. Shale units which overlie both limestones are also differ significantly from one another.

Unit 16 (black unit; about 30 m in thickness). It is subdivided in the description into two parts.

Subunit 16a (shale part of the black unit; about 20 m in thickness). It is represented by dark gray to black lime-free mudstone with pyrite interlayers (millimeters to a few centimeters) and fine-grained dark gray, sometimes brownish, Fe-carbonate beds (and clayey dolostone (?); centimeters to a few decimeters). Carbonate beds are commonly cracked perpendicular to the bedding; they macroscopically resemble siltstone, contain up to 1–2% of fine siliciclastic grains, and are

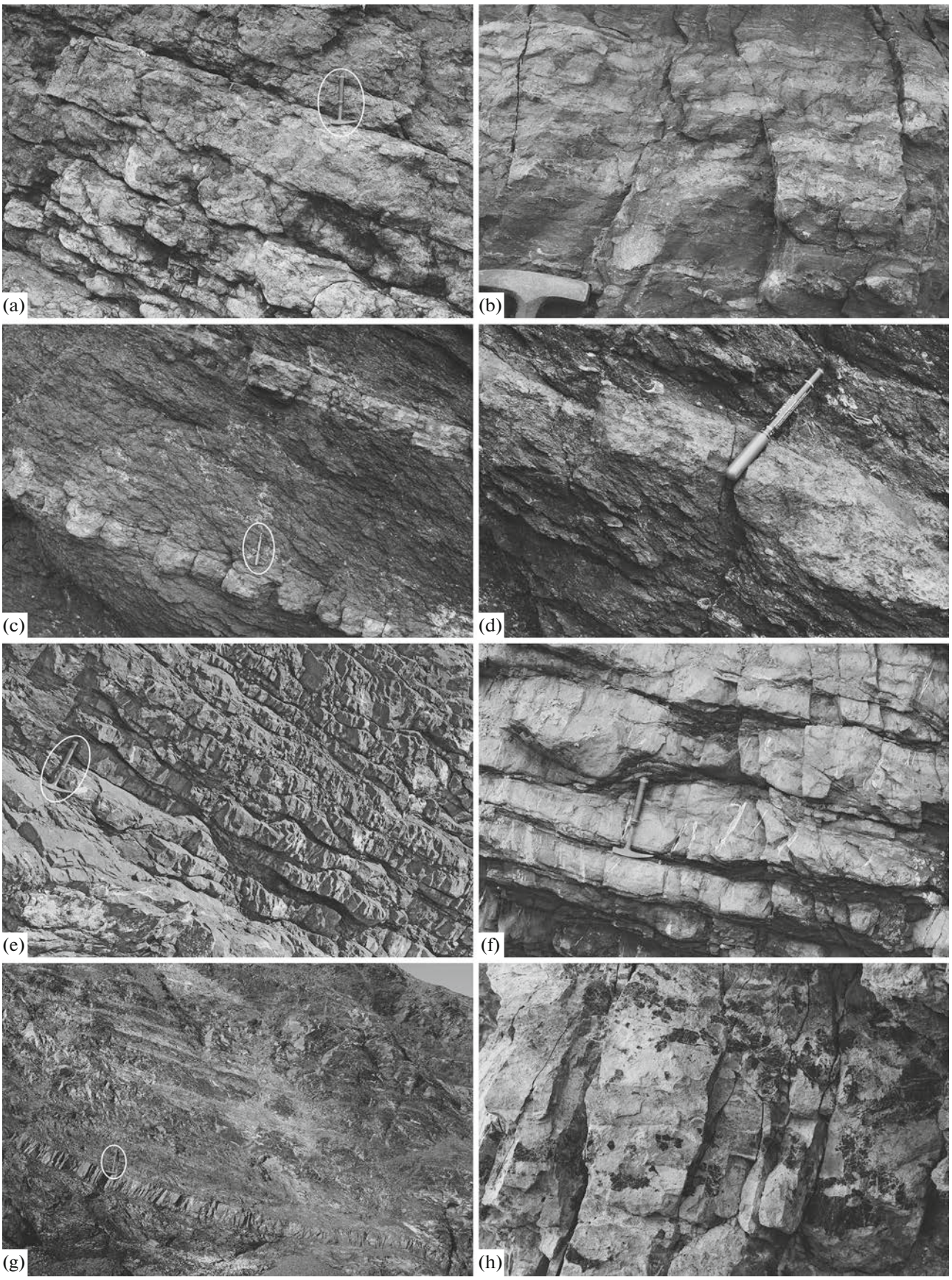
(a)
(b)
(c)
(d)
(e)
(f)
(g)
(h)

Fig. 9. The most typical rock varieties in the middle part of the Tas-Ary Formation. In photos (a), (c), (e), and (g), a hammer is circled in a white oval. (a) Evenly bedded gray bioclastic limestone of the unit 12; (b) bioturbated concretion-shaped interlayers of silty limestone in darker finely laminated clayey limestone (near the top of unit 12); (c, d) the upper part of unit 13: rare interlayers of bioturbated clayey limestones in calcareous shales (both of them contain a huge amount of fauna, as can be seen in Fig. 9d); (e) general view of the section in the middle part of unit 15, showing "bumpy" bedding surfaces; (f) lower horizons of unit 15, close up: more pronounced clayey layers and occurrence of chert nodules (for example, left of the hammer); (g) general view of the lower part of the black shale unit 16; the hammer stands at the top of the ferrous carbonate layer with characteristic vertical cracks; (h) numerous black chert nodules in the limestone of unit 19 emphasized by leaching of the host rock (photograph is 25 cm high).

confined mainly to the upper third of the interval. The two most notable such layers were found near the top and the base of subunit 16a (Fig. 9g). There are rare interlayers of clayey limestone as well, some with sponge spicules, visible in thin sections. Shales contain rare large flattened sideritic (up to 15 cm) and clayey–carbonate concretions (up to 50 cm in length) and jarosite horizons. Siderite concretions are especially abundant at the top of the interval. This very part of the black unit crops out several times to the north (Fig. 3, almost up to site 593), in a faulted section. The overlying rocks are not exposed north of site 761.

Subunit 16b (transitional part of the black unit; about 10 m in thickness). Dark gray fine-grained clayey limestones containing numerous sponge spicules and fine siliciclastic admixture (not less than 5%), with interlayers of black mudstone, including calcareous varieties (up to 0.5 m). There are also more light-colored fine-grained limestones, rare pyritized fossils, and thin pyrite interlayers (tabular concretions (?)). Rocks are cleaved, and lamination in the unit is hard to identify. The top (Fig. 3, site 760) consists of black lime-free mudstone (about 0.5 m) overlaid by dark gray fine-grained dolostone (?) (0.2 m).

Upper Part of the Tas-Ary Formation

From site 760 (Fig. 3) to the south, the section is generally homoclinal. Here the upper part of the Tas-Ary Formation (Fig. 4, units 17–21) was studied. The thickness of these units was estimated graphically. However, in contrast to the lower seven units which thicknesses were calculated on the basis of interpolated bedding attitudes, the thickness of the upper part of the Tas-Ary Formation was estimated on the basis of the general structure. In this (southern) area, the coastline strike approximately coincides with the axis of the syncline (Fig. 3); in other words, the coastal outcrops reveal its near-core part, where the thickness is likely higher. Therefore, when calculating the thickness, the length of the outcrop for a particular unit (across the strike) was taken not along the coast (actually observed), but away from the fold core (according to the compiled geological map). Dip angles measured in the cliff were used in the calculation. This approach led to inevitable inaccuracies; however, we assume them to be smaller than those resulting from measurements in a near-core part of the syncline.

Unit 17 (cleaved dark limestone; apparent thickness is 110 m). Indistinctly laminated limestones with spicules, fine- and very fine-grained, mostly clayey (ESM_1 fig. S3c), similar to those of the underlying unit. The clay content decreases up the section; in some layers, the amount of siliciclastic admixture reaches 15% (grains are very small). In limestones, rare fragments of crinoids are macroscopically noticeable; in the lower part, partially pyritized brachiopod shells and sporadic thin pyrite interbeds can be found at several levels. Rocks are highly cleaved and bioturbated (the latter, however, is not very noticeable) (Fig. 11): the cross sections of tunnels made by burrowing animals and fine dashed lamination can be seen. Bedding in the section is visible from afar, but it is hardly distinguishable in a close view due to a well-defined cleavage. Bioclastic interlayers appear in the upper half of the unit: firstly, dark fine-grained limestones with large relatively rare fossil fragments, and gray coarse-grained clastic ones above. In the upper part of the section both fine-grained cleaved rocks and coarse-grained limestone contain abundant fauna of crinoids, brachiopods, and corals. Rock enriched in siliciclastic material (well seen in a thin section) was found there:

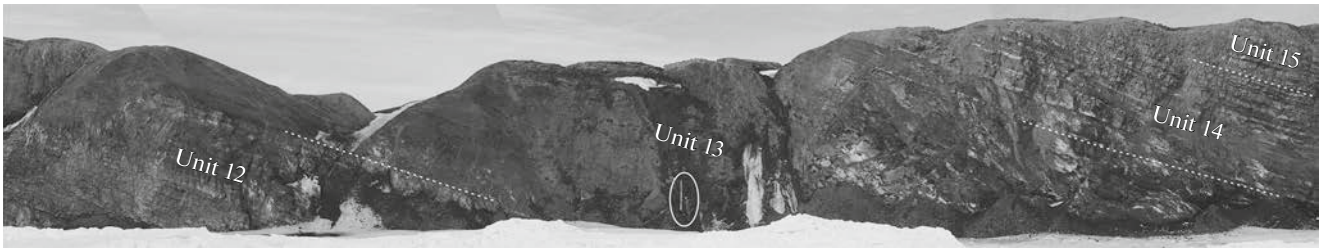

Fig. 10. Fragment of panoramic photograph of the southwestern coast of the Tas-Ary Peninsula showing a monoclinal section of the Tas-Ary Formation in the interval from the upper part of unit 12 to the bottom of unit 15. A man with a range pole (2.5 m in height) is outlined in an oval.

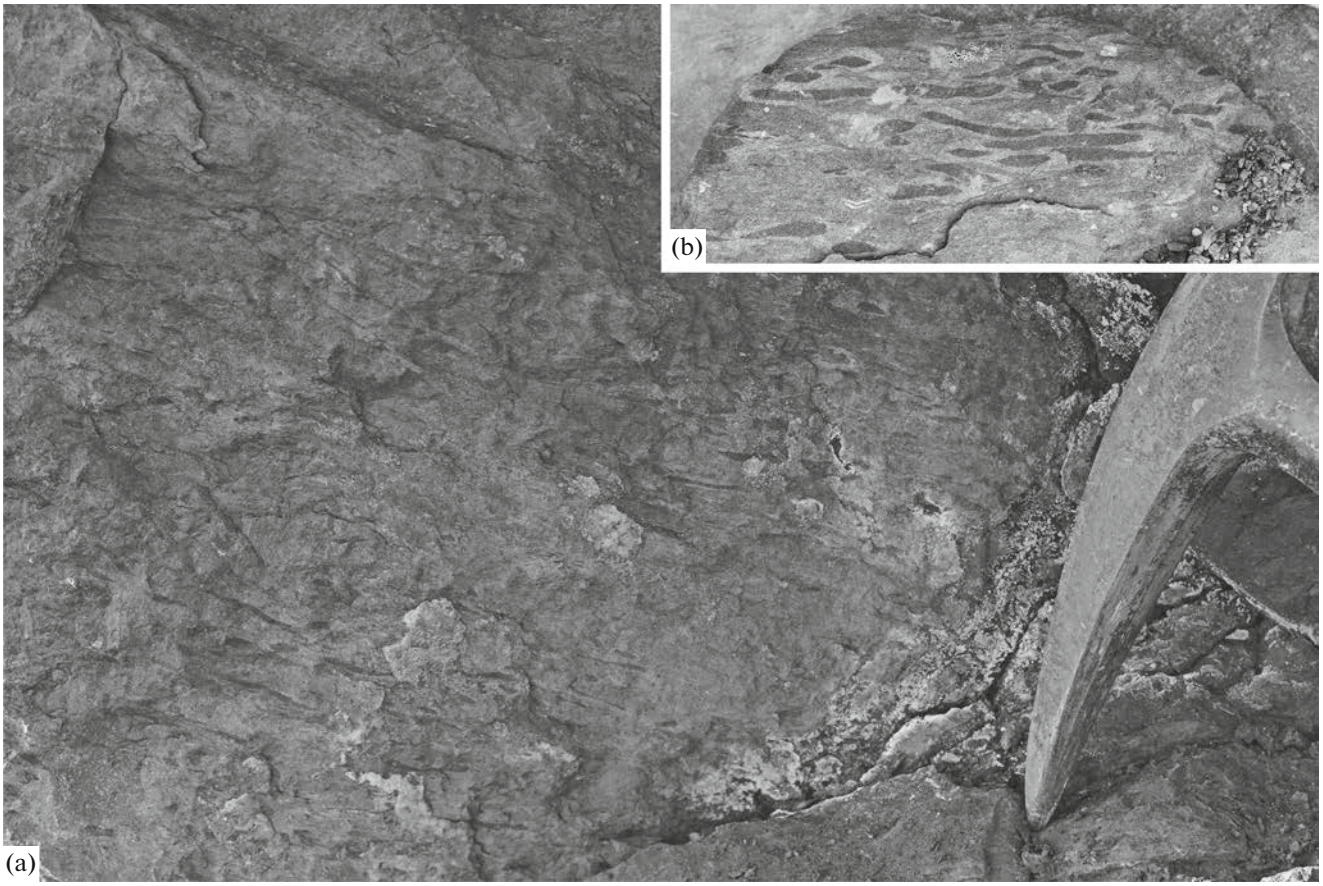

Fig. 11. (a) Bioturbated fine-grained clayey limestone of unit 17; poorly defined bioturbation is characteristic of the whole unit; (b) analogous clearer structures in the limestone fragment on the beach near the Lagerny Creek mouth (probably from higher horizons of the section): cross-section of winding tunnels (sample cut at right angles to layering) dug by some benthic organisms (such tunnels are visible in the plates split along layering); photograph is 8 cm wide. These structures resemble *Phycosiphon* surface feeding traces which are typical of extremely low-energy settings (Frey, 1975).

it is represented by recrystallized limestone with large bioclasts, quartz and chert silt and fine sand (about 30% of the rock). The top of the unit is composed of gray crinoid limestones (a few meters thick; sporadic unbroken stems) forming plates (up to a few decimeters) with clayey surfaces.

Further on, the section is interrupted by a long wide beach and the mouth of the Lagerny Creek. No outcrops were found between sites 755 and 767 over a distance of 140 m (Fig. 3). The thickness of the unexposed interval, according to our estimates, reaches 70–90 m (at a dip angle of 24° and 30°, respectively).

Unit 18 (the second unit of cleaved dark limestone; apparent thickness is 30 m). In the visible base of the section, there are about two meters of interbedded limestone and black calcareous shale. They are overlain by relatively dark gray fine to very fine-grained limestones with rare fossil fragments (mainly crinoids). There are beds of thin-platy to fissile clayey limestones. Trace fossils similar to those of unit 17 were observed on the bedding planes. The boundaries between limestones of both types are often poorly defined. The gray limestones prevailing in the unit, in contrast to the underlying ones, are somewhat more competent; meanwhile, at some intervals, they still contain clay (especially in the upper part of the unit); very fine siliciclastics and numerous sponge spicules are still present. Rocks include fine pyrite dissemination and rare small pyrite nodules.

Unit 19 (limestone with chert; approximately 210 m in thickness). The rocks at the base of the unit are similar to those at the top of the underlying one, but contain centimeter-thick black fissile clayey limestone interbeds at a step of 10–20 cm on average. Up the section, the rocks become more light-colored, and the thickness of clayey interlayers decreases. At a distance of 7–8 m from the bottom of the unit, there is a bed about 15 cm thick composed of highly clayey limestone. Its middle part contains a concretion-shaped interlayer of gray fine-grained limestone with fine pyrite dissemination, rare small crinoid columnals, and numerous sponge spicules (visible in thin sections). Above this, a thick monotonous section of brownish gray very fine-grained hard micrite-contain-

ing limestone often silicified to some extent (fragmentary development of secondary siliceous cement), with numerous nodules of black (sometimes dark brown) irregularly shaped chert, starts (Fig. 9h). Tabular chert concretions are widespread in some intervals of the section. Limestones form beds with a thickness of 10–30 cm, sometimes more, separated by thin clayey interlayers (clayey limestone, calcareous shale; a few millimeters, less often, a few centimeters). Limestone layers are massive, without internal lamination, usually with uneven boundaries. Macrofauna remains are very rare in the lower part of the unit, and crinoid columnals occur higher. Spicules, sometimes numerous (ESM_1 fig. S3e–S3h), can be identified in both limestone and chert under a microscope.

Much of the section is greatly altered in the weathering crust. For 155 m from site 768 to the south (Fig. 3), deposits of the unit are almost unrecognizable. They are leached and turned into light porous rocks of black, pinkish gray, yellow color, resembling siltstone and sandstone. Slightly weathered fragments of the section, represented by the same very fine-grained limestone with chert, are sometimes exposed further to the south (up the section), in the lower part of the cliff. From the point of +230 m to the south of site 768, the rocks are "fresher" and react with hydrochloric acid, but the cliff is severely fractured, occasionally rusty. Limestones are thick-platy there (layers are up to 0.8 m in thickness). Above, the thickness of the layers decreases again. The rocks at the top of the unit are bleached, but their composition does not change.

Unit 20 (fissile clayey limestone; 30 m in thickness). The unit is composed of dark gray limestone, fissile clayey and harder (slightly fissile) less clayey ones. Both varieties are fine-grained and contain fauna and fine pyrite grains. The transition from one limestone variety to another is vague, and it is not possible to trace the layers. The rocks contain silt-sized quartz and chert grains, occasionally abundant (up to 40%). Limestone layers similar to those in the underlying unit are rare. The upper part of unit 20 is enriched in fossils (solitary corals, brachiopods, and crinoids) oriented chaotically. In general, these are fragments (even crinoid columnals are crushed) which form individual small segregations at some levels (Fig. 12a). Implicit competent lenticular interlayers and lenses can be identified among clayey limestones (Fig. 12b). Sedimentary structures are not visible. The lower and upper boundaries of the unit are indistinct owing to gradual transitions.

Unit 21 (upper limestone with cherts and fauna; 35–40 m in thickness). The base (several meters) is composed of heavily fractured limestones with rare clayey interlayers, which are still harder than those in the underlying unit. The clayey interlayers are enriched in fossil fragments; hard limestones contain only a few fragments of foraminifera and crinoid columnals. Major part of unit 21 is represented by limestones, gray from the surface and darker inside, making up massive layers of 0.1–1 m thick (commonly a few decimeters), with cherts. Limestones are fine-grained; some varieties appear to be recrystallized. The layers are separated by thin clayey horizons (up to a few centimeters); boundaries are usually uneven. Cherts are distributed throughout the section (in the lower horizons, these are partially silicified nodules). The unit is similar to lower "limestone with chert" (unit 19), and the main difference is the presence of numerous macrofauna fragments. They are noted throughout the unit, usually quite rare and small, but they are more numerous in some layers and sometimes form accumulations; in general, the number of fossils in the rocks increases up the section. There are also unbroken specimens, in particular, large brachiopods, less often, coral colonies. In one case, two spherical colonies were observed next to each other (possible fragments) (Fig. 13a). Apparently, all of them were buried in a displaced position. In the upper part of the unit, bioclastic limestones contain chert pebbles. The thin sections show that rocks of unit 21, as well as those of the unit 19, contain sponge spicules; a siliciclastic material is more abundant there (mainly silt; up to 10% at the top of the section). Silicification features are somewhat different: chert nodules developed in both units, but limestones in unit 21 are usually not "saturated" with siliceous cement; only bioclasts are partially silicified.

Near the top of the unit, there is a limestone bed (0.3 m) with an unclear parallel lamination. Above, approximately 0.7 m is occupied by almost black clayey–silty limestone with brachiopods. It is overlain by dark gray–black fissile clayey rocks which we assigned to the Bel'kov Formation (Fig. 13b).

BEL'KOV FORMATION

The Bel'kov Formation crops out on the southwestern and southeastern coasts of the Tas-Ary Peninsula, in different limbs of the syncline (Fig. 3). The best exposures are confined to the southwestern cliff, but upper horizons of the section do not crop out there there. We managed to correlate the sequence in the western and eastern limbs, although it was not always unambiguous. The formation consists of ten subdivisions called in the text "members" (Fig. 14). Some of them were additionally subdivided into units. Here we provide the description of members 1–7 for southwestern coastal exposure, while overlying members were described along the southeastern coast.

We drew the lower boundary of the formation along the base of the black fissile unit lying over massive light-colored limestones forming the top of the Tas-Ary Formation. However, this unit, as well as the entire lower portion of the Bel'kov Formation, is characterized by rapid changes in facies and thickness along the strike. Near site 771 (Fig. 3), where the black unit first appears at the top of the cliff, judging from the photographs, it is composed mainly of shale and

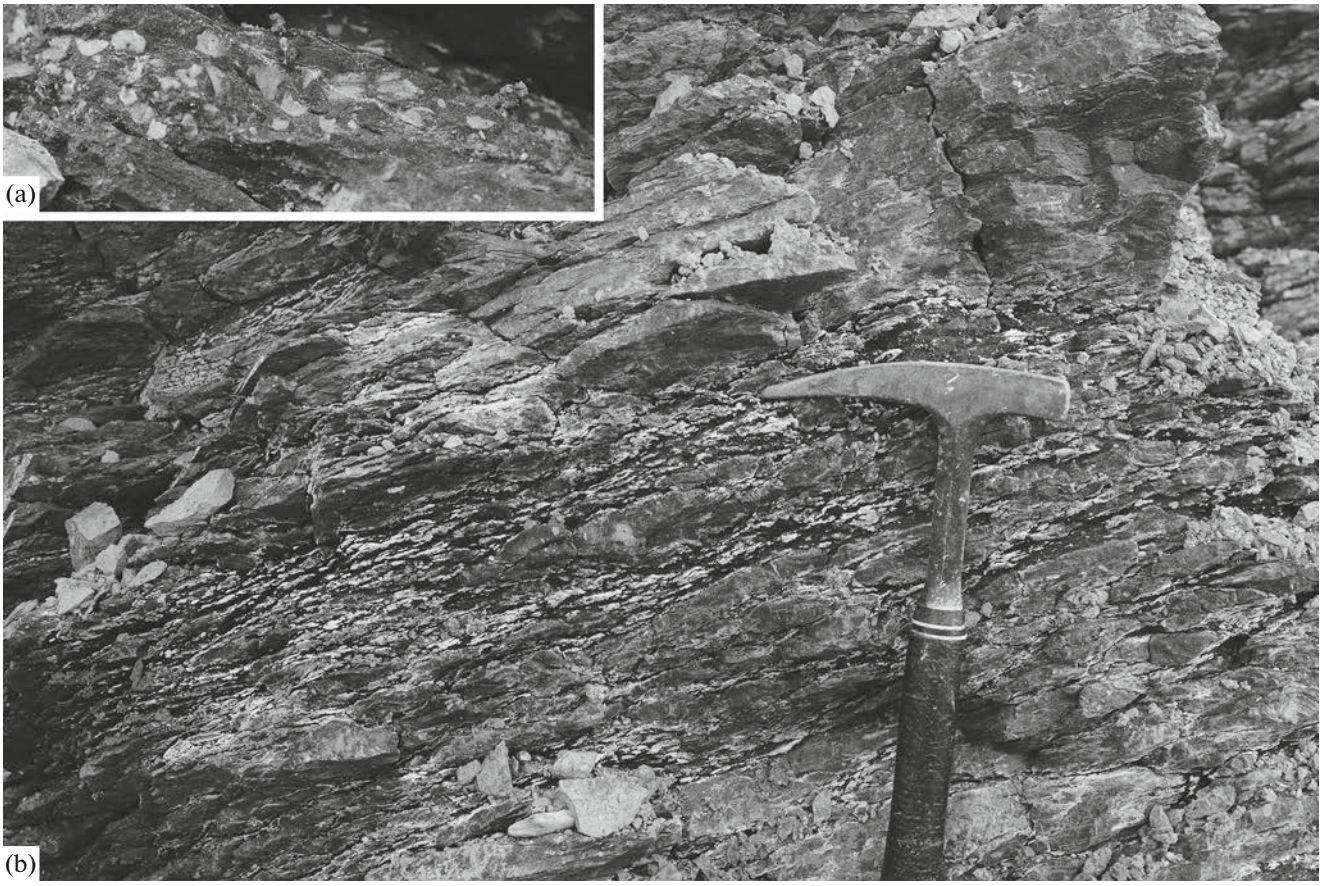

Fig. 12. Lithological features of the rocks in the upper part of unit 20. (a) Accumulation of crinoid fragments in fine-grained limestone (the photograph is 12 cm wide); (b) unclear lenticular interlayers composed of a slightly harder rock than the host clayey limestone.

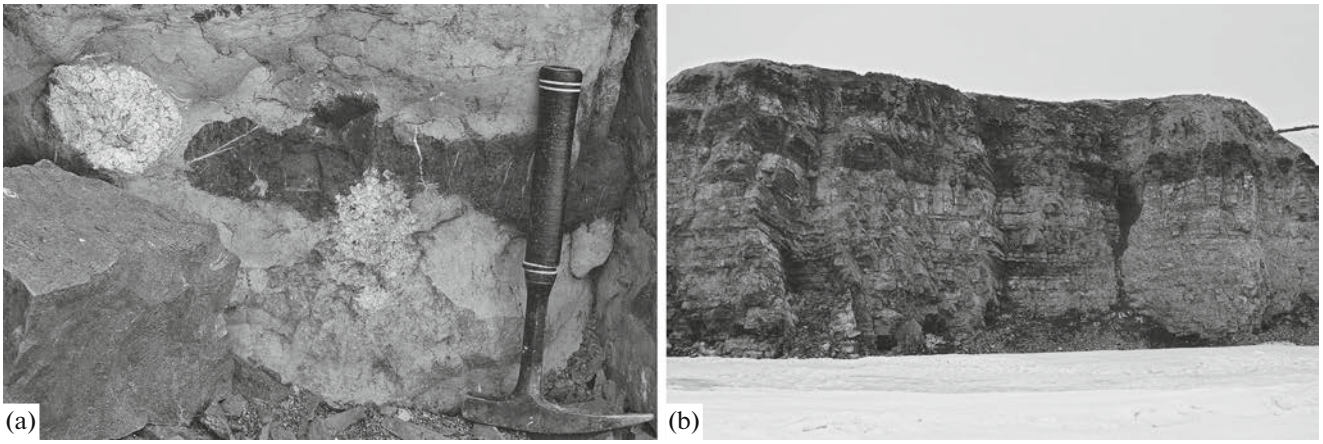

Fig. 13. (a) Two large coral colonies and black chert nodules in the uppermost unit of the Tas-Ary Formation; (b) top of the Tas-Ary Formation and overlying black limestones and shales of the Bel'kov Formation (the cliff height is about 20 m).

dark clayey limestone with interlayers of massive limestone (Fig. 13b), and it is lithologically drastically different from the underlying rocks. To the southeast, where the unit goes down to the beach, its thickness increases by 2.5 times, and massive limestones prevail in its composition. However, it demonstrates the facies which are absent in the Tas-Ary Formation (see below). The position of the boundary between the Tas-Ary Formation and the Bel'kov Formation that we adopted differs from that published by the geologists of the Arctic Geology Research Institute (Kos'ko et al., 1985). These researchers drew a boundary 50 m

(65 m according to their data) up the section, apparently at the base of member 4 (in our classification). The reason for this decision is not clear: with this approach, the Tas-Ary Formation appears to include sandstones and carbonaceous shales with phosphatic concretions, which are not characteristic of it, but are characteristic of the overlying Bel'kov Formation. The total apparent thickness of the latter, according to our estimates, is at least 300 m (Fig. 14).

Lower Member of the Bel'kov Formation

Unit 1 (bottom black unit; 3–3.5 m in thickness). The base of the unit is represented by black cleaved clayey limestones (0.5–0.6 m). Up the section, similar rocks with rhythmic interlayers of hard black limestone of 3–5 cm thick (0.8–1.0 m in total) crop out. This facies was not found lower in the Carboniferous section. Cleaved limestones are overlain by a clastic limestone layer composed of skeletal fauna fragments (largely crinoid columnals; 0.7 m). The top of the unit is made of limestone similar to that in its base, but containing corals and brachiopods (1 m; the thickness increases to 1.5 m to the southeast).

Unit 2 (limestone with "bulging"; 1.5–8 m in thickness). This unit is composed mostly of massive gray limestone. Its thickness rapidly increases from NW to SE. The upper and lower boundaries of the unit become less defined in the same direction, because massive limestone interlayers also appear in the underlying and overlying rocks. The unit has a maximum thickness near site 766 (Fig. 3); from the sea, it looks like a bulge (Fig. 15; ESM_3 file in Supp. Data), but to a large extent, it is a semblant bulging caused by a combination of beds altitude (tilted towards the slope) and the configuration of the coastline. It can be assumed that the thickness of the unit increases even more significantly to the southeast. At site 766, the unit has the following composition (from bottom to top):

Subunit 2a (1.2 m in thickness). Massive gray limestone sometimes splitted into two or three layers with numerous crinoid columnals at the bottom. Brachiopod shells can also be found there.

Subunit 2b (1.3 m in thickness). The same limestone in alternation with dark cleaved clayey limestone. Crinoid fragments were noted.

Subunit 2c (1.6 m in thickness). Relatively hard homogeneous limestone 0.2–0.3 m thick occurs at the base; upwards, it is replaced by dark gray–black clayey cleaved limestone. Fragments of brachiopod shells are sporadic.

Subunit 2d (3.8 m in thickness). A series of several beds of massive recrystallized limestone are well seen in the cliff. The number of layers distinguishable in the outcrop depends on the degree of rock weathering: additional exfoliation planes appear in more weathered areas. Predominantly, three distinct (up to 1.3 m) layers separated by black clayey limestone interlayers with a thickness of 1–10 cm can be seen; these interlayers occasionally contain fauna. In massive limestones at some levels, there are fragments of brachiopod shells, sometimes traced as a chain; a trilobite

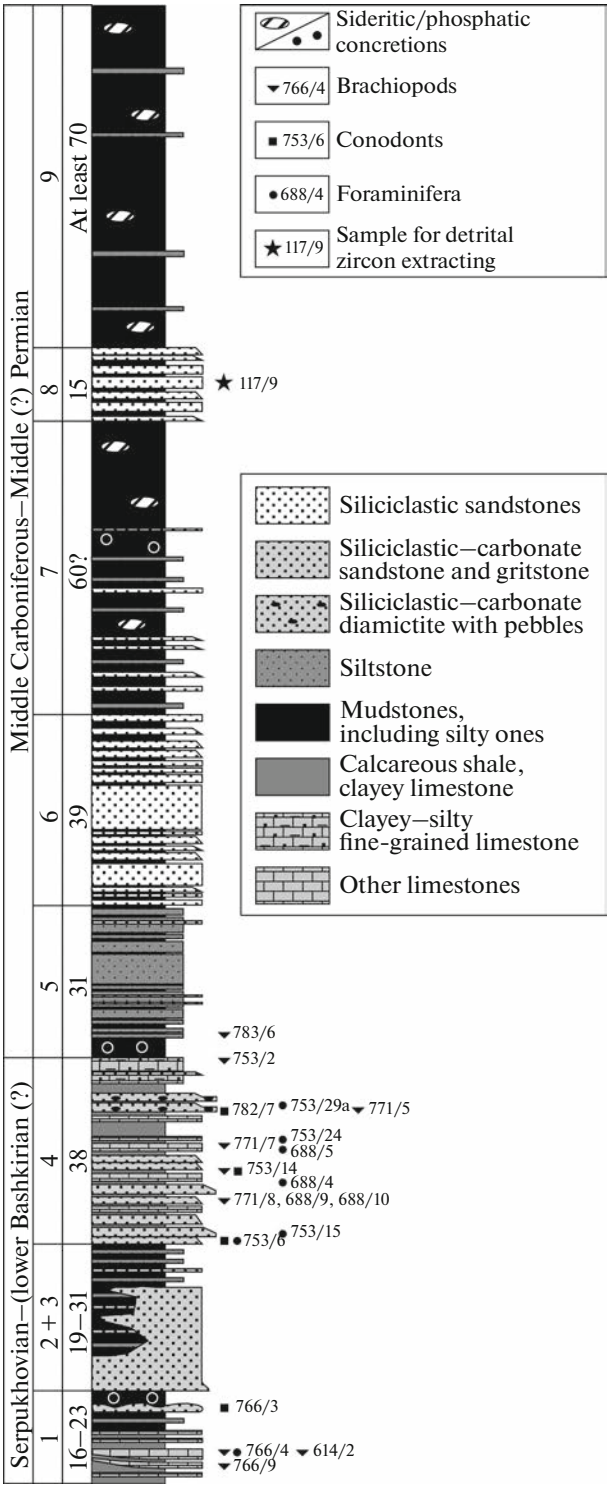

Fig. 14. Stratigraphic column of the Bel'kov Formation. Series/stages, numbers of members and thickness in meters are written left of the column.

Fig. 15. Fragment of panoramic photograph of the southwestern coast of the Tas-Ary Peninsula showing the lower horizons of the Bel'kov Formation (member 1). The top of the Tas-Ary Formation is indicated with a solid white line. Men with a range pole (2.5 m in height) is outlined in an oval.

fragment was also found. The top of the middle layer is marked by small chert nodules.

Unit 3 (the second black unit; 11–12 m in thickness) is composed of four contrast parts clearly visible in a photograph (Fig. 16).

Subunit 3a (3.8 m in thickness). Alternation of limestone, as in the upper part of the underlying unit, and dark calcareous shale. Brachiopods and rugose corals are rare. In the upper half of the interval, limestones predominate and form thick layers; limestone beds are thin (5–20 cm) in the lower half and at the top of the unit.

Subunit 3b (3.8 m in thickness). Dark gray mudstone, black bituminous at the base (1.8 m) and at the top (0.7 m). In the lower part, there are implicit interlayers of relatively competent rocks. In the middle part (1.3 m), mudstones are rhythmically interbedded with siltstones and, likely, fine-grained sandstones. The thickness of siltstone interlayers decreases up the section. Rocks in the middle part of the interval include gypsified varieties.

Subunit 3c (1–2 m in thickness). "Lava-like bed" of poorly sorted siliciclastic–carbonate gravelly sandstone with bulges. The rock is composed in large part of crushed crinoid columnals and bryozoan fragments. The volume of the siliciclastic material reaches 30–40%; it is represented, as down the section, by chert and quartz grains (ESM_1 fig. S4a, S4b). In addition, mudstone and siltstone lithoclasts with clay–carbonate cement were noted; some fragments of microcrystalline chert resemble a matrix of felsic volcanic rocks. Sandstone also contains chert interlayers likely formed owing to sponge spicules. Because of recrystallization, only a few cross sections of spicules among fine-grained chalcedony can be identified in thin sections. The characteristic shape of the bed is due to sediment fluidization (Danukalova and Kuzmichev, 2016; see below).

Subunit 3d (2.5 m in thickness). Fissile black mudstone with phosphatic concretions and gypsum. These concretions are small (a few centimeters), spherical, and flattened. Thin interbeds of more competent gray siltstone were also observed. The subunit was strongly folded in the base of the massive unstratified "sill" (see below): hinges of recumbent folds stretching along the slope are well seen. Black carbonaceous shales make up about 30% of the thickness of the subunit.

The total thickness of the lower member of the Bel'kov Formation is 16–23 m.

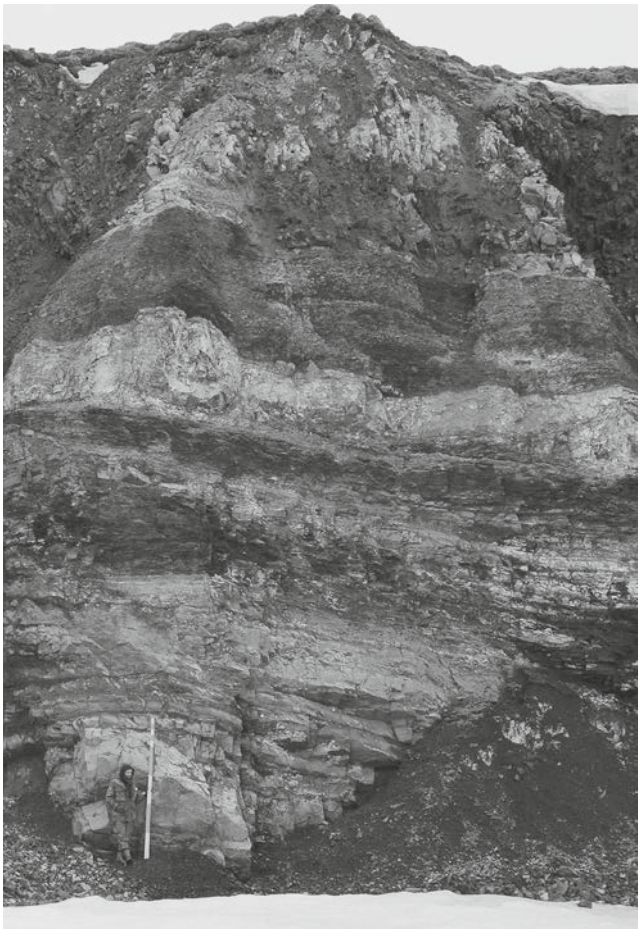

Fig. 16. The whole unit 3 of the lower member of the Bel'kov Formation in the coastal cliff. The base of the cliff is composed of massive limestone of the uppermost part of unit 2; its top is located at the upper end of the range pole (2.5 m in height). The upper part of the cliff consists of unstratified sill-like sandstone of member 2. Unit 3 is divided into four intervals (see the text): (a) limestone with shale interlayers, (b) mudstone and siltstone, (c) lava-like sandstone bed, and (d) black shale.

Member 2 (Sill-like Sandstone)

This member is represented by an impressive sandstone body whose base appears conformable with the host rocks, while the roof is irregular, with curved "prominences" disturbing the sedimentary sequence (Fig. 17). The thickness of this body increases from 8 to at least 20 m at a distance of 50 m to the southeast and is further cut off by the fault. Sandstone is homogeneous, fine- to medium-grained. It is devoid of sedimentary structures and, at first glance, resembles an igneous rock. Its composition is similar to the above-described lava-like bed, but more equigranular; it contains more siliciclastic material (about 50%) and less bioclasts (ESM_1 fig. S4c, S4d); abundant pyrite, fragments of phosphatic concretions, a few fragments of andesites and basalts and plagioclase occur locally. At the bottom there is a basal layer with a thickness from a few centimeters to a few decimeters, which is composed of poorly sorted sandstone with crushed fossils and a large number of lithoclasts (mudstone, siltstone, limestone, and altered volcanic rocks). Up the section, the rock gradually becomes finer grained. In the lower one and a half meters, there are poorly defined structures resembling water-escape ones (dish structures) (Stow, 2012), as well as signs of amalgamation.

The described sandstone body is interpreted as an in situ bed which was fluidized under compaction of the host carbonaceous clayey deposits and mobilized in the fault zone, which led to injections into overlying sediments (Danukalova and Kuzmichev, 2016). Only separate thinner sand sills and dikes connecting them are visible in the cliff to the southeast of the fault, in the downthrown block. We assume that initially sandstone (as in the lava-like bed) had a turbidite nature; the crushed fauna fragments came from the coastal part of the basin. The lowermost part of the layer, which retained primary sedimentary structures, was not mobilized.

Fig. 17. Line drawing of a panoramic photograph fragment of the Tas-Ary Peninsula's southwestern coast demonstrating a thick layer of siliciclastic–carbonate sandstone which gave injections (clastic dikes and sills) into overlying shale as a result of mobilization in the fault zone (shown with a dotted line). The cliff height is 20 m. Boundaries of the sandstone body are outlined; host deposits are darkened.

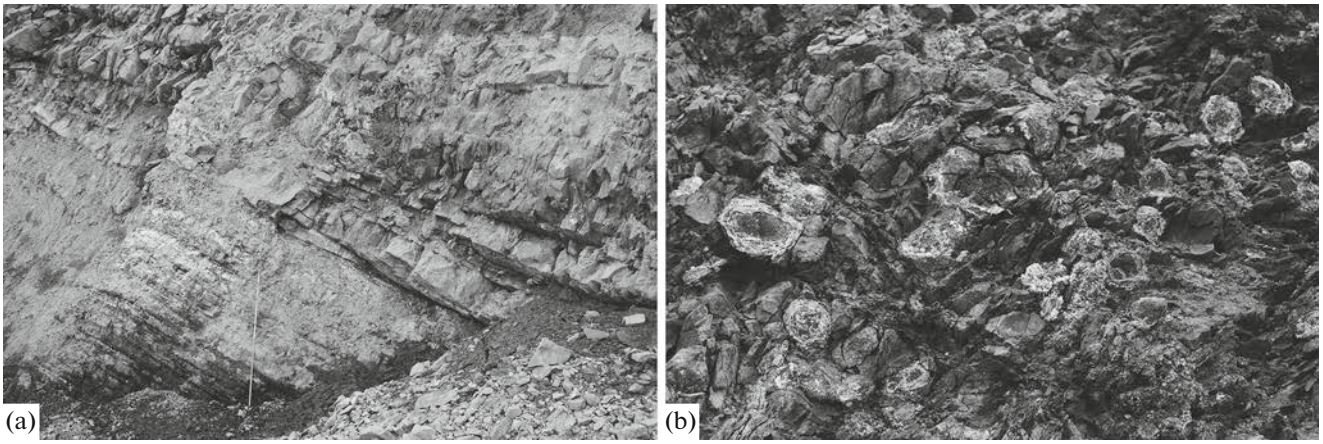

Fig. 18. Some rocks in the middle part of the Bel'kov Formation. (a) Upper horizons of member 3 ("over-sill"), which are represented by a thin intercalation of mudstone and silicified siltstone with jarosite efflorescences, and overlying siliciclastic–carbonate sandstone and gritstone of the carbonate member in the key section (southwestern coast of the Tas-Ary Peninsula). The height of the range pole is 2 m. (b) Decomposed phosphatic concretions (whitish) in member 5 (southeastern coast of the Tas-Ary Peninsula). The photograph is 40 cm wide.

Member 3 ("Over-Sill")

The member does not crop out in cliff entirely. Southeast of the above fault, the maximum part of the unit is visible, but it contains numerous injections of underlying sandstone. The total thickness of visible fragments of this member reaches 11 m. It is represented by dark gray and black mudstone and siltstone, including bituminous sooty varieties. In some fragments of the member, these rocks are rhythmically interbedded with highly silicified, occasionally clayey siltstone 3–10 m thick (Fig. 18a). Rocks are often rusty and yellow owing to a coating of iron hydroxide and jarosite. At 1.5–1 m below the top, there are horizons with spherical and flattened phosphatic (?) concretions. Similar concretions were also found down the section in other sequence fragments. Both concretions and host rocks contain radiolarians and a few sponge spicules, as well as dispersed pyrite.

Member 4 (Carbonate)

Rocks of this interval of the section are partially exposed along the Quaternary fault zone and turn into tectonic breccia. The bottom of the member is the best preserved (unit 1); in addition, a fresh gully uncovered the top of the section (unit 4 top–unit 6) in 2009. These intervals are described more thoroughly.

Unit 1 (sandstone; 4 m in thickness). It is composed of gradational layers (up to 1.3 m) of siliciclastic–carbonate sandstone and gritstone separated by thin mudstone interlayers (Fig. 19a). The rocks demonstrate horizontal lamination, dish structures, and convolute lamination. Along the strike, individual beds often split into several ones (Fig. 18a), which is indicative of a partial amalgamation; the boundaries between them are sometimes uneven, and thicknesses vary. The ratio of carbonate and siliciclastic material is not constant: some rocks contain a maximum 30% of siliciclastics and some rocks are dominated by it. It is represented mainly by quartz and chert; plagioclase grains are rare. Clastic rocks are poorly sorted (ESM_1 fig. S4e, S4f). Siliceous cement developed at the bottom of the unit; some rocks contain calcite cement (locally). Sandstone and gritstone contain lithoclasts of limestone, mudstone, carbonate and quartz siltstone with a fine-grained carbonate matrix, and volcanic rocks; bioclasts (fragments of bryozoans, brachiopod shells, crinoids, etc.); phosphate grains; pyrite; and secondary Fe-carbonate. Thick gravelly sandstone in the middle part of the unit contains many peloids and micritized bioclasts. The listed sedimentological and lithological characteristics of the rocks in unit 1 allow us to interpret them as turbidites.

Unit 2 (with bioclastic limestone; 17–18 m in thickness). It is a muddy, intensely fractured, boudinaged interval, again dominated by massive carbonate rocks. They are represented by bioclastic sandy limestones (contain up to 15% of silicate silt and sand), extremely poorly sorted siliciclastic–carbonate diamictites (contain a material from clay to gravel), and mainly carbonate and mixed sandstones and siltstones. Where it is possible to trace the layers, they have a thickness from a few decimeters to 1 m. Normal grading and horizontal lamination can be seen in some beds, as in the underlying unit. Fissile clayey limestones and mudstones are also present in the section. Chert and phosphatic concretions were also observed. The base of the unit is composed of a single (?) thick (2 m) layer of fine- and medium-grained carbonate–siliciclastic sandstone with large bioclasts and fragments resembling felsic and intermediate volcanic rocks. Bioclastic limestone (0.6 m) occurs at the top of the unit. The total thickness of the unit was estimated using a panoramic photograph.

Unit 3 (about 2 m in thickness). Interbedding of calcareous shale and clayey fine-grained limestone.

The rocks are greenish black in the lower half of the unit and black above. The unit is poorly exposed. It is seen under a microscope that limestones at the bottom of the unit are bioclastic wackestones; the top is also composed of fine-grained rocks, but with a significant content of carbonate and siliciclastic silt, fissile, with organic matter along the cracks and without bioclasts.

Unit 4 (with conglomerate-like limestone; about 4 m in thickness). Rocks are similar to those of unit 2. A distinctive feature of unit 4 is conglomerate-like limestones, i.e., the rocks which are similar to diamictites down the section, but containing clayey–carbonate pebbles up to a few centimeters in size, showing greater contrast in size between grains and the matrix and including rare, chaotically oriented shells of large brachiopods. The matrix is represented by fine-grained carbonate and silty grains, while sand is scarce. This rock makes up, in particular, the lower part (0.75 m) of a thick rhythm in the middle of the unit (Fig. 19b, layer 1a). A lenticular bed at the top of the unit (0.35–0.5 m) (Fig. 19b, layer 2) demonstrates a gradual transition from coarse-grained bioclastic grainstone (base of the bed) with an admixture of fine siliciclastics to carbonate–silicate (50 : 50) sandy siltstone (top of the bed) with horizontal lamination. Siltstone is overlain along the sharp boundary by fissile limy mudstone (0.1–0.3 m).

Unit 5 is represented by a single rhythm 1.7 m thick. Its lower part (1.2 m) is composed of bioclastic gritstone–diamictite with rare carbonate pebbles. It is overlain by siliciclastic–carbonate sandstone (0.5 m) with a clear normal grading and horizontal lamination. Cross-lamination can be noted at its top. The transition from gritstone to sandstone is rough (Fig. 19b).

Unit 6 (2 m in thickness). Interbedding of detrital siliciclastic–carbonate rocks (1–50 cm) and dark calcareous shale–clayey limestones. The latter form about half the thickness of this unit. Its composition is shown in Fig. 19b.

Unit 7 (about 5.5 m in thickness). It is composed of pale greenish (prevailing) and dark gray-brown fine-grained clayey–silty limestone. The base consists of a diamictite layer (0.1 m) with large clasts, which gradually passes into fine-grained sandstone up the section. Small brachiopod shells were found in the upper part.

The total thickness of the carbonate member is 38 m.

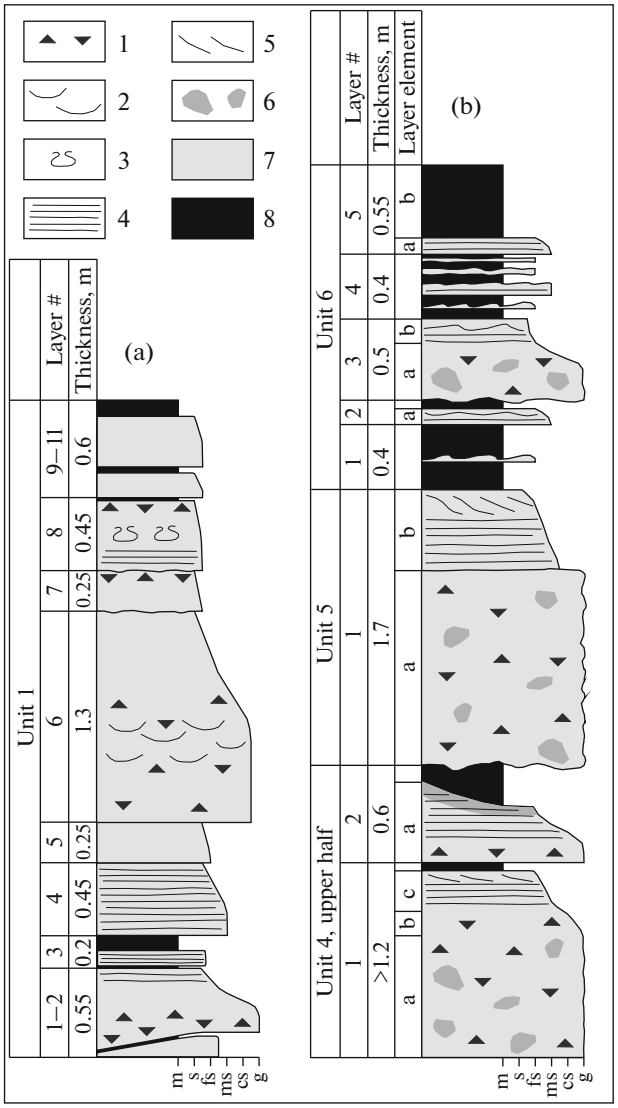

Fig. 19. Lithological columns (a) for unit 1 and (b) for the upper half of unit 4–unit 6 of the carbonate member of the Bel'kov Formation. (*1*) Frequent gravel-sized bioclasts; (*2*) dish structures; (*3*) convolute lamination; (*4*) horizontal lamination; (*5*) cross-lamination; (*6*) pebble of clay–carbonate rocks; (*7*) siliciclastic–carbonate rocks (gritstone, sandstone, and silty sandstone); (*8*) shale and highly clay limestone. The granulometric scale designations under the columns: (m) mudstone, (s) siltstone, (fs) fine-grained sandstone, (ms) medium-grained sandstone, (cs) coarse-grained sandstone, (g) gritstone.

Member 5 (Clayey Cherty–Phosphatic)

Nearly the entire section of the member is exposed on the dirty slope probably oriented approximately along the fault zone. The layering in this part of the cliff is not visible, and beds are identifiable only in unit 4 (see below). Most rocks are ground and crushed, contain multi-oriented blocks, and only a few fragments of the section maintain a normal stratification.

Unit 1 (4 m in thickness). It is composed mainly of black and brown mudstone and sandy mudstone. At the lower larger part of the unit, the rocks are mostly nonfissile and unexpectedly hard and contain phosphatic concretions. Reddish layered mudstones and siltstones lie at upper part of the unit. The latter are bituminous, with numerous sponge spicules and local siliceous cement. At the top, there are bitumen-saturated varieties which are not crushed with a hammer due to their rubber-like consistence. There are also cherty varieties that are split into small cubes.

Unit 2 (about 4 m in thickness). Deep black disintegrated carbonaceous shale with spherical phosphatic

concretions (Fig. 18b) separated every 0.2–1 m by sets (0.5–1.5 m) of rusty harder rocks (silty mudstone and sandy slightly clayey silicified siltstone). There are approximately three such rhythms. The thicknesses change greatly because of faults. Clayey rocks in the outcrop are light yellow owing to jarosite. Radiolarians and pores filled by bitumen can be seen in concretions in thin sections. Hard mudstones and siltstones are also bituminous. Some siltstones are dominated by angular grains; in addition to quartz and rare cherts, these rocks contain a considerable amount of plagioclase.

Unit 3 (7 m in thickness). Gray and dark gray siltstone and mudstone. The base comprises silicified siltstone with secondary (?) dolomite. Above, the rocks are platy, with filamentous sandy interlayers. A normal grading is occasionally visible in siltstone.

Unit 4 (5.5–6 m in thickness). It is composed of nonfissile (massive) silicified siltstones, as in the lower part of the underlying unit. They are light greenish and pinkish on the fresh cut and rusty from outside. In the lower part of the unit, the rocks are homogeneous, almost devoid of lamination; in the upper part, lamination is more distinct, and some flagginess appears.

Unit 5 (about 10 m in thickness). Ash gray homogeneous siltstones and mudstones are exposed beyond the fault zone. They are slightly fissile and, as a rule, indistinctly laminated on the fresh cut; siltstone is occasionally marked by filamentary sand interlayers and rare horizons of black mudstone. In the upper part of the unit, rocks are poorly sorted; thin silty sandstone interlayers containing numerous plagioclase grains as well as basalt and microcline fragments occur. The rocks are locally bioturbated. The unit is exposed mostly in the scree.

The total thickness of the clayey member is estimated at 31 m.

Member 6 (the First Sandstone Member)

The member is dominated by siliciclastic sandstones. The lower contact is exposed badly and is interrupted by a fault, but its amplitude is low. Rocks of this member are brecciated and exposed in the muddy cliff, and sedimentary features are not always visible. The bottom of the section was observed in the strippings and in the blocks which fell from the higher part of the slope. The whole section is composed of similar rocks, and their general description is given below. Two assemblage types can be identified: (1) a rhythmic alternation of sandstones (layers have a thickness from a few decimeters to 1 m) and thin interbedding intervals of sandstones and shales; (2) thick (a few meters) layers of amalgamated sandstone (Figs. 20a, 20b; ESM_4 file in Supp. Data). Individual sandstone beds from assemblage 1 are characterized by the following set of structures. Their lower part is composed of homogeneous unstratified sandstone, while the upper part is marked by a horizontal, rarer, cross-lamination with a more or less gradual transition to a clayey uppermost part of the rhythm (Fig. 20b). Mudstone clasts (rip-up) are present at different levels in sandstones; they were formed due to erosion of underlying clayey rocks (Fig. 2e); bottom marks are locally developed. Sandstones are poorly sorted, consist mainly of quartz and plagioclase, and contain numerous fragments of volcanic rocks (basic rocks are confidently identified), as well as cherts, phosphate fragments, muscovite, and microcline. Some layers contain many carbonate grains. Grains range in size from fine silt to coarse sand (ESM_1 fig. S4g, S4h). We interpret such sandstones as turbiditic.

Thinly bedded intervals separating thick sandstone layers in assemblage 1 also contain thin, often lenticular, sandstone interlayers deposited by along-slope bottom currents (Fig. 20d). They are commonly finer grained in relation to those considered above. We assume that these currents deposited the material transported by waning turbidity flows. Bioturbation observed in some horizons is indicative of quiet periods characterized by colonization of the sea floor.

Assemblage 2 is represented by two separate layers 4.5 and 9.0 m thick (Fig. 20c) located in the lower and middle parts of the section. They are composed of dark gray sandstone, which is similar to the assemblage 1 sandstones, but contains up to 30% of clay in the matrix. In the outcrop, both layers seem unstratified homogeneous, irregularly fractured. At closer examination, clay prominences, folded fragments of a layered succession, and ball-and-pillow sandstone structures can be observed (Fig. 20f). Thus, the assemblage 2 rocks result from mixing and incomplete

Fig. 20. Rocks of the first sandstone member of the Bel'kov Formation (member 6). (a) Fragment of this member exposed in the cliff of the southwestern coast of the Tas-Ary Peninsula. A thick layer in the middle part of the cliff is nine-meter diamictic sandstone (see the text). The height of the range pole (circled) is 2.5 m. (b) Detail of the section showing the transition from massive sandstone in the lower part of the turbidite rhythm to laminated sandstone of the upper part (left side of the photo). In the right part of the photo, the laminated element of this rhythm is fissile, and the upper boundary of the massive part of the considered rhythm seems sharp. Such a situation is typical of the rocks in this member. This photo shows that the massive part of the rhythm actually consists of two individual, partially amalgamated sandstone layers separated by a wavy clayey surface. One division of the range pole is 10 cm in length. (c) Schematic lithological column of member 6 (see the text); sandstone is shown with dotted pattern; shale and intervals of thin intercalation of sandstone and shale are indicated in black. (d) Fragment of the thin sandstone–shale alternation package separating thick beds of turbidite sandstones. Sandy horizons in this package were also deposited by currents, likely both contour and turbidity. Current ripples can be seen at the top of the photo image. Photograph is 20 cm wide. (e) Rip-up clasts in sandstone; (f) structures of chaotic mixing of the material due to subaqueous slumping in a 4.5-m (Fig. 20c) sandstone layer; photograph is about 1 m high.

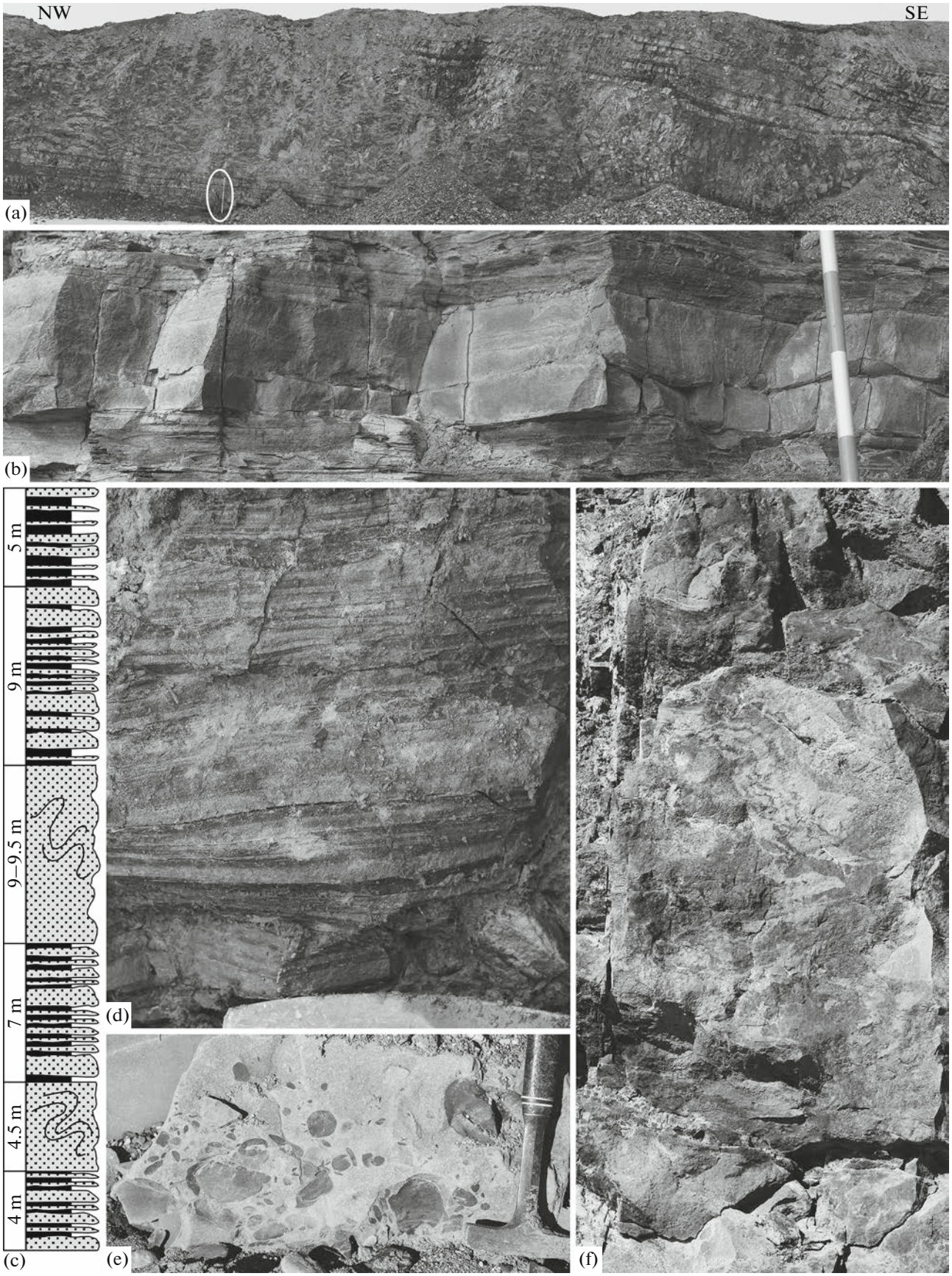
NW
SE
(a)
(b)
5 m
9 m
9–9.5 m
7 m
4.5 m
4 m
(c)
(d)
(e)
(f)

Fig. 21. Trace fossils, which are similar to the ichnogenus *Hillichnus*, in the deposits of member 7 of the Bel'kov Formation. The photo shows a boundary between two rhythms with normal grading from light-colored laminated sandstone to dark-colored mudstone.

homogenization of some levels of a stratified section which slid down the slope.

In the upper part of the member, individual beds of massive sandstone are separated by relatively thick thin-bedded intervals (up to 0.5 m, possibly more), similar to that shown in Fig. 20d. Plant debris occurs on the bedding planes. The boundary with the overlying member is drawn along the top of the last noticeable layer of laminated sandstone. Although this layer (and a number of similar ones) looks massive and stands out in the section, it is also composed of thin sandy–clayey alternation, but enriched in a sand fraction.

The thickness of the sandstone member is estimated at 39 m.

Member 7 (with "Fucoids")

As well as three underlying members, the rocks of this interval in large areas represent a tectonic breccia confined to the along-slope normal faults. In addition, they rarely form rocky outcrops, but are exposed on a muddy slope. For this reason, it was not possible to make a layer-by-layer description of this member. In general, it is composed of dark siltstone and mudstone with interbeds of light-colored fine-grained sandstone, petrographically similar to sandstones of member 6. The thickness of such interbeds is measured in centimeters. They often show a sharp base and a graded top. In addition, sole marks, horizontal and cross-lamination, and current ripples were noted. The rocks of the member are bioturbated. It seems that mudstone and siltstone prevail at the section top, while the lower part is dominated by sandstone and siltstone. Some intervals of the section have a rhythmic architecture. The observed sedimentary structures make it possible to interpret sandy interbeds as a result of bottom currents, presumably contoured. Beds with normal grading can be distal turbidites. Approximately 10 m above the base, there are two layers of a specific rock with characteristic structures referred to in the field as "fucoids" (Fig. 21). We found similar layers in the Bel'kov Formation on Bel'kov Island, as well as in the Permian deposits in the well AH-2 (Southeastern Taimyr), and nowhere else. The described structures are interesting formations which are similar in their form to plants or algae. They resemble rare *Hillichnus* ichnofossils which are described in the deep-sea Palaeocene deposits of California and in some other sections and are considered as traces of deposit-feeding bivalves (Bromley et al., 2003; Clifton, 2013).

The tops of the SW cliff section on the peninsula are composed of black and dark gray mudstone and siltstone with rare sideritic concretions (up to 15 cm). To the south, the rocks are changed to clay in the weathering crust and contain rare spherical phosphatic concretions in the visible top of the section. The apparent thickness of member 7 in this outcrop is about 30 m.

The higher horizons of the Bel'kov Formation crop out only at the southeastern end of the Tas-Ary Peninsula, in the opposite limb of the syncline (Fig. 3). Exposures are fragmentary there; the rocks are altered in the Tertiary weathering crust and often differ in outer appearance from those observed in the cliff of the southwestern coast. This fact complicates correlation and thickness calculation. The total thickness of the rocks attributed in this outcrop to member 7 was estimated graphically at least as 60 m; this estimation is approximal due to above-mentioned reasons. Meanwhile, some sedimentary features are better seen there (Fig. 22). On the southeastern coast, the upper third of the member is composed of leafy black mudstones, sometimes unevenly colored (stripes) owing to jarosite and limonite, with rare large siderite concretions (Fig. 23a). The same rocks sporadically occur down the section of member 7 in this outcrop.

Fig. 22. Sedimentary structures visible only in a wave-polished block (under water). Intense bioturbation, cross-lamination in sandy lenses, and syndepositional microfaults caused by irregular sediment compaction can be seen. Similar structures are typical also of the Bel'kov Formation on Bel'kov Island. Photograph is 25 cm high.

Member 8 (the Second Sandstone Member)

It is composed of rhythmically interbedded gray calcareous-free turbidite sandstones (Fig. 23b) and dark gray shale changing into sets of fine sandy–clayey alternation. The thickness of the sandstone layers is up to 1 m, while the thickness of mudstones and interbedding sets is up to 20 cm, rarely up to 0.5 m. Sandstones are similar to rocks of member 6, but often contain iron hydroxides as lumps, spots, and gouges in the cracks (visible in thin sections), sometimes, brownish carbonate (siderite (?)). Some varieties contain a black bituminous (?) cement. Mudstone clasts (rip-up) are present. The member is 15 m in thickness.

Member 9

The member is exposed in the syncline core on the southeastern coast of the Tas-Ary Peninsula. It is composed of monotonous dark gray mudstones, including silty varieties, with sideritic concretions and gray siltstone interlayers (up to 0.5 m). Radiolarians can be seen in thin sections of concretions. The apparent thickness is 70 m.

BIOSTRATIGRAPHY AND BIOGEOGRAPHY

Macrofauna (brachiopods and corals) was found in the studied section at many levels of the Tas-Ary Formation and in the lower part of the Bel'kov Formation; conodonts were identified in twelve samples; foraminifera from the first and fourth Bel'kov members were studied. The position of fossil samples in the section is shown in Figs. 4 and 14; their locality on map, in the ESM_5 file in Supp. Data. The list of fauna determinations for all samples is also reported in the Supplementary Data (file ESM_6), as well as the distribution of fossil assemblages in the section (file ESM_7).

Brachiopods

In the Upper Palaeozoic section of the Tas-Ary Peninsula, the most representative brachiopod assem-

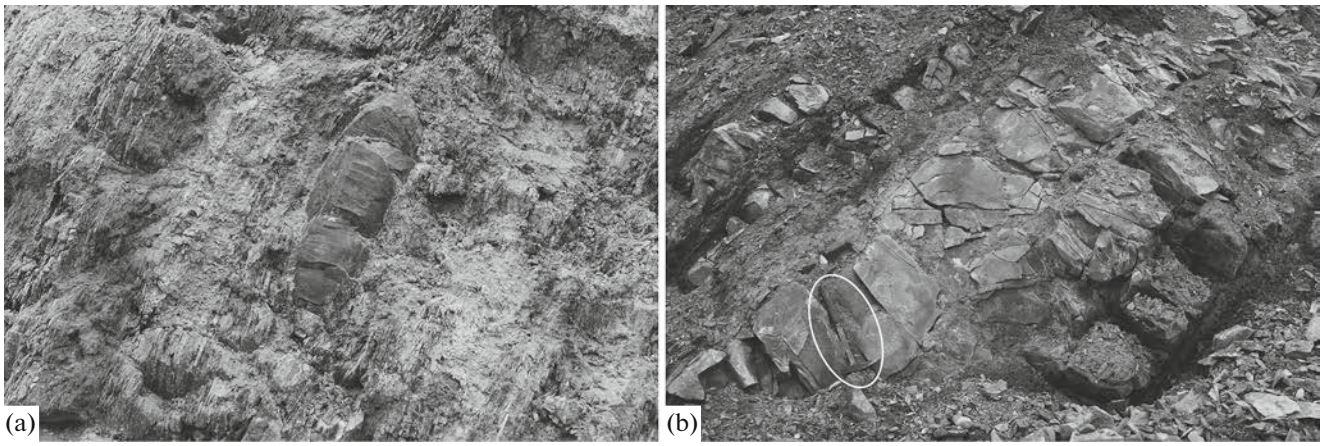

Fig. 23. Rocks in the upper visible part of the Bel'kov Formation exposed on the Tas-Ary Peninsula. (a) Siderite concretion in fissile shales in the upper part of member 7 (photograph is 40 cm wide); (b) rocks of the second sandstone member. A hammer is circled.

blages characterize the Tas-Ary Formation (Plate I; Plate II, figs. 9–11; Plate III, figs. 1–3, 5, 6). In the lower part of Bel'kov Formation, brachiopod association is not rich in either the number of specimens or the systematic composition (Plate II, figs. 2, 3, 5–8; Plate III, fig. 4).

In the Tas-Ary Formation, the first few remains of the shells were found only at a distance of 240–260 m from its base (unit 7), and they are represented by the forms which are characteristic in general of the Early Carboniferous. In addition to unidentified shell imprints and cores, they include *Unispirifer* cf. *teodorovichi* (Fotieva), *Un.* aff. *pesasica* (Tolmatschow), and *Torynifer* cf. *cooperensis* (Swallow). The first rather numerous forms which are similar to the characteristic Tournaisian forms include *Syringothyris* aff. *hannibalensis* (Swallow) and *Unispirifer taidonensis* (Tolmatschow) and occur 40 m higher (unit 9).

The most numerous and richest taxonomic assemblage is characteristic of units 12–14 (Plate I; Plate II, figs. 9–11; Plate III, figs. 1–3, 5, 6). The following forms were determined: *Leptaenella* sp. indet., *Rhipidomella altaica* (Tolmatschow), *Rh.* aff. *kusbassica* Besnosova, *Schellwienella* sp., *Tolmatchoffia* cf. *robusta* (Tolmatschow), *Marginatia deruptoides* Sarytscheva, *M.* aff. *deruptoides*, *M. burlingtonensis* (Hall), *Tomiproductus elegantulus* Sarytcheva, *T. fomikhensis* Sarytcheva, *Setigerites newtonensis* (Moore), *Syringothyris scinderi* Sokolskaja, *Palaeochoristites cinctus desinuatus* (Lissitzyn), *P.* sp. nov. no. 1, *P.* sp. nov. no. 2, *Unispirifer duchovae* (Besnosova), *Eomartiniopsis elongata* Sokolskaja, and *Lamellosathyris* aff. *lamellosa* (Leveillé). The listed forms belong to nine families and twelve genera. In general, it is a rich and diverse assemblage which characterizes the normal marine shelf facies. This assemblage is distinguished by semireticulate productids represented by the genera *Marginatia*, *Tolmatchoffia*, and *Tomiproductus* and also spiriferids such as *Unispirifer* and especially numerous large shells of *Palaechoristites*. Some layers are enriched in representatives of the genera *Rhipidomella* and *Lamellosathyris*. The considered complex is relatively typical of the upper Tournaisian.

The brachiopod association at the top of the next unit 15 differs from the previous one in generic composition. It includes *Rhipidomella* sp. indet., numerous *Stegacanthia pustuloides* (Nalivkin), and also *Tolmatchoffia robusta*, *Marginatia burlingtonensis*, *Tomiproductus* sp., *Krotovia* aff. *spinulosa* (Sowerby), *Setigerites* cf. *setigerus* (Hall), and *Mucrospirifer roemerianus* (Koninck). Only three genera, i.e., *Tolmatchoffia*, *Marginatia*, and *Tomiproductus*, relate this complex to the previous one. A complete disappearance of *Palaechoristites* representatives is noteworthy. Meanwhile, it includes *Stegacanthia* and also genera *Krotovia*, *Setigerites*, *Mucrospirifer*, which were absent earlier. Despite these differences, the host deposits apparently also belong to the upper Tournaisian, which is indicated, first of all, by representatives of the genera *Tomiproductus*, *Setigerites*, and *Mucrospirifer*, characteristic of the Tournaisian Stage of Siberia, Kuzbass, and North America.

When describing the Tournaisian brachiopod assemblage of the Tas-Ary Formation in general, it should be taken into account that the biogeography of the Tournaisian Age, especially of its second half related to the wide late Tournaisian transgression, is poorly differentiated. The observed differences in the regional Tournaisian assemblages are related not so much to their biogeography as to biofacial features. In general, the Tournaisian brachiopods are essentially cosmopolitan. The forms and especially the dominants of the considered assemblage represented in units 12–15 of the Tas-Ary Formation are indicative of the fact that it is analogous to the assemblages in the Kizelian Regional Substage of the Urals, the Chernyshinskian Regional Substage of the Moscow Syneclise, the Nizhnetersinskian Regional Substage of Kuzbass, and in the upper Tournaisian of the Omolon Block (Sarycheva and Sokolskaya, 1952; Sarycheva et al., 1963; Nalivkin, 1979). In Taimyr, age analogs of units 12–15 of the Tas-Ary Formation are likely represented in the Binjudinskian Regional Substage, although the assemblage of the latter is poorer than the Tas-Ary one (Tschernjak et al., 1972); in particular, it does not contain the characteristic *Tolmatchoffia* and *Palaechoristites*. Meanwhile, these faunas are similar owing to the presence of representatives of the typical late Tournaisian genera such as *Setigerites*, *Tomiproductus*, *Marginatia*, and *Unispirifer* and the absence of large high-arheic *Syringothyris*, which are characteristic of the Tournaisian of America, Kuzbass, and the Urals.

A major part of the 110-m unit 17 is devoid of fauna. Only its middle part contains a few *Camaratoechia* sp. shell imprints, which are too negligible to determine the rock age. A few fossils near the top of the unit are more informative. *Brachythyris* sp. indet.? and *Grandispirifer subgrandis* (Rotai) were identified there (Plate III, fig. 7). The genus *Grandispirifer* was first described in the Visean deposits of China. In the

Plate I. Brachiopods from the Carboniferous deposits of Kotel'ny Island, Tas-Ary section. Collection kt-014 is kept at the Geological Institute, Russian Academy of Sciences. Abbreviation: (u.) unit. All images are full-size. (1) *Pustula pilosa* Thomas, 1914, Sample 763/4, specimen k-27, fragment of shell with articulated valves, Tas-Ary Formation, u. 13, upper Tournaisian substage; (2, 3) *Tolmatchoffia robusta* (Tolmatchow, 1924): (2a–2c) Sample 592/1, specimen k-20, ventral valve in three positions, Tas-Ary Formation, u. 15, (*3*) Sample 763/5, specimen k-22, external print of dorsal valve, same place, u. 12, the same age; (4a, 4b) *Setigerites newtonensis* (Moore, 1928), Sample 764/6, specimen k-30, ventral valve in two positions, Tas-Ary Formation, u. 14, upper Tournaisian substage; (5, 6) *Tomiproductus fomikensis* Sarytcheva, 1963, Tas-Ary Formation, u. 13, upper Tournaisian substage: (5a–5c) Sample 763/4, specimen k-23, ventral valve in different positions; (6) Sample 763/4, specimen k-24, ventral valve.

Plate I

Northeast of Russia and in Kuzbass, *G. subgrandis* can be found in both the upper Tournaisian and the lower Visean.

Macrofauna was not found in the overlying part of the section with a thickness of 320 m (taking into account the unexposed interval). Unit 20 is a last level in the Tas-Ary Formation where identifiable brachiopod remains were found (Plate II, fig. 1). It contains the following assemblage: *Avonia* sp. indet., *Stegacanthia* cf. *sibirica* Sarytcheva, *Tolmatchoffia* sp. indet., *Tomiproductus* sp. nov., *Antiquatonia ustyensis* (Sarytcheva), *Punctospirifer* sp. indet., *Unispirifer similis* (Tolmatschow), *Spirifer* aff. *parabisulcatus* Semichatova, *Torynifer* cf. *pseudolineatus* (Hall), and *Eomartiniopsis* aff. *maximovae* Besnosova. Except for antiquatonias, other fossils in the unit are poorly preserved. Nevertheless, the occurrence of *Antiquatonia*, *Punctospirifer*, and *Spirifer* ex gr. *parabisulcatus*, which are characteristic representatives of the Visean–Serpukhovian deposits of the Moscow Syneclise and other regions, together with relics of the Tournaisian forms such as *Tomiproductus* and *Unispirifer*, is indicative of the Visean age of the host deposits.

In the Bel'kov Formation base (member 1) only two brachiopod specimens were found—a fragmented shell with articulated valves belonging to the subfamily Gigantoproductinae, genus *Beleutella* (Plate II, fig. 4), and a ventral valve of the genus (?) *Sajakella*. The genus *Beleutella* was first described in the Serpukhovian deposits of Kazakhstan (Litvinovich, 1967). In the Moscow Syneclise, as well as in Taimyr, Gigantoproductinae are distributed almost throughout the interval of the Visean and Serpukhovian stages. The genus *Sajakella* was also described for the first time in the Carboniferous deposits of Kazakhstan. In the Northeast and Taimyr sections, representatives of this genus are widespread, but commonly above the Gigantoproductinae layers, in the Serpukhovian–lower Bashkirian interval. Owing to a limited amount of material, a more accurate determination of the age of the host deposits than the Visean–Serpukhovian is impossible. No fauna was found in the second and third members of the Bel'kov Formation.

The brachiopod association—relatively numerous, quite characteristic of and endemic to Eastern Siberia, in particular, Taimyr—was identified in member 4 and the lowermost part of member 5 (Plate II, figs. 2, 3, 5–8; Plate III, fig. 4). Collections of 2009 and 2014 include the following fossil assemblage: *Chonetes ischimicus kusbassicus* Sokolskaja, *Paeckelmannia* sp., *Stegacanthia sibirica artyshtensis* (Sarytsceva), *Calliprotonia taimyrensis* (Einor), *Eomarginifera librovitchi* (Alexandrow), (?) *Kutorginella* cf. *stepanovi* Abramov et Grigorieva, (?) *Praehorridonia* sp. indet., (?) *Antiquatonia* sp. indet., *Brachythyris* aff. *atbasarica* Nalivkin, *Spirifer* cf. *bisulcatus* Sowerby, *Spirifer engelgardthi* Tschernjak, *Spirifer* (?) cf. *pseudotrigonalis* Semikhatova, *Spirifer attenuatiformis* A. Ivanov et E. Ivanova, and *Camerisma* sp. This association is present in the brachiopod assemblages of the Magar Regional Substage of the Kolyma–Omolon region, the Tiksi Formation and its Verkhoyansk analogs, and the Nizhnemakarian (Kholodninskian) Regional Substage of Taimyr (Ustritskii and Tschernjak, 1963; *Stratigrafiya...*, 1970; Ganelin and Tschernjak, 1996). The Magar brachiopod assemblage characterizes a significant age interval from the end of the Late Visean to the first half of the Bashkirian. Insufficient data on the stratigraphy of this interval within the whole of Eastern Siberia occasionally complicate a more detailed identification of its individual divisions. As for the considered assemblage from the Bel'kov Formation, its forms such as *Chonetes ischimicus kusbassicus*, *Stegacanthia sibirica artyshtensis*, *Calliprotonia taimyrensis*, *Inflatia taraiaensis* (Einor), *Spirifer* cf. *bisulcatus*, *S.* cf. *pseudotrigonalis*, and *S. attenuatiformis* are more typical of the Visean part of the Magar interval. Along with that, we should note the occurrence of the forms such as (?) *Kutorginella* cf. *stepanovi*, (?) *Praehorridonia* sp. indet., and *Spirifer engelgardthi* Tschernjak which are characteristic of higher parts of the Magar interval, which allows us to suggest a possible belonging of the host deposits to the Serpukhovian Stage.

Corals

The location of rugose corals on the Tas-Ary Peninsula was known for a long time. During the geological survey in 1970, Yu.G. Rogozov made the collection of Tournaisian–Visean rugose corals, the layer-by-layer definitions of which were published in the Explanatory Note to the State Geological Map 1 : 1000000 and subsequent editions (*Gosudarstven-*

Plate II. Brachiopods from the Carboniferous deposits of the Kotel'ny Island, Tas-Ary section. Collection kt-014 is kept at the Geological Institute, Russian Academy of Sciences. Abbreviations: (u.) unit, (m.) member. All images, unless otherwise stated, are full-size. (1a–1c) *Antiquatonia ustyensis* Sarytcheva, 1949, Sample 770/5, specimen k-39, ventral valve in three positions, Tas-Ary Formation, u. 20, Visean Stage; (2a–2c) *Inflatia taraiensis* (Einor, 1939), Sample 688/10, specimen k-39, ventral valve in different positions, Bel'kov Formation, m. 4, (?) Serpukhovian Stage; (3) *Praehorridonia* sp. indet (?), Sample 688/10, specimen k-41, ×1.5, ventral valve with a partially preserved thick shell layer, Bel'kov Formation, m. 4, (?) Serpukhovian Stage; (*4*) *Beleutella tulensis* (Bolkhovitinova, 1938), Sample 766/9, specimen k-42, fragment of ventral valve, Bel'kov Formation, m. 1, Visean–Serpukhovian; (5–7) *Kutorginella* cf. *stepanovi* Abramov et Grigorieva, 1983: (5a–5c) Sample 771/7, specimen k-43, ventral valve in different positions, Bel'kov Formation, m. 4, (?) Serpukhovian Stage; (6) Sample 771/7, specimen k-44; (7) Sample 771/7, specimen k-45: imprints of external surface of dorsal valves, the same location and age; (8–10) *Palaechoristites* sp. nov. no. 1: (8a–8c) Sample 763/4, specimen k-49, ventral valve in different positions, Tas-Ary Formation, u. 13, upper Tournaisian substage, (9) Sample 763/4, specimen k-50, (10) Sample 84/9, specimen k-48: ventral valves, Tas-Ary Formation, u. 14, the same age.

Plate II

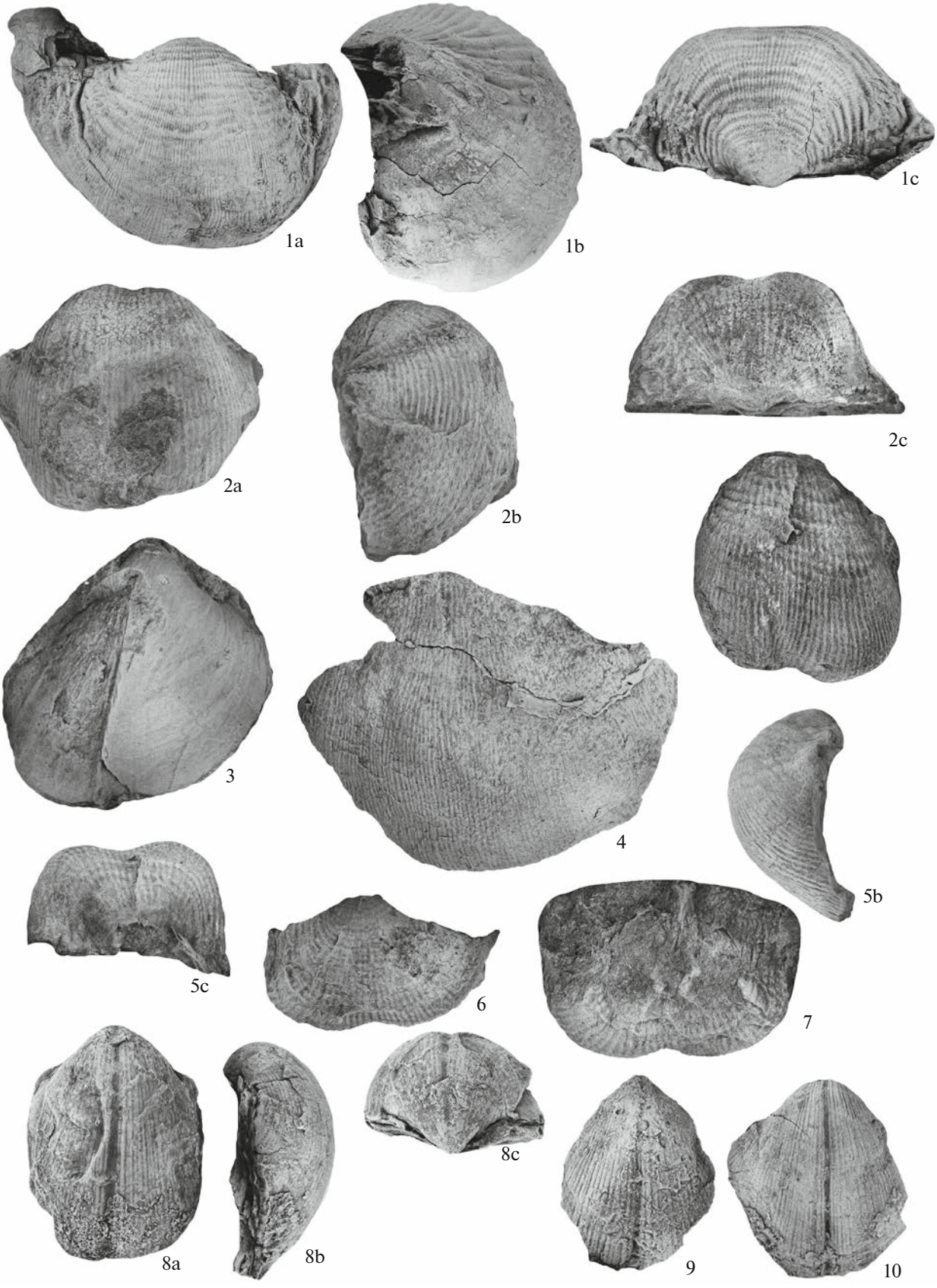

naya..., 1999, pp. 28–31). The Tournaisian species included *Cyathoclisia tabernaculum* Dingwall, *Sychnoelasma* ex gr. *konincki* (Milne–Edwards et Haime), *S. urbanowitschi* (Stuckenberg), *Enniskillenia enniskilleni* (Milne–Edwards et Haime), and *Thysanophyllum* ex gr. *acystosum* Rogozov; the latter species was initially described in the Falabigayan Regional Substage of Taimyr. In Taimyr, this species was found at the top of the section, which, according to a jointly occurring assemblage of foraminifera, belongs to the Serpukhovian (Rogozov, 1972; Tschernjak et al., 1972). Corals of Taimyr, as well as in the Tas-Ary assemblage, include the taxa which were first identified in the Mississippian of Canada (Sutherland, 1958). Despite a significant number of publications, most of which belong to the 1970s, the Tournaisian corals remain almost unknown. Coral collections from the Tournaisian–Visean deposits of the Kyrgyz steppe (Gorskii, 1932) and the Southern Urals (Voinovskii–Kriger, 1934) were described in the 1930s. Some of these collections are currently being reconsidered (Fedorowski and Kullmann, 2013; Fedorowski, 2017).

Description of the Collection

The author's collection of corals originates from the Tas-Ary Formation consists of about 50 specimens. The material is represented only by solitary forms, except for two locations of syringoporids (units 7 and 20) and one level with colonial rugose at the top of the section (unit 21). Rugose corals are dominated by forms without dissepiments, i.e., a "Cyathaxonia fauna" (Hill, 1938) which is characteristic mainly of rather deep (cold-water) sedimentation settings. Numerous findings of this fauna are confined to calcareous shales in units 9 and 13. A feature is the high species diversity with a limited number of specimens of each species. Corals with dissepiments, typical representatives of a shallow biota, are quite rare. The collection includes some new taxa which were not previously described either in the Russian or in the foreign literature. The collection, especially its late Tournaisian part, is dominated by genera which are widespread in the Urals and Western Europe, but some taxa are encountered in the Asian part of Russia (Kuznetsk basin, Omolon Block) and in Kazakhstan. An exception is the genus *Ekvasophyllum* Parks, known only from the Mississippian of North America. Three assemblages can be distinguished by variations in the taxonomic composition: (1) *Lophophyllum*–"*Zaphrentites*," (2) *Sychnoelasma*–*Uralinia*, and (3) *Amplexizaphentis*.

Analysis of Coral Assemblages

Assemblage 1. The unit 9 assemblage (Sample 758-24) includes about 25 specimens of largely small corals which were partially ascribed to new species and, occasionally, genera. The host deposits are dated to the second half of the early Touraisian (formerly, the middle substage of the Tournaisian Stage of Belgium, Hance et al., 2006; ESM_8 file in Supp. Data file) or to the late Tournaisian on the basis of the first appearance of representatives of the genus *Cyathoclisia* Dingwall known from the Cherepetian deposits of the Urals (Sayutina, 1973) and the interval of the genus *Lophophyllum* Milne–Edwards et Haime (Poty et al., 1991).

The stratigraphic position of the species *Ekvasophyllum* aff. *inclinatum* Parks (Plate IV, figs. 7, 8) was established presumably in the middle part of the Mississippian (upper Tournaisian–lower Visean) of northeastern British Columbia (Sutherland, 1958) and in the Tournaisian of the northwestern United States (Sando and Bamber, 1985). *Variaxon* sp. 1 (Plate V, fig. 11), similar to the species *V. radians* Fedorowski (upper Serpukhovian, Czech Republic) (Fedorowski, 2010), was also identified in unit 9. A single specimen of the species *Bifossularia* sp., characterized by the development of dissepiments, was found in unit 9. The genus is distributed in the Kuznetsk basin, where its first representatives appear in the Taidonian Regional Substage of the lower (middle) Tournaisian and also in the Nizhnetersinskian and Pod'yakovian regional substages of the upper Tournaisian and lower Visean (Dobrolyubova et al., 1966). In the upper Tournaisian and lower Visean deposits, the genus is also mentioned in Belgium and France (Boland, 2002; Vuillemin, 1990).

Cyathoclisia (?) sp. (Plate IV, figs. 3–5) found at the same level is similar in its ontogenetic development and morphology to typical representatives of the genus *Cyathoclisia* Dingwall (Sayutina, 1973). The difference is in a more compact morphology of the axial structure. The first species appear in the Cherepetian Regional Substage in the upper part of the lower Tournaisian (according to the correlation by Menning et al., 2006); however, the maximum species diversity is characteristic of the second half of the Tournaisian. This genus is unknown in the Visean deposits (according to a new

Plate III. Brachiopods from the Carboniferous deposits of Kotel'ny Island, Tas-Ary section. Collection kt-014 is kept at the Geological Institute, Russian Academy of Sciences. Abbreviations: (u.) unit, (m.) member. All images, unless otherwise stated, are full-size. (1–3) *Palaechoristites cinctus* (Keyserling, 1846), Tas-Ary Formation, u. 14, upper Tournaisian substage: (1a–1c) Sample 764/6, specimen k-52, ventral valve in different positions; (2a, 2b) Sample 84/9, specimen k-46, ventral valve from two sides; (3) Sample 84/9, specimen k-47, ×1.2, fragment of ventral valve core, thick dental plates; (4) *Brachythyris* aff. *atbasarica* Nalivkin, 1937, Sample 688/10, specimen k-44, ×1.2, ventral valve, Bel'kov Formation, m. 4, (?) Serpukhovian Stage; (5a–5c) *Palaechoristites* sp. nov. no. 2, Sample 764/6, specimen k-53, ventral valve in different positions, Tas-Ary Formation, u. 14, upper Tournaisian substage; (6a, 6b) *Syringothyris scinderi* Sokolskaja, 1963, Sample 763/4, specimen k-55, ventral valve from two sides, Tas-Ary Formation, u. 13, upper Tournaisian substage; (7) *Grandispirifer subgrandis* (Rotai, 1938), Sample 755/2, specimen k-73, ×1.5, fragment of ventral valve, Tas-Ary Formation, u. 17, upper Tournaisian–lower Visean.

Plate III

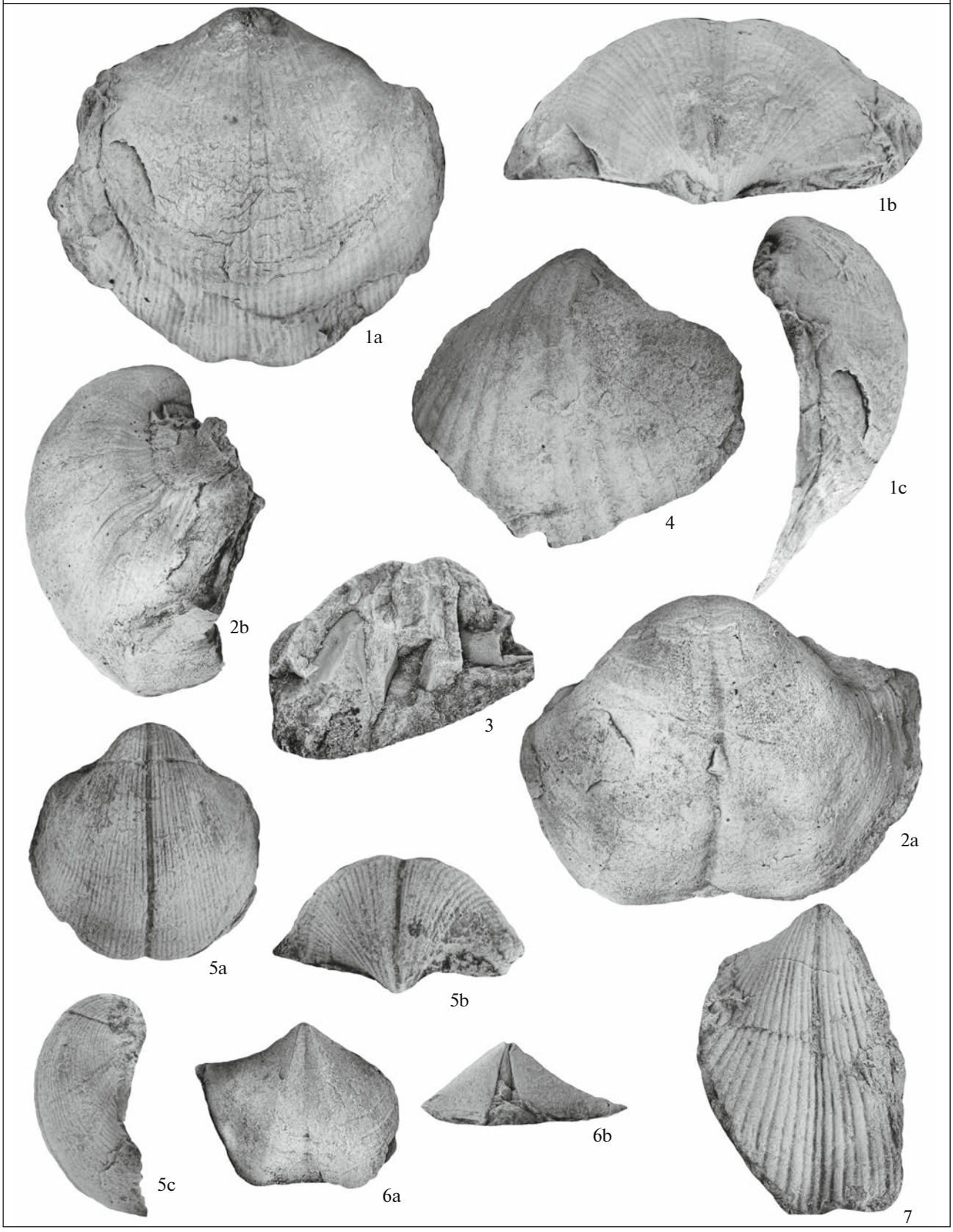

position of the lower boundary of the Visean in the International Stratigraphic Scale). Outside the Urals, the genus is distributed in Western Europe and is also described in the upper Tournaisian deposits of the Omolon Block (Shilo et al., 1984).

Lophophyllum sp. (Plate V, fig. 12) belongs to the genus *Lophophyllum* Milne–Edwards et Haime, which, apparently, was one of the most common taxa of the second half of the Tournaisian (Denayer et al., 2011). Its stratigraphic distribution is from the upper part of the lower Tournaisian (= parts of the middle Tournaisian of Belgium) to the lower part of the upper Tournaisian (Poty et al., 1991) at a three-member division of the stage. One of the species found in the Tournaisian deposits of the lower reaches of the Lena River was mistakenly identified by Ivanovskii (1967, pl. 2, fig. 3) as *Sychnoelasma* ex gr. *konincki* (Milne–Edwards et Haime). *Lophophyllum* sp. also occurred in the upper Tournaisian substage of the Rügen Island, the Baltic Sea (Weyer, 1993).

Eostrotion sp. (Plate V, fig. 6) belongs to the genus which can be found in the upper Tournaisian of Belgium. Earlier, forms with such a morphology were included in the species *Caninia cornucopiae* Michelin in Gervais (Denayer et al., 2011, pl. 3, figs. A–D). It is currently known only from the upper Tournaisian of Belgium and, perhaps, of England.

The specimen referred to Gen. et sp. nov. (aff. *Zaphrentites* Hudson, 1941) (Plate V, figs. 9, 10) differs in a trabiticular microstructure of septa from typical representatives of the genus. Corals of the genus *Zaphrentites* are common in the Tournaisian and Visean deposits and are characteristic of the Cyathaxonia fauna complex.

Assemblage 2. Different corals of various sizes were found at the top of unit 12 and in units 13 and 14 of the Tas-Ary Formation. It includes typical Late Tournaisian taxa (sometimes continued in the Visean Age), common throughout the basins of Europe and Asia. Nevertheless, the corals of assemblage 2 from the Tas-Ary section are also distinguished by a peculiar morphology. According to the fauna composition, the age of this assemblage can be estimated at the late Tournaisian. Its index species include *Uralinia* sp. aff. *gracilis* (Ludwig) and *Sychnoelasma* aff. *urbanowitschi* (Stuckenberg).

Sychnoelasma aff. *urbanowitschi* (Plate V, figs. 7, 8) was found at the top of unit 12. The species is distributed in the Kizelian and Kosvian regional substages of the Urals (upper Tournaisian substage), in the late Tournaisian deposits of Poland, in the Visean deposits of Novaya Zemlya, and in the lower substage of the Visean in England, Ireland, Belgium, France, and Donbass (Sayutina, 1976; Poty, 1981; Mitchell and Somerville, 1988). The stratigraphic range of the genus, in particular, the species *S. urbanowitschi* s.l., includes the upper part of the Tournaisian and the lower part of the Visean (Bobrikian Regional Substage). The taxonomy of this genus and its species should be revised.

In addition, the top of unit 12 contains *Variaxon* sp. 2 (Plate IV, figs. 11, 12). *V. radians* Fedorowski is the most similar to it. *Variaxon* sp. differs from this species (except for the age range) in a greater number of septa and a larger size. Today, the phylogenetic line of this genus which was found so far only in the Serpukhovian deposits remains uncertain (Fedorowski, 2010). Its possible origin from the Tournaisian corals, in particular, those described by Gorskii (1932) in the Kyrgyz steppe, is considered as a hypothesis (Fedorowski, 2017).

The species *Uralinia* sp. aff. *gracilis* (Ludwig) (Plate V, figs. 9, 10) was found at the top of unit 13. Typical specimens of *U. gracilis* were described in the Tournaisian deposits near the city of Kizel (Shtukenberg, 1895), but later were not restudied. The genus *Uralinia* Stuckenberg is widespread in the Tournaisian deposits of the Urals, Belgium, Omolon Block, Central Kazakhstan, etc. It is most characteristic of the second half of the Tournaisian (the Urals, Poland, and Germany).

The genus *Zaphrufimia* Fedorowski, to which the species *Zaphrufimia* (?) sp. 1 (Plate V, figs. 4, 5) of unit 13 belongs, was identified when studying the collection of Serpukhovian corals in Poland (Fedorowski, 2012). The typical species *Z. disjuncta* (Carruthers) was found in the upper Serpukhovian deposits of Scotland. Findings from more ancient intervals were not earlier indicated. The internal structure of the coral from the Tas-Ary Formation corresponds to the genus diagnosis.

The species *Keyserlingophyllum* sp. was identified in the same unit (Plate IV, figs. 1, 2). Its affiliation to the genus was determined by comparison of a range of successive sections of young stages and ontogenesis of the species *Keyserlingophyllum obliquum* (Keyserling) described in the upper Tournaisian deposits of the Northern Urals (Soshkina, 1960). The genus is char-

Plate IV. Rugosa corals from the Tournaisian deposits of the Tas-Ary Formation, Tas-Ary section, Kotel'ny Island. The collection is kept in the Chernyshev Central Research Exploration Museum. Abbreviation: (u.) unit. (1, 2) *Keyserlingophyllum* sp., Sample 762/7, specimen 762/7-1 (×3), successive cross sections, u. 13, upper Tournaisian substage; (3–5) *Cyathoclisia* sp., Sample 758/24, specimen ko-5, u. 9, upper part of the lower Tournaisian substage: (3) external form of coral (×3), (4, 5) successive cross sections (×10); (*6*) *Cyathoxonia* sp., Sample 763/3-1, specimen ko-25, cross section (×10), u. 14, upper Tournaisian substage; (7, 8) *Ekvasophyllum* sp. aff. *inclinatum* Parks, 1951, Sample 758/24, specimen ko-2, successive cross sections (×8), u. 9, upper part of the lower Tournaisian substage; (9, 10) Gen. et sp. nov. (aff. *Zaphrentites* Hudson, 1941), Sample 758/24, specimen ko-4, successive cross sections, u. 9, upper part of the lower Tournaisian substage: (9) (×12), (10) (×10); (11, 12) *Variaxon* sp. 2, Sample 762/11, specimen 762-11-1, successive cross sections, u. 12, roof, upper Tournaisian substage: (11) (×5), (12) (×4).

Plate IV

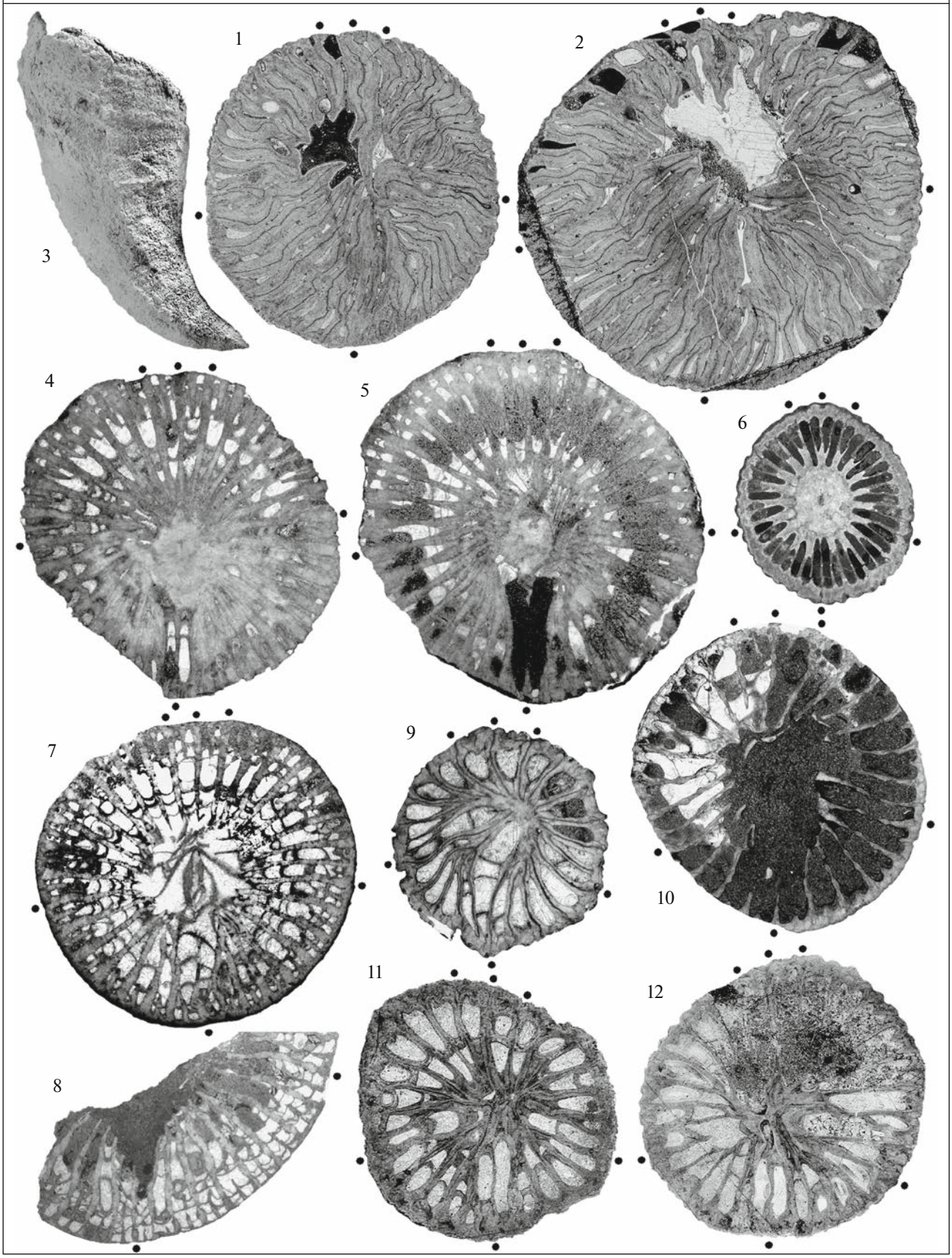

acteristic of the upper Tournaisian of the Urals and is also known in the contemporaneous deposits of Germany, Belgium, Poland, Central Kazakhstan (Ulitina, 1975), Kuznetsk basin, Omolon Block (Ganelin and Tschernjak, 1996), and China (Wang et al., 2001).

Corals of the genus *Cyathaxonia* Michelin, despite a wide stratigraphic range (lower Famennian–Lower Permian), are a typical element of the Belgium upper Tournaisian deposits (Poty et al., 1991). The genus is ubiquitous (for example, the upper Tournaisian of the Rügen Island, the southern part of the Baltic Sea) (Weyer, 1993; etc.). The species *Cyathaxonia* sp. aff. *cornu* Michelin (Plate IV, fig. 6) was found in unit 14 of the Tas-Ary Formation, dated to the late Tournaisian according to the accompanying complex.

Assemblage 3. The most significant changes and depletion in taxonomic composition of the corals are characteristic of deposits above unit 14. The last corals were found in unit 20. Assemblage 3 is characterized by rare findings of solitary corals of the genus *Amplexizaphrentis* Vaughan, which is characteristic mainly of the Visean. The location of one species of this genus *A. zapense* Denayer is known in the Köprülü Formation in Turkey (Denayer and Hosŋgör, 2014). In the western part of North America, the genus was also described in the Tournaisian deposits (Sando and Bamber, 1985). In the Tas-Ary Peninsula section, numerous rugose corals of the genus *Amplexizaphrentis* were also found at the top of unit 13 dated to the late Tournaisian. Thus, on the basis of the rugose determination, the age of assemblage 3 remains the late Tournaisian–Visean. Meanwhile, the conodont assemblage found in this part of the section makes it possible to accept the age of assemblage 3 as the Visean.

Amplexizaphrentis sp. (Plate V, figs. 1, 2) identified at the bottom of unit 15 in the Tas-Ary Formation is the most similar to the species *Amlexizaphrentis enniskilleni* (Milne–Edwards et Haime). The latter is widespread in the Visean deposits of England, Ireland, and Canada (Sutherland, 1958). A few findings were made in the Taidonian and Nizhnetersinskian regional substages of Kuzbass. Numerous findings were recorded in the Pod'akovian Regional Substage (Dobrolyubova et al., 1966) belonging to the lower part of the Visean (Alekseev, 2008). A similar species, *A. hastatus* Rogozov, was described in the Binjudinskian Regional Substage of Taimyr (Rogozov, 1972). The second level including corals is the top of unit 17 with only a few specimens of rugose corals found, of which we identified *Amplexizaphrentis* sp. indet. (Sample 755/2-4). The last finding was made in unit 20 and contains one identifiable specimen also belonging to *Amplexizaphrentis* sp. (Plate V, fig. 3).

Conodonts

When studying the key section of the Upper Palaeozoic deposits on the Tas-Ary Peninsula, carbonate rocks boiling rapidly in HCl were sampled for conodonts. Such rocks turned out to be irregularly distributed along the section. We managed to extract conodonts from all samples, except for one. Most samples with conodonts were taken from the Tas-Ary Formation, and only a few findings were made in the lower part of the Bel'kov Formation. The conodont assemblages of the Tas-Ary Formation are not rich in their number and systematic composition, while the Bel'kov assemblages demonstrate a great diversity of species.

In the Tas-Ary Formation, conodonts are present in all three parts of the section. In the lower part of the formation (units 1–11), they were found in units 5, 6, 7, and 9 (ESM_6 file in Supp. Data). The middle part of the formation (units 12–15) contains conodont assemblages only at the base: in the visible foot and near the top of unit 12; only one species was identified higher (top half of unit 15). The top of the section of the Tas-Ary Formation (units 16–21) was not sufficiently assessed in terms of conodonts. The latter were found at the top of unit 17, where they were represented by a small association including two species. The overlying Bel'kov Formation contains conodonts only in the lower part, in the first and fourth members.

The biostratigraphic analysis of conodonts makes it possible to distinguish in the key section three assemblages belonging to the Tournaisian, Visean, and Serpukhovian stages of the Lower Carboniferous.

Assemblage 1 covers the lower part and base of the middle part of the Tas-Ary Formation units (5–12) and includes the following species: *Siphonodella crenulata* (Cooper), *S. isosticha* (Cooper), *Polygnathus parapetus* Druce, *Po. inornatus* Branson et Mehl, *Po. communis communis* (Branson et Mehl), *Patrognathus variabilis* Rhodes, Austin et Druce, *Bispathodus aculeatus aculeatus* (Branson et Mehl), *Bi. aculea-*

Plate V. Rugosa corals from the Tournaisian and Visean deposits of the Tas-Ary Formation, Tas-Ary section, Kotel'ny Island. The collection is kept in the Chernyshev Central Research Exploration Museum. Abbreviation: (u.) unit. (1, 2) *Amplexizaphrentis* sp., Sample 764/4, specimen 764-4-1, successive cross sections (×3), u. 15, Visean Stage; (3) *Amplexizaphrentis* sp., Sample 770/5, specimen 770-5-1, cross section (×2), u. 20, Visean Stage; (4, 5) *Zaphrufimia* sp., Sample 763/2-1, specimen ko-26, successive cross sections, u. 13, upper Tournaisian substage: (4) (×10), (5) (×8); (6) *Eostrotion* sp., Sample 758/24, specimen ko-3, cross section (×9), u. 9, upper part of the lower Tournaisian substage; (7, 8) *Sychnoelasma* sp. aff. *urbanowitschi* (Stuckenberg, 1895), Sample 763/5, specimen 763-5, successive cross sections, u. 12, roof, upper Tournaisian substage: (7) (×3), (8) (×2); (9, 10) *Uralinia* sp. aff. *gracilis* (Ludwig, 1862), Sample 762/7, specimen 762-7-0, successive cross sections (×3), u. 13, upper Tournaisian substage; (11) *Variaxon* sp. 1, Sample 758/24, specimen ko-20, cross section (×12), u. 9, upper part of the lower Tournaisian substage; (12) *Lophophyllum* sp., Sample 758/24, specimen ko-7, cross section (×8), the same location and age.

Plate V

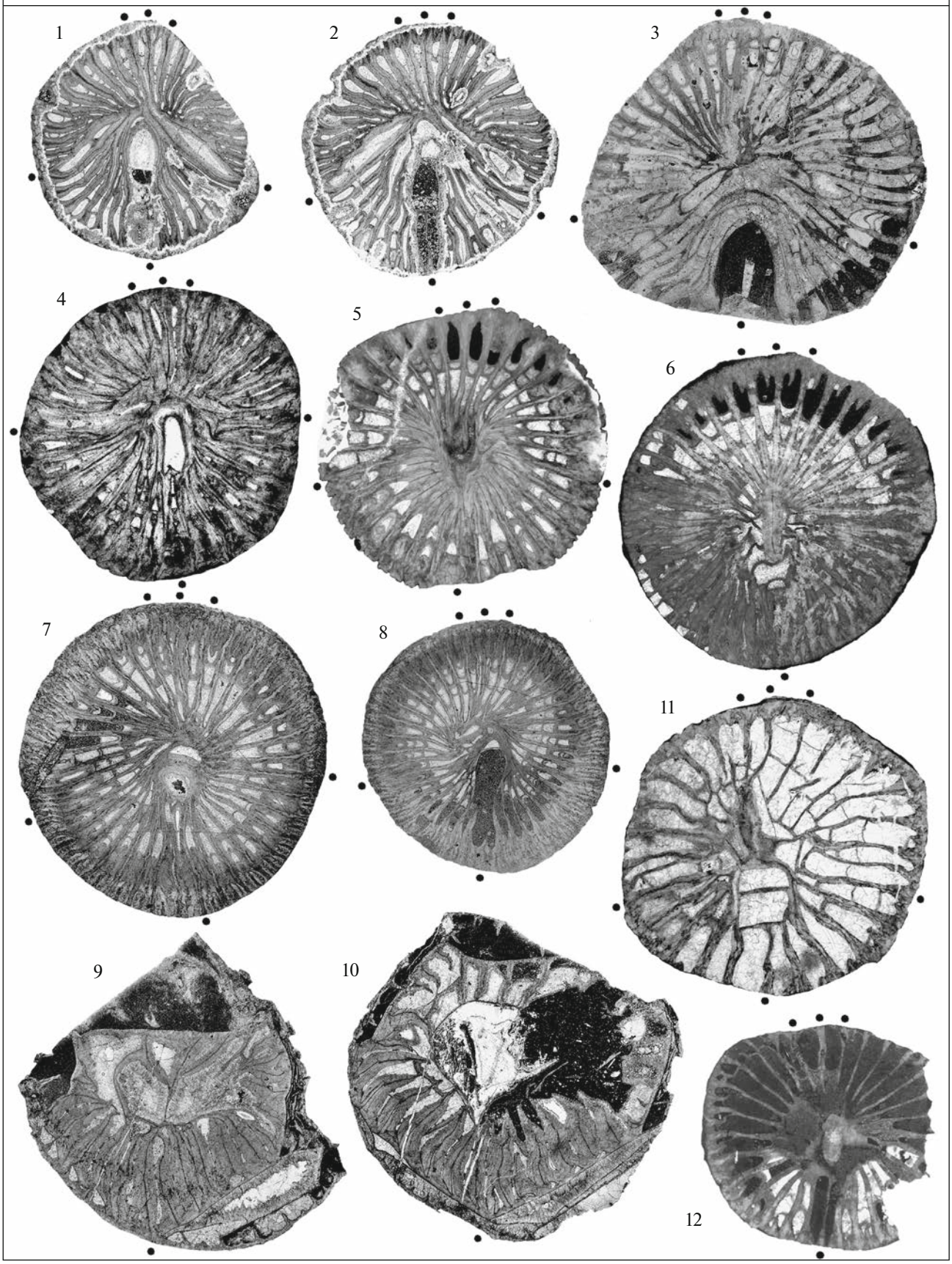

tus plumulus (Rhodes, Austin et Druce), *Pseudopolygnathus nodomarginatus* (E. Branson), *Ps. multistriatus* Mehl et Thomas, *Ps. pinnatus* Voges, *Gnathodus pseudosemiglaber* Thompson et Fellows, *Gn*. aff. *praebilineatus* Belka, and *Hindeodus cristulus* (Youngquist et Miller). The major species include the following: *Siphonodella crenulata* (Plate VI, fig. 10), *S. isosticha* (Plate VI, fig. 4), *Patrognathus variabilis* (Plate VI, figs. 5, 6), *Polygnathus parapetus* (Plate VI, fig. 9), *Pseudopolygnathus nodomarginatus* (Plate VI, fig. 1), *Ps. multistriatus* (Plate VI, fig. 2), and *Gnathodus pseudosemiglaber*. Many of the above-mentioned species are zonal types of the Tournaisian conodont scale. For example, *Siphonodella crenulata* is considered as an index species of the cognominal zone of the North American scale, while *S. isosticha* is a zonal species of the European scale. The species are characterized by a wide geographic distribution and can be found in Europe, Asia, Australia, Canada, and North America. In Russia, the considered zones were traced in the Southern Urals (Pazukhin, 2010), in the north of the Urals and the Chernyshev Ridge (Zhuravlev, 2003; Plotitsyn, 2016), and also in the Prikolymian Uplift of the Northeastern region (Gagiev, 2009). *Patrognathus variabilis* was found in many regions of the world in the lower Tournaisian deposits formed in the extremely shallow water settings (Austin, 1976). The species is known in England, where it was described for the first time (Rhodes et al., 1969). In Belgium, the Patrognathus variabilis–Spathognathodus plumulus or Patrognathus variabilis–Polygnathus inornatus Zone (Austin et al., 1970) was identified at the base of the Carboniferous. In Ireland, *Patrognathus variabilis* is also widespread in the local conodont lower Tournaisian Polygnathus spicatus and Polygnathus inornatus zones (Johnston and Higgins, 1981). The latter zone contains the species *Siphonodella cooperi* Hass, on the basis of which it is correlated with the top of the Siphonodella duplicata Zone and also with the S. sandbergi and S. crenulata zones of the standard scale. In Alaska (United States), the species was found in the lower part of the Mississippian deposits (Mull et al., 1995). In Russia, *Patrognathus variabilis* is known in the lower Tournaisian deposits of the Malevkian and Upian formations in the central regions of the Russian Platform (Barskov et al., 1984), north of the Urals (Zhuravlev, 2003), and the Abyshevian Regional Substage in the south of Western Siberia (Bushmina and Kononova, 1981). *Polygnathus parapetus* is frequent in occurrence in the lower Tournaisian (Druce, 1969; Bouckaert and Groessens, 1976; Kozitskaya et al., 1978; Gagiev, 1979, 2009; Bushmina and Kononova, 1981; Barskov et al., 1984; Alekseev et al., 1994; Zhuravlev, 2003; Kislyakov and Eikhvald, 2004; Pazukhin, 2009; Bahrami et al., 2011). *Pseudopolygnathus nodomarginatus* was found in the lower Tournaisian of Europe, North America, and Australia (Rhodes et al., 1969; Druce, 1969). *Pseudopolygnathus multistriatus* can be found in the upper Tournaisian, from the isosticha–Upper crenulata Zone to the lower part of the anchoralis–latus Zone (Lane et al., 1980). In Iran, the species occurs in the range of the isosticha–Upper crenulata and typicus (bottom) zones (Bahrami et al., 2011). In the Southern Urals, *Ps. multistriatus* was noted in the upper Tournaisian Siphonodella isosticha–Gnathodus punctatus zones (bottom of the Kizelian Regional Substage) (Pazukhin, 2009). *Gnathodus pseudosemiglaber* was found in the upper Tournaisian deposits of Europe, Asia, and North America. The species distribution begins in the anchoralis–latus Zone (upper Tournaisian) and passes into the texanus Zone (lower Visean) (Lane et al., 1980).

On the basis of the data given above, the Tournaisian part of the Tas-Ary Formation can be subdivided into two parts. The first part (units 5–9) corresponds to the lower Tournaisian (ConA1a), while the second part (units 10(?)–12) corresponds to the upper Tournaisian (ConA1b). The Tournaisian conodont assemblagees are represented by the species with a wide biogeographic distribution; thus, the palaeobasins of Europe, Asia, and the Midcontinent (North America) had stable relations which were strongly pronounced at the time of the late Tournaisian transgression.

Plate VI. Lower Carboniferous conodonts from the key section of the Tas-Ary Peninsula (Kotel'ny Island). the length of the scale bar is 0.1 mm for figs. 1, 4–10 and 0.3 mm for figs. 2, 3. The conodont collection is kept at the Lomonosov Moscow State University under the no. NOKTAS 362. Abbreviation: (u.) unit. (1) *Pseudopolygnathus nodomarginatus* (E. Branson, 1934), Pa element, Sample no. 758/3, specimen NOKTAS 362-1: (1a) top view and (1b) bottom view, lower part of the Tas-Ary Formation, u. 6, lower Tournaisian substage; (2) *Pseudopolygnathus multistriatus* Mehl et Thomas, 1947, Pa element, Sample no. 762/17, specimen NOKTAS 362-2: (*2a*) top view and (2b) bottom view, middle part of the Tas-Ary Formation, u. 12, upper Tournaisian substage; (3) *Pseudopolygnathus pinnatus* Voges, 1959, Pa element, Sample no. 762/17, specimen NOKTAS 362-3: (3a) top view and (3b) bottom view, middle part of the Tas-Ary Formation, u. 12, upper Tournaisian substage; (4) *Siphonodella isosticha* (Cooper, 1939), Pa element, Sample no. 758/10, specimen NOKTAS 362-4, side view, lower part of the Tas-Ary Formation, u. 7, lower Tournaisian substage; (5, 6) *Patrognathus variabilis* Rhodes, Austin et Druce, 1969, lower part of the Tas-Ary Formation, u. 5, lower Tournaisian substage: (5) Pa element, Sample no. 758/1, specimen NOKTAS 362-5, side view; (6) Pa element, Sample no. 758/1, specimen NOKTAS 362-6, top view; (7) *Bispathodus aculeatus plumulus* (Rhodes, Austin et Druce, 1969), Pa element, Sample no. 758/10, specimen NOKTAS 362-7, side view, lower part of the Tas-Ary Formation, u. 7, lower Tournaisian substage; (8) *Polygnathus communis communis* (Branson et Mehl, 1934), Pa element, Sample no. 762/17, specimen NOKTAS 362-8: (8a) top view and (8b) bottom view, middle part of the Tas-Ary Formation, u. 12, upper Tournaisian substage; (9) *Polygnathus parapetus* Druce, 1969, Pa element, Sample no. 758/1, specimen NOKTAS 362-9: (9a) top view and (9b) bottom view, lower part of the Tas-Ary Formation, u. 5, lower Tournaisian substage; (10) *Siphonodella* cf. *crenulata* (Cooper, 1939), Pa element, Sample no. 758/30, specimen NOKTAS 362-10, top view, lower part of the Tas-Ary Formation, u. 9, lower Tournaisian substage.

Plate VI

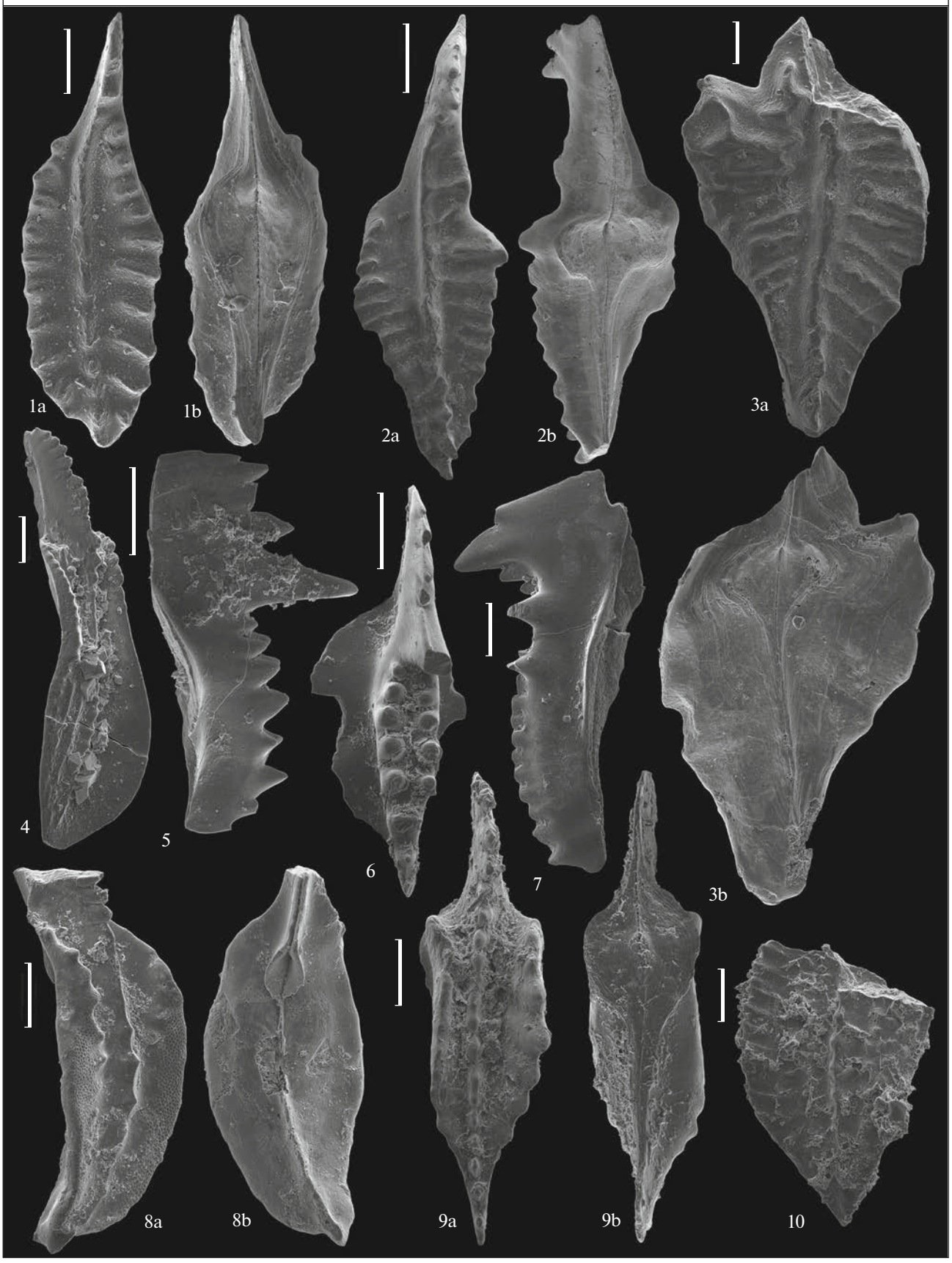

Assemblage 2 was identified in units 15–17 and includes the following species: *Lochriea commutata* (Branson et Mehl) (Plate VII, fig. 2), *Vogelgnathus postcampbelli* (Austin et Husri) (Plate VII, fig. 1), and *Cavusgnathus unicornis* (Rhodes, Austin et Druce) (Plate VII, fig. 10). *Lochriea commutata* is widespread in the Lower–Middle Carboniferous of Eurasia (Bischoff, 1957; Higgins and Bouckaert, 1968; Rhodes et al, 1969; Rhodes and Austin, 1971; Kozitskaya et al., 1978; *Nizhnii...*, 1993; Nemyrovskaya et al., 1994; Dzik, 1997; Blanco-Ferrera et al., 2005; Nemyrovska, 2005; Kabanov et al., 2009; Pazukhin, 2011; Nemyrovska et al., 2011) and in the Upper Mississippian of North America (Branson and Mehl, 1941; Scott, 1942; Krumhandt et al., 1996). *Vogelgnathus postcampbelli* can be found in the upper Visean–lower Serpukhovian (Gnathodus bilineatus–Lochriea ziegleri conodont zones) of Europe and in the Upper Mississippian (late Chesterian) of North America (Cavusgnathus monocerus Zone (= Adetognathus unicornis) (Nemyrovska, 2005). *Cavusgnathus unicornis* occurs in the upper Velmeyeran–Chesterian of North America, Visean–Serpukhovian of Western Europe, Visean (Utting Formation) of Northwestern Australia, and Tournaisian–Serpukhovian of Donbass (Kozitskaya et al., 1978). In Alaska, the species is widespread in the upper Meramecian–uppermost Chesterian (Upper muricatus conodont subzone) (Krumhardt et al., 1996). On the Russian Platform, this species was described in the upper Visean–Serpukhovian deposits (Paragnathodus nodosus–P. multinodosus zones) (*Nizhnii...*, 1993). On the basis of the data cited above, the described conodont assemblage can characterize the Visean Stage. The occurrence of cosmopolitan Visean conodonts in the Tas-Ary Formation is indicative of the preserved biogeographic relations of the studied palaeobasin to both the European and Asian and the North American palaeobasins in the Visean Age.

Assemblage 3 originated from the lower part of the Bel'kov Formation (members 1 and 4) and is represented by *Mestognathus bipluti* Higgins, *Vogelgnathus postcampbelli*, *Cavusgnathus naviculus* (Hinde), *Lochriea commutata*, *L. scotiaensis* (Globensky), *Gnathodus girtyi gyrtyi* Hass, *Gn. girtyi simplex* Dunn, *Pseudognathodus homopunctatus* (Ziegler), *Rhachistognathus muricatus* (Dunn), *Rh. prolixus* Baeseman et Lane, and *Declinognathodus bernesgae* Sanz–Lopez, Blanco–Ferrera, Garcia–Lopez et Sanchez de Posada. Major species defining the Serpukhovian age of the host deposits are as follows: *Gnathodus girtyi simplex* (Plate VII, fig. 14), *Declinognathodus bernesgae* (Plate VII, fig. 16), and *Rhachistognathus muricatus* (Plate VII, fig. 15). *Gnathodus girtyi simplex* is largely characteristic of the uppermost part of the Mississippian (Chesterian), slightly touching the base of the Pennsylvanian, the conodont zones Gnathodus bilineatus–Declinognathodus noduliferous–Rhachistognathus primus (Krumhardt et al., 1996). In Europe, the species was found in the Visean and Serpukhovian (Rhodes and Austin, 1971; Higgins, 1975; Tynan, 1980). *Declinognathodus bernesgae* originates from the upper Serpukhovian–lower Bashkirian deposits in the northern part of Spain (Sanz–Lopez et al., 2006). In Europe, the species is frequent in occurrence at the boundary between the Serpukhovian and the Bashkirian (Nemirovska et al., 2011). *Rhachistognathus muricatus* was described in the Late Mississippian Bird Spring Formation in Nevada (Dunn, 1965). This species is the most widespread in the United States. It was found in deposits from the late Chesterian (Late Mississippian) to the early Morrowan in southern Nevada,

Plate VII. Lower Carboniferous conodonts from the key section of the Tas-Ary Peninsula (Kotel'ny Island). Length of the scale bar is 0.1 mm. Abbreviations: (u.) unit, (m.) member. (1) *Vogelgnathus postcampbelli* (Austin et Husri, 1974), Pa element, Sample no. 755/1, specimen NOKTAS 362-11, side view, upper part of the Tas-Ary Formation, u. 17, Visean Stage; (2) *Lochriea commutata* (Branson et Mehl, 1941), Pa element, Sample no. 753/14, specimen NOKTAS 362-12, top view, lower part of the Bel'kov Formation, m. 4, Serpukhovian Stage; (3) *Lochriea scotiaensis* (Globensky, 1967), Pa element, Sample no. 766/3, specimen NOKTAS 362-13, top view, lower part of the Bel'kov Formation, m. 1, Serpukhovian Stage; (4) *Gnathodus* aff. *praebilineatus* Belka, 1985, Pa element, Sample no. 763/6, specimen NOKTAS 362-14, top view, middle part of the Tas-Ary Formation, u. 12, upper Tournaisian substage; (5) *Pseudognathodus homopunctatus* (Ziegler, 1960), Pa element, Sample no. 753/6, specimen NOKTAS 362-15, top view, lower part of the Bel'kov Formation, m. 4, Serpukhovian Stage; (6, 9) *Mestognathus bipluti* Higgins, 1961: (6) Pa element, Sample no. 753/6, specimen NOKTAS 362-16, top view, lower part of the Bel'kov Formation, m. 4, Serpukhovian Stage; (9) Pa element, Sample no. 766/3, specimen NOKTAS 362-17, side view, lower part of the Bel'kov Formation, m. 1, Serpukhovian Stage; (7) *Hindeodus cristulus* (Youngquist et Miller, 1949), Pa element, Sample no. 758/3, specimen NOKTAS 362-18, side view, lower part of the Tas-Ary Formation, u. 6, lower Tournaisian substage; (8) *Cavusgnathus naviculus* (Hinde, 1900), Pa element, Sample no. 766/3, specimen NOKTAS 362-19, side view, lower part of the Bel'kov Formation, m. 1, Serpukhovian Stage; (10) *Cavusgnathus unicornis* (Rhodes, Austin et Druce, 1969), Pa element, Sample no. 41/1, specimen NOKTAS 362-20, top view, middle part of the Tas-Ary Formation, u. 15, Visean stage; (11) *Rhachistognathus prolixus* Baeseman et Lane, 1985, Pa element, Sample no. 753/14, specimen NOKTAS 362-21, top view, lower part of the Bel'kov Formation, m. 4, Serpukhovian Stage; (12) *Gnathodus girtyi gyrtyi* Hass, 1953, transitional form to *Gnathodus girtyi simplex* Dunn, 1966, Pa element, Sample no. 753/14, specimen NOKTAS 362-22, top view, lower part of the Bel'kov Formation, m. 4, Serpukhovian Stage; (13) *Rhachistognathus* sp., Pa element, Sample no. 753/14, specimen NOKTAS 362-23, top view, lower part of the Bel'kov Formation, m. 4, Serpukhovian Stage; (14) *Gnathodus girtyi simplex* Dunn, 1966, Pa element, Sample no. 782/7, specimen NOKTAS 362-24, top view, lower part of the Bel'kov Formation, m. 4, Serpukhovian Stage; (15) *Rhachistognathus muricatus* (Dunn, 1965), Pa element, Sample no. 753/6, specimen NOKTAS 362-25, top view, lower part of the Bel'kov Formation, m. 4, Serpukhovian Stage; (16) *Declinognathodus bernesgae* Sanz-Lopez, Blanco-Ferrera, Garcia-Lopez et Sanchez de Posada, 2006, Pa element, Sample no. 782/7, specimen NOKTAS 362-26, top view, lower part of the Bel'kov Formation, m. 4, Serpukhovian Stage.

Plate VII

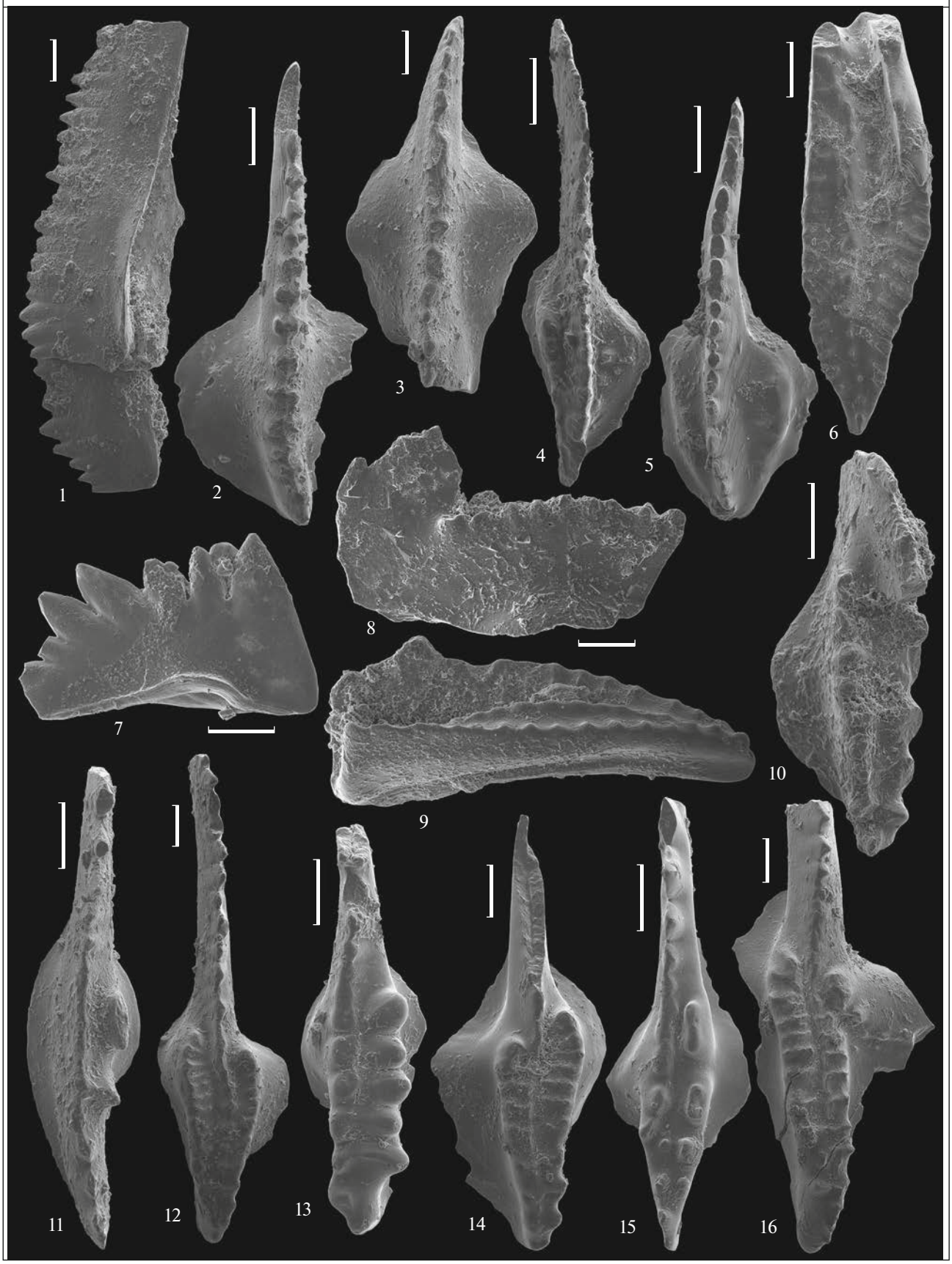

western Texas, southern and eastern Oklahoma, and northern Arkansas, as well as from the Morrowan to the early Atokan in eastern Idaho and central Montana (Lane and Straka, 1974; Baesemann and Lane, 1985). In Alaska, the species can be observed in Wahoo limestones (uppermost Chesterian to Morrowan; Upper muricatus Subzone to lower minutus Fauna) (Krumhardt et al., 1996). In the European sections, including Russian, the species is very rare. A few findings of *Rhachistognathus muricatus* were made in the Yogian Formation of the Yana–Kolyma region (Northeast of Russia); on the basis of these findings, the formation was dated to the Serpukhovian–early Bashkirian (Gagiev, 2009). *Mestognathus bipluti* (Plate VII, figs. 6, 9), *Vogelgnathus postcampbelli*, *Cavusgnathus naviculus* (Plate VII, fig. 8), *Lochriea commutata*, *L. scotiaensis* (Plate VII, fig. 3), *Gnathodus girtyi gyrtyi* (Plate VII, fig. 12), *Pseudognathodus homopunctatus* (Plate VII, fig. 5), and *Rhachistognathus prolixus* (Plate VII, fig. 11) are transit species from the Visean Stage, which are the most abundant in the Serpukhovian.

Owing to the fact that the transitional Serpukhovian–Bashkirian conodont species were found in the lowermost Bel'kov Formation, there is a question of attributing these deposits to a particular stage. The predominance of the Serpukhovian conodonts in the association makes it possible to consider this part of the section as Serpukhovian. From the biogeographic point of view, the presence of the genus *Rhachistognathus* conodonts in the Serpukhovian assemblage of the Bel'kov Formation of the studied palaeobasin closely approximates it to the North American palaeobasin, where the genus was most fully assessed both systematically and quantitatively.

Foraminifera

Foraminifera were studied on the Tas-Ary Peninsula in the lower part of the Bel'kov Formation (members 1 and 4). The degree of preservation of the shells, their relative rarity in the rock, and the small number of specimens recorded in thin sections make it difficult to identify the material and explain the use of an open nomenclature. Some identified taxa are defined only up to the genus, while others are considered as possibly related, and their definition is given largely conditionally (Plate VIII).

Foraminifera from the deposits of member 1 occur in Sample 766/4. The found assemblage is represented by the following genera: *Endotaxis* Bogush et Brazhnikova, 1983, *Tetrataxis* Ehrenberg, 1854, *Planoarchaediscus* A. Miklukho–Maclay, 1956, *Archaediscus* Brady, 1873, *Paraarchaediscus* Orlova, 1955, and (?) *Rectocornuspira* Warthin, 1930. This assemblage is dominated by archaediscides of three genera: *Planoarchaediscus* (Plate VIII, figs. 21–25, 28–30), which is widespread in the Visean–Serpukhovian; *Archaediscus* (Plate VIII, figs. 14–17, 19, 20, 26, 27), which can be found in the Lower Carboniferous (Visean) and Lower Permian; *Paraarchaediscus* (Plate VIII, figs. 31), which occurs in the Visean–Serpukhovian, likely, in the Bashkirian Stage (*Spravochnik...*, 1993). The analyzed assemblage includes *Planoarchaediscus duxundaensis* Bogush et Juferev (Plate VIII, figs. 21, 22), which is described in the Visean deposits of the Kolyma Block (Bogush and Yuferev, 1970), and also *Planoarchaediscus spirillinoides* (Rauser) (Plate VIII, figs. 28–30), which is widespread in the Visean deposits of the Moscow Syneclise and western slope of the Urals. *Archaediscus krestovnikovi* Rauser is present together with the above-mentioned species. The species holotype was described in the Visean deposits of Central Kazakhstan (Rauzer–Chernousova, 1948), but *Archaediscus krestovnikovi* Rauser is known at both the top of the Visean Stage and the bottom of the Serpukhovian Stage in the Serpukhovian stratotypical section of the Moscow Syneclise (Gibshman, 2003). This species is indicated in the lower Serpukhovian substage of the Timan–Pechora province (Durkina,

Plate VIII. Foraminifera from the Bel'kov Formation of the Tas-Ary section, Kotel'ny Island. Length of the scale bar is 0.1 mm. The collection of thin sections no. 4918 is kept at the Geological Institute, Russian Academy of Sciences. Corals in Sample 766/4 originate from member 1, Visean (?)–lower Serpukhovian. Other samples are taken from member 4, upper Serpukhovian–lower Bashkirian (?). (1) *Eostaffella* ex gr. *pseudostruvei* Rauser et Beljaev, 1936, Sample 753/24, specimen no. 4918/1; (2) *Eostaffella* sp., Sample 688/4, specimen no. 4918/10; (3–5) *Eostaffella* cf. *prisca* Rauser, 1948, Sample 688/4: (3) specimen no. 4918/11, (4) specimen no. 4918/12, (5) specimen no. 4918/13; (6) *Eostaffella* ex gr. *postmosquensis* Kireeva, 1951, Sample 753/24, specimen no. 4918/2; (7) *Endostaffella* sp., Sample 753/24, specimen no. 4918/3; (8, 9) *Eostaffellina paraprotvae* (Rauser), 1948, Sample 753/24: (8) specimen no. 4918/4, (9) specimen no. 4918/5; (10–12) *Plectostaffella* sp., Sample 688/4: (10) specimen no. 4918/14, (11) specimen no. 4918/15, (12) specimen no. 4918/16; (*13*) *Eostaffella* sp. (ex gr. *postmosquensis* (?)), Sample 753/24, specimen no. 4918/6; (14, 15) *Archaediscus pauxillus* Shlykova, 1951: (*14*) Sample 688/4, specimen no. 4918/17; (15) Sample 688/5, specimen no. 4918/20; (16, 17) *Archaediscus kolymensis* Mikluho-Maclay, 1960, Sample 688/5: (16) specimen no. 4918/21, (17) specimen no. 4918/22; (18) *Asteroarchaediscus* sp., Sample 688/4, specimen no. 4918/18; (19, 20) *Archaediscus krestovnikovi* Rauser, 1948: (*19*) Sample 688/4, specimen no. 4918/19; (20) Sample 766/4, specimen no. 4918/24; (21, 22) (?) *Planoarchaediscus duxundaensis* Bogush et Juferev, 1970, Sample 766/4: (21) specimen no. 4918/25, (22) specimen no. 4918/26; (23–25) *Planoarchaediscus* ex gr. *monstratus* (Grozdilova et Lebedeva, 1954) Sample 766/4: (23) specimen no. 4918/27, (24) specimen no. 4918/28, (25) specimen no. 4918/29; (26, 27) *Archaediscus* ex gr. *moelleri* Rauser, 1948: (*26*) Sample 753/24, specimen no. 4918/7; (27) Sample 766/4, specimen no. 4918/30; (28–30) *Planoarchaediscus spirillinoides* (Rauser, 1948): (28) Sample 766/4, specimen no. 4918/31; (29) Sample 753/24, specimen no. 4918/8; (30) Sample 753/24, specimen no. 4918/9; (31) *Paraarchaediscus* sp., Sample 766/4, specimen no. 4918/32; (32, 33) *Tetrataxis* sp.: (32) Sample 688/5, specimen no. 4918/23; (33) sample 766/4, specimen no. 4918/33; (34) (?) *Rectocornuspira* sp., Sample 766/4, specimen no. 4918/34; (35, 36) *Endotaxis brazhnikovae* Bogush et Juferev, 1966, Sample 766/4: (35) specimen no. 4918/35, (36) specimen no. 4918/36.

Plate VIII

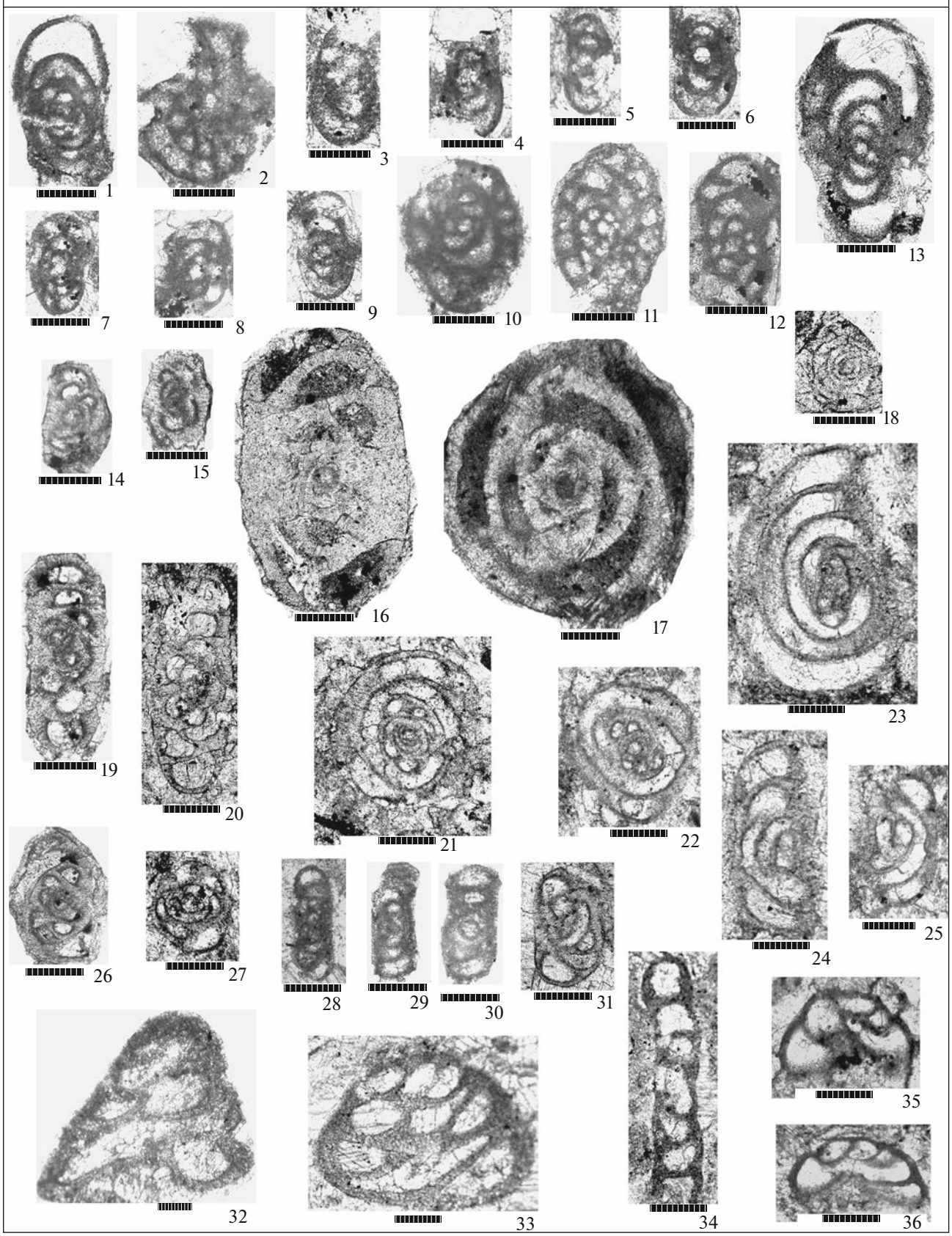
1
2
3
4
5
6
7
8
9
10
11
12
13
14
15
16
17
18
19
20
21
22
23
24
25
26
27
28
29
30
31
32
33
34
35
36

2002), as well as in the Serpukhovian Stage of Chukotka (Solov'eva, 1975).

Thus, the archaediscides composition of the analyzed assemblage is represented by transit species appearing as early as the Visean Stage, but common in the Serpukhovian deposits. A distinctive feature of this assemblage is the presence of *Endotaxis brazhnikovae* Bogush et Juferev (Plate VIII, figs. 35, 36). This species, although described in the Middle Visean, is usually characteristic of the Serpukhovian deposits. *Endotaxis brazhnikovae* Bogush et Juferev is present at the bottom of the Serpukhovian stratotypical section in the type area (Gibshman, 2003) and in the Serpukhovian key section in the Southern Urals (Kulagin and Gibshman, 2002). In general, the considered assemblage of foraminifera from member 1 of the Bel'kov Formation is transit Visean–Serpukhovian. It is hard to determine a more accurate age-related reference of this assemblage owing to the lack of original data on this fauna group from underlying deposits. However, given the previously known findings of Serpukhovian foraminifera at the top of the Tas-Ary Formation, such as *Eostaffellina* cf. *paraprotva* (Rauser), *Eosigmoilina explicata lata* Ganelina, and *Eostaffella* ex gr. *pseudostruvei* Rauser et Beljaev (Kos'ko et al., 1985), the age of the lower unit of the Bel'kov Formaition can presumably be estimated as the early Serpukhovian. As for the age of the top of the Tas-Ary Formation, it is impossible to solve this issue using the author's materials, because there are no new data on foraminifera which would confirm or disprove the information obtained by the previous researchers.

The general assemblage of foraminifera from the deposits of member 4 is similar in generic and species composition to the assemblages of foraminifera from both the Eosigmoilina explicata–Eostaffellina paraprotva and Planoarchaediscus stilus–Eostaffella pseudostruvei layers. These layers were described earlier in the Tas-Ary Peninsula section by Solov'eva (1975). The first ones were identified as analogous to the Protvinskian Regional Substage of the Serpukhovian Stage of the Lower Carboniferous in the Russian Platform, while the second ones characterize the bottom of the lower Bashkirian of the Middle Carboniferous. Comparison of the newly obtained assemblage of foraminifera of member 4 in the Tas-Ary section with the previously known assemblagees of the above-mentioned layers indicates the following. The species *Eostaffellina paraprotva* (Rauser) (Plate VIII, figs. 8, 9), accepted as one of the index species of the lower layers, is recorded in four out of five samples provided for the study of foraminifera. First described in the Protvinskian Regional Substage of the Serpukhovian of the Moscow Syneclise (Rauzer–Chernousova, 1948), this species and its subspecies are characterized by a wide geographic distribution. They are known from the top of the Serpukhovian and the bottom of the Bashkirian of the Russian Platform, Donbass, the Urals, Timan, Yugorsky Peninsula, and Primorye. The presence of eosigmoilins in the assemblage as the second index species is doubtful. Sample 753/24 contains a few oblique cross sections of shells which are presumably related to (?) *Eosigmoilina* (Plate VIII, fig. 31).

The analyzed assemblage also includes *Plectostaffella* sp. (Plate VIII, figs. 10–12) and *Eostaffella* ex gr. *pseudostruvei* Rauser et Beljaev (Plate VIII, fig. 1), whose presence "makes younger" the late Serpukhovian age of the considered community. The genus *Plectostaffella* is characteristic of the lower Bashkirian deposits of the Bashkirian stratotypic region. The first appearance of a few forms is possible already at the top of the Serpukhovian (Kulagina et al., 2001). A similar stratigraphic distribution is typical of the forms which are similar to the group *Eostaffella pseudostruvei*. The community of foraminifera from Sample 753/24 has the "youngest" outer appearance. Eostaffellae are relatively diverse in this community. The group *Eostaffella pseudostruvei* is accompanied by *Eostaffella postmosquensis* (Plate VIII, figs. 6, 13). In the updated stratigraphic scheme of the Bashkirian Stage, its lower part is associated with diverse plectostaffellae (Kulagina et al., 2000) for the East European Platform and the Southern Urals, as well as with the Eostaffella postmosquensis–Eostaffella pseudostruvei zonal complexes for the Northern Urals, Northwest Timan, and Timan–Pechora province (Durkina, 2002; Kossovaya et al., 2006).

In general, the assemblage of foraminifera identified in member 4 has a depleted species composition, although it includes ten definable generic taxa and two supposedly related ones. The species diversity of taxa is more pronounced among archaediscides. They are characterized by a wide geographical distribution and are known in Eurasia on the East European Platform, in Donbass, in the Urals, in Kazakhstan and in other regions. The exception is the species *Archaediscus kolymensis* Miklukho-Maclay (Plate VIII, figs. 15, 16) described in the Visean deposits of the Kolyma basin in Northeastern Siberia (Miklukho-Maclay, 1960). Obviously, this species should be considered as endemic.

Hence, a joint location of the genera *Plectostaffella*, *Eostaffellina*, and *Eostaffella* representatives is critical for dating of the deposits of member 4. The assemblage includes zonal species and other forms which have a wide geographic distribution and are characteristic of the Serpukhovian and Bashkirian boundary interval. On this basis, the deposits containing such a complex are dated to the late Serpukhovian–early Bashkirian. The obtained new data on the Tas-Ary foraminifera of Kotel'ny Island confirm the earlier known information (Solov'eva, 1975) on the presence of foraminifera there, which are characteristic of the tropical biogeographic region.

General Conclusion on the Age of Deposits and Palaeogeography Based on Different Fossil Groups

The lower part of the Tas-Ary Formation is definitely Tournaisian in age, which is confirmed by con-

clusions on three fossil groups. Nevertheless, it cannot be ruled out that the lowest horizons of the formation (units 1–4), devoid of fauna, may belong to the Upper Devonian. The Tournaisian–Visean boundary in the Tas-Ary section is located not lower than the top of unit 14. During the State Geological Survey, judging by the description in (Kos'ko et al., 1985), the upper part of unit 15 in our nomenclature (in the cited paper, unit 19) was assigned to the Visean Stage, while all (?) underlying deposits were assigned to the Tournaisian. The data we obtained, as shown above, do not make it possible to unambiguously draw a clear boundary between the Tournaisian and Visean in the Tas-Ary Peninsula section. We have to single out a transitional interval (unit 15) in the column (Fig. 4), corresponding in age to the late Tournaisian–early Visean, which contains representatives of both the late Tournaisian and Visean fauna. The lower part of the formation up to the top of unit 9 refers to the lower Tournaisian, while units 12–14 are upper Tournaisian. The latter, presumably, also covers units 10–11, where no taxa of a narrow stratigraphic range were found.

All overlying deposits, up to the top of unit 20, should be attributed to the Visean. The upper unit of the Tas-Ary Formation may be the Serpukhovian in age. Its middle part contains displaced coral colonies resembling *Thysanophyllum* ex gr. *acystosum* Rogozov, previously identified by Yu.G. Rogozov at the bottom of the Bel'kov Formation (Kos'ko et al., 1985, unit 26 of the Tas-Ary Formation, survey experts' nomenclature). This fact is also confirmed by the aforementioned findings of the Serpukhovian foraminifera in the upper part of the Tas-Ary Formation made during the State Geological Survey. Thus, the boundary between the Tas-Ary and the Bel'kov formations passes inside the Serpukhovian Stage, most likely in its lower part.

The age of the highest interval of the studied section, which contains fossil remains, i.e., member 4 of the Bel'kov Formation, can be estimated at the late Serpukhovian or, possibly, the late Serpukhovian–early Bashkirian, as evidenced by the microfauna data. The results of brachiopod identification do not contradict this conclusion. Fossils were not found in the overlying part of the Bel'kov Formation, except for *Camerisma* sp. indet. brachiopods at the bottom of member 5, which are characteristic of the Carboniferous–Permian and therefore are not important for specification of the host rock age.

In general, the fauna remains of the Tas-Ary section are represented by taxa of a wide geographic distribution. This fact is not surprising, considering that the Pangea assembly already started in the Early Carboniferous, and Laurussia was relatively close to Siberia; in addition, both Laurussia and a large part of the Siberian palaeocontinent (whose Taimyr margin was turned at that time toward the Baltica) were located in tropical latitudes. The position of the continental blocks such as Kazakhstan and Northern and Southern China is reconstructed in the same latitudes (Domeier and Torsvik, 2014). However, the Serpukhovian time is marked by close relations of the studied palaeobasin to the basin(s) of Taimyr, Verkhoyansk, and Kolyma–Omolon regions, as indicated by the characteristic brachiopod associations and endemic species of foraminifera in the Bel'kov Formation, earlier known only in the Kolyma River basin. It should be noted that the conodont assemblages from the Serpukhovian deposits of the Tas-Ary Peninsula, including species of a wide geographic distribution, are the most similar to the North American assemblages.

THE AGE OF THE UPPERMOST BEL'KOV FORMATION BASED ON DETRITAL ZIRCONS

Detrital zircons were extracted from sandstone in the middle part of member 8 in the Bel'kov Formation (Fig. 14, Sample 117/9). Zircons are 50–150 μm in size. They are mostly euhedral, less often, semirounded. One hundred crystals were dated in the Isotope Laboratory of the University of California, Santa Cruz (LA-ICP-MS). Almost all of them are of Palaeozoic age, with the prevailing Carboniferous–Permian zircons evidently related to the Northern Taimyr orogenesis. A few crystals appeared to be Neoproterozoic, Palaeoproterozoic, and Archean. The description of dating methods and results will be given in a special paper. Here we report only the data on the youngest crystals to substantiate the maximum depositional age of the upper part of the Bel'kov Formation. The analyses of the Late Palaeozoic zircons (45 dated grains) form an almost continuous sequence on the Pb/U isotopic diagram, filling the age interval of 330–260 Ma (Fig. 24a; ESM_9 file in Supp. Data). The three youngest crystals form a concordant cluster with an age of 261 ± 5 Ma, MSWD = 1.08 (Fig. 24b). This value is accepted as the maximum depositional age of the visible top of the Bel'kov Formation on the Tas-Ary Peninsula (upper Middle Permian). Similar data on the detrital zircon age in the Bel'kov Formation on Bel'kov Island are given in (Ershova et al., 2015; Pease et al., 2015). The actual age of upper horizons of the Bel'kov Formation on the Tas-Ary Peninsula can turn out to be younger. Firstly, the dated sample was collected not from the very top of the formation: above the sampled sandstones, there is a thick shale unit. Secondly, the Late Palaeozoic zircons are characterized by normal magmatic oscillatory zoning and small elongation, and, most likely, they originate from the Late Palaeozoic granites of the Northern Taimyr belt and its assumed eastern continuation, while their volcanic origin is less likely. Before being eroded, granites had to be exhumed, which requires an additional period of time likely lasting for a few million years.

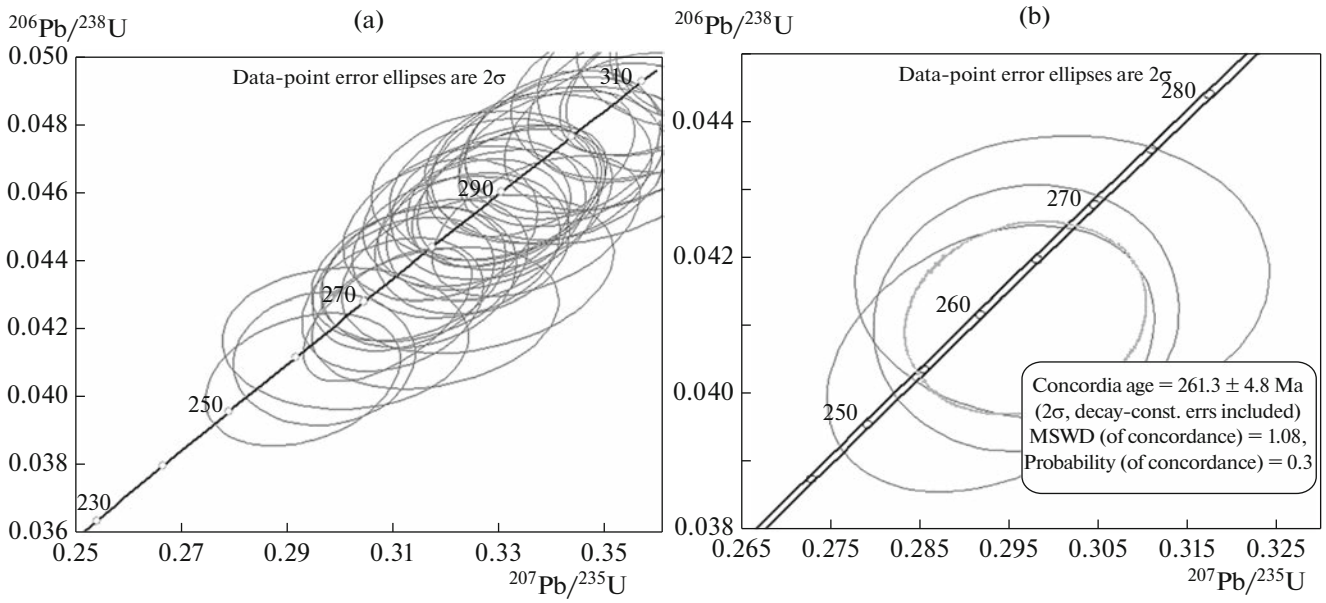

Fig. 24. Pb/U isotopic diagrams for detrital zircons from the upper part of the Bel'kov Formation. (a) Late Palaeozoic zircons form a continuous sequence in the diagram, indicating a long-term continuous magmatism related to the Northern Taimyr granites; (b) age of the concordant cluster of the three youngest crystals.

EVOLUTION OF THE DEPOSITIONAL SETTINGS DURING THE CARBONIFEROUS–PERMIAN

The coastal marine environments of the late Devonian were replaced by some basin deepening at the beginning of the Tournaisian, accompanied by a decreased supply of siliciclastics from the land. These processes favoured the development of carbonate-producing organisms and the accumulation of mixed siliciclastic–carbonate sediments composing the lower part of the Tas-Ary Formation. The absence of Lower Carboniferous rocks in the northern and central areas of Kotel'ny Island points that at that time either this area was dry land, or the Lower Carboniferous deposits were thin and underwent erosion. In any case, it can be assumed that, at the beginning of the Carboniferous, the coastline shifted somewhat to the northeast, still being close to the recent Tas-Ary Peninsula. Highly bioturbated rocks of the lower four units of the Tas-Ary Formation were most likely formed in a calm lagoon. They are almost devoid of macrofossils and signs of active hydrodynamics (wave ripples and cross-lamination are sporadic).

The higher horizons of the Lower Tournaisian demonstrate a gradual transition to an open shallow shelf environment which was favorable for the settlement of benthic fauna and exposed to waves. Silty and sandy bioclastic limestones appeared in the section become predominant; carbonate sandstone and gritstone with quartz and chert grains, ooids, and intraclasts, as well as quartz cross-laminated sandstone, and wave ripples occur. Unit 6 is composed of grainstones with corals and brachiopods being the first in the section. The abundance of intraclasts and displaced fossils indicates redeposition of sedimentary material. Environments become even more active in the middle part of the Tournaisian: numerous sandstones and gritstones with a storm-generated cross-stratification, both mixed siliciclastic–carbonate and oligomictic (quartz and chert grains) are widespread, sometimes with plant detritus. Bioclastic limestones and sandstone are often poorly sorted. Such rocks were apparently deposited at a greater distance from the coast, under the influence of storm waves and currents which carried clastic material from the coastal part of the basin. Some beds demonstrate bioturbation at their tops corresponding to the calm conditions between the storms. Predominantly clayey deposits of overlying units 9 and 10 were presumably accumulated at somewhat greater depths; quartz sandstone interlayers with current ripples and load marks could have been deposited as relatively distal tempestites. The origin of numerous ooids in the black shales at the top of unit 10 remains unclear. Outwardly, these rocks resemble the Mesozoic tasmanite shales.

The upper Tournaisian and lower Visean limestone and calcareous shale containing numerous fossils and devoid of wave- and storm-induced structures could have been formed either in the protected lagoon or in the open shelf or ramp (in the nomenclature of Pomar, 2001) slightly below the storm wave base. We prefer the second possibility for the following reasons. Solitary corals abounding in this part of the section (units 12–15) are characteristic of a relatively deep-water "Cyathaxonia fauna." Storm deposits are widespread down the section relative to the considered interval, while

deeper water rocks are located higher (see below). There are no signs of reef facies in the Lower Carboniferous on the New Siberian Islands; the Tas-Ary Formation rocks were most likely deposited not in the rimmed shelf. We should clarify that our interpretation of deposits at the base of the formation (units 1–4) as lagoon types implies a narrow shallow coastal lagoon restricted by some shoal, as in the model proposed by (Burchette and Wright, 1992) for a carbonate ramp. This is not about a vast shelf lagoon separated by a barrier reef from the deep-sea basin. During the late Tournaisian–early Visean, the depositional settings generally remained fairly stable although some sea level fluctuations obviously took place.

A new phase of basin deepening started in the early Visean. Its beginning is marked in the section by black shales with pyrite and siderite (unit 16a). The entire overlying part of the Tas-Ary section is represented by fairly uniform facies dominated by fine-grained spiculite limestones being bioturbated and clayey in the lower half. Macrofossils in this part of the formation includes almost only crinoid fragments; corals and brachiopods (displaced) were found only at a few levels. Pyrite is present. Near the top of the Tas-Ary Formation, rocks contain more siliciclastic material and lots of displaced fossil fragments. The transition to the Bel'kov Formation is gradual, but fast. This is due to a relatively abrupt change in the depositional settings at the end of the Visean–Serpukhovian: the facies of the open, although fairly deep, shelf are replaced by the "basin" ones. Black carbonaceous shales appear in the lower, transitional, part of the section, but carbonate rocks still play a significant role. However, almost all of the latter were deposited by turbidity flows, like carbonate–siliciclastic sandstones and gritstones, which are common there. Clastic rocks are enriched in crushed fauna fragments; they could have been ground only in an upper shoreface to foreshore zone or on some shoals, where the siliciclastic material was also supplied. Turbidity currents transported coastal sand to the deep anoxic part of the basin. Presumably, the accumulation of these rocks was preceded by the drainage of incompletely lithified carbonate sediment in the source area, its erosion, and crushing by waves. A new clastic source appeared at the end of the Early Carboniferous on land resulted in admixture of feldspar and volcanic rock fragments in sandstones. This source became a major one for sandstones and siltstones of the Middle Carboniferous–Permian.

The carbonate clastics almost disappeared in the Bashkirian. The entire overlying section is represented by mudstone (including carbonaceous shales) and siltstone with units of siliciclastic turbidite sandstone. Taking into account the fact that the deposits of member 8 of the Bel'kov Formation were accumulated no earlier than at the end of the Middle Permian (Chapter 6), the Middle Carboniferous–Middle Permian interval (50–60 m.y.) is only approximately 140 m thick. Given that a significant part of this interval is composed of turbidite sandstones deposited almost instantly, the background sedimentation during this period was extremely slow, and the section is condensed.

Hence, the Carboniferous–Permian section studied in the Tas-Ary Peninsula demonstrates a gradual change in the depositional settings from the shallow shelf to the deep-water basin. The Tas-Ary Formation is marked by small-order cycles complicating the general trend. They are most pronounced in the middle part of the formation (Fig. 4, units 13–15, 16–17). The cycles are asymmetrical: the transition (up the section) from relatively deep-water to shallower-water rocks is gradual, while the reverse replacement is very fast. The latter could have been caused by syndepositional faulting. We interpret the Tas-Ary Formation as deposits of homoclinal (?) ramp with a mixed sedimentation pattern: the formation is dominated by carbonate rocks containing siliciclastic admixture throughout the section, abundant in some intervals. The largest proportion of siliciclastic material is characteristic of the shallowest (above the storm wave base) and, on the contrary, the deepest facies of the Tas-Ary Formation. Although we observe their replacement in a vertical section, it can be assumed that it largely corresponds to a lateral distribution of the ramp facies. This idea is aligned with the model (Yancey, 1991) for the carbonate–siliciclastic shelf according to which there is an intermediate carbonate accumulation zone between the shallow and deep-water zones where predominantly siliciclastic material accumulates.

The Bel'kov Formation deposits correspond to a different stage in the basin development. It can be assumed that its bottom profile changed in the late Visean–early Serpukhovian: a bend separating the shallow shelf (narrow at that time) from the deep-water basin appeared. This transformation was likely related to active normal faulting. The Bel'kov Formation is represented by slope deposits. In the visible upper part of the formation, they are more distal and could have been accumulated at the toe of the slope.

PALAEOGEOGRAPHY OF THE NEW SIBERIAN ISLANDS IN THE LATE PALAEOZOIC AND CORRELATION WITH TAIMYR AND SIBERIAN PLATFORM

M.K. Kos'ko et al. (for example, Kos'ko and Korago, 2009) established the facies zoning inherited from the Late Devonian for the Lower–Middle Carboniferous deposits of Kotel'ny and Bel'kov islands. Two zones were identified: the southwestern deep-water zone covering Bel'kov Island and the southwestern half of Kotel'ny Island, and the northeastern shallow zone. The deposits of most part of the Tournaisian-Serpukhovian were previously believed to be absent on the Bel'kov Island. According to our observations (Pease et al., 2015; Chapter 8.2), deposits of the Bel'kov For-

mation conformably overlie the Upper Devonian rocks on this island. Considering this, it seems appropriate to point out a transition facies zone. This zone is assumed to include the southwestern part of Kotel'ny Island (including the Tas-Ary Peninsula), where the Lower Carboniferous deposits are lithologically different from those on Bel'kov Island (Fig. 2).

The Carboniferous–Permian Deposits in Other Areas of Kotel'ny Island

In the southwestern part of Kotel'ny Island (transition zone), the Lower Carboniferous is represented by the Tas-Ary Formation (M.K. Kos'ko's nomenclature, including the Serpukhovian deposits). This formation, except for the Tas-Ary Peninsula, crops out in two areas: south of the peninsula (lower reaches of the Khos-Teryuttyakh River) and in the southeast of the island. In both regions, the lithology of the formation is similar to that in the key section (Kos'ko et al., 1985). Within the northeastern shallow facies zone, the Lower Carboniferous deposits form a vast field in the east of Kotel'ny Island (near the proposed boundary with the intermediate zone), and they are also known in the local outcrop in the north of the island. In the first case, they are represented by a formation of fine-grained and clayey limestones 300–400 m thick containing bioclastic interlayers with upper Tournaisian, Visean, and Serpukhovian fossils. This limestone unit overlies older rocks with an angular unconformity; conglomerates with quartz and chert pebbles were noted at its base (Kos'ko et al., 1985). Scattered debris of dark gray mudstones of presumably continental genesis with Visean miospores were described in the northern part of the island (Dibner, 1982; Kos'ko and Korago, 2009).

The younger deposits of the Upper Palaeozoic in the transitional facies zone, except for the Tas-Ary Peninsula, were also mapped in a small outcrop in the southeast of Kotel'ny Island. These rocks were attributed to the Bel'kov Formation. The age of the exposed part likely does not go beyond the Middle Carboniferous. In the shallow-water zone, the upper parts of the Palaeozoic section are assigned to a single thin Middle Carboniferous–Permian formation overlying with a stratigraphic unconformity the Devonian rocks (Kos'ko et al., 1985). This formation is composed of shallow-water carbonate rocks in the center of Kotel'ny Island, with a total thickness of a few tens of meters. In the northwest, it has a more diverse composition and a greater thickness. Limestones form only its lower part (not less than 70 m), while the higher horizons of the section consist of shallow-marine mudstone with siltstone and sandstone interlayers (about 200 m). According to the earlier suggestions, the boundary between the carbonate and terrigenous units approximately corresponds to the base or the lowest part of the Permian (Kos'ko et al., 1985; Konstantinov, 2001 and references therein), but the recent findings of Artinskian foraminifera and brachiopods at the top of the carbonate section (Filimonova et al., 2015) make us doubt this. This question requires further studies.

The Carboniferous–Permian on Bel'kov Island (Deep-Water Zone)

The upper part of the Palaeozoic section on Bel'kov Island was mapped as a part of the Bel'kov Formation which was identified in this area by V.F. Nepomiluev (Kos'ko et al., 1985). This barren formation was previously attributed to the Middle Carboniferous (Bashkirian) by analogy with the section on the Tas-Ary Peninsula. According to our data, it conformably overlies limestones with the upper Famennian–lower Tournaisian fauna, and the age of the formation covers the interval from the beginning of the Carboniferous to the Early Permian inclusively (not older than 280 Ma) (Pease et al., 2015). The upper part of the section is likely much younger: it contains subvolcanic basaltic intrusions which were emplaced into the semiliquid sediment and are similar in age and petrographic and geochemical features to the Siberian traps (Kuzmichev and Pease, 2007). It is possible that the formation also includes a part of the Triassic. Thus, the lower boundary of the Bel'kov Formation is diachronous: it roughly corresponds to the Visean–Serpukhovian boundary on Kotel'ny Island and to the lower part of the Tournaisian on Bel'kov Island (in this area, the lower part of the formation is coeval with the Tas-Ary Formation).

The deposits of the Bel'kov Formation on Bel'kov Island are similar in lithology to those in the Tas-Ary section, but are generally more distal. They are represented mainly by dark gray and black shales, occasionally bioturbated, and contain siderite and phosphatic concretions and intervals with thin siltstone and sandstone interlayers, sometimes interrupted by slump folds and syndepositional faults. We interpret such intervals as distal turbidites partly redeposited by along-slope bottom currents. The upper half (?) of the section contains rare packs of turbidite sandstones. In mineral composition, they are similar to sandstones of the top of the Tas-Ary Peninsula section. The total thickness of the formation on the Bel'kov Island is more than 1 km.

The Upper Palaeozoic of Taimyr, North of the Siberian Platform, and Northern Verkhoyansk Fold Belt

Taimyr. The Lower Carboniferous of Taimyr is traditionally interpreted as deposits of the Siberian passive margin (for example, Nikishin et al., 2010). In general, they are represented mainly by carbonate rocks; in the western part of the peninsula, clayey shales also play an important role (Sobolev, 1999). The deposits of this age are most thoroughly studied in the Lake Taimyr area; the Lower Carboniferous key

section was described there (upper reaches of the Nyunkaraku-Tari River) (Mikhailov and Tschernjak, 1972; Bezzubtsev et al., 1986; Sobolev, 1999). The Tournaisian–lower Visean (75 m) deposits in this section are represented by detrital limestone, sometimes silty (cross-stratification was noted), usually with abundant benthic fauna; silty shale interlayers and packs can be observed. Bauxites are located at the base. Such lithological composition (except for bauxites) is similar to that in the upper part of the upper lower Tournaisian–upper Tournaisian on the Tas-Ary Peninsula. The middle part of the Visean of the Taimyr key section (70 m) is characterized by fine-grained, clayey, and bioclastic limestones; detrital limestones with fossils are predominant up-section (100 m); very fine-grained limestones and dolostones are minor; the rocks contain sand and silt at some levels. The upper part of the Visean (50 m) is composed of very fine-grained limestone with chert nodules, while the Serpukhovian (about 100 m (?)) is composed of detrital limestone, including numerous fossils; chert concretions are still observed. A considerable quartz sand and silt admixture appear at the top of the Lower Carboniferous section.

It can be concluded from the above description that the considered section has much in common with the Tas-Ary section also in its Visean part: in both areas, clayey and fine-grained limestones are widespread in the middle Visean, while very fine-grained (micritic?) limestones with cherts occur in the upper part. A large amount of siliciclastic material in detrital limestones at the top of the Serpukhovian in Taimyr can be aligned with the presence of siliciclastic–carbonate sandstones in the lower part of the Bel'kov Formation on Kotel'ny Island. Taking into account such analogies, we can suggest that the Early Carboniferous in the central Taimyr and southwest of Kotel'ny Island were characterized by similar depositional environments, and they changed approximately synchronously. It should be noted that relatively deep-water Lower Carboniferous facies were observed to the south of the Taimyrian key section (*Gosudarstvennaya...*, 2009; Sobolev, 1999). This fact was likely caused by local reasons (depression in the shelf (?)), and it does not contradict the general trend of the Taimyr basin deepening to the north–northeast.

As in the Tas-Ary Peninsula, carbonate deposits in Taimyr disappear from the section approximately at the Early–Middle Carboniferous boundary. From this time and until the end of the Permian, a thick formation composed of sandstone, siltstone, and mudstone in various combinations, containing hard coal seams have been accumulated throughout the Mountain Taimyr region (more than 5 km thick in the east of Taimyr) (Proskurnin et al., 2013). This formation is characterized by regressive cycles. Carbonate rocks can be found in some sections in the lower, transitional, part of the formation (Bashkirian). The Middle Carboniferous–Permian terrigenous deposits of Taimyr are considered to be formed in the foreland basin which developed in front of the Northern Taimyr orogen in the course of collision of the Kara block and Siberia (for example, Kuzmichev, 2009; Nikishin et al., 2010).

North of the Siberian Platform. In the north of the Siberian Platform near the Nordvik Peninsula, the Lower Carboniferous is also composed mainly of carbonate rocks which occasionally overlie older deposits with a stratigraphic unconformity (*Gosudarstvennaya...*, 2009; Proskurnin et al., 2013). They are represented by limestone with calcareous shale interbeds (Tournaisian and upper part of the Visean); the lower Visean is characterized by bioclastic limestone with anhydrite and gypsum interlayers. Oolitic limestones are common for the upper Visean in some sections. The total thickness of the Lower Carboniferous rocks reaches 600–850 m (in the most complete sections). They are overlain by the terrigenous mostly marine Permian deposits of about 1.5 km thick with a ravinement surface at the base. To the east, up to the Lena River delta, the Carboniferous deposits are not exposed; the Permian deposits are more widespread and demonstrate the same composition as in the Nordvik area. To the south, they rapidly decrease in thickness and change to the continental facies (Ershova et al., 2016 and references therein).

Northern Verkhoyansk fold belt. In the lower reaches of the Lena River (Kharaulakh mountains), deposits of the deformed margin of the Siberian Platform, mapped as a part of the Verkhoyansk belt, are exposed. The Tournaisian deposits in this area are similar to those in the Tas-Ary section. Its lower part consists of sandy dolostones and limestones (50 m), while the upper part is dominated by bioclastic limestones with chert nodules and limy mudstone interlayers (Yuferev, 1973; Ershova et al., 2011). The Visean was marked by basin deepening as well as in the west of the Kotel'ny Island; however, the rock composition was different. The Verkhoyansk complex began to accumulate in the northeastern margin of Siberia. Heterogeneous facies are characteristic of the Visean here. In the northwesternmost section (Bykov channel head of the Lena River delta), the Visean deposits were described as sandy turbidites with conglomerates and gritstones; in the upper part, as fine-grained turbidites (total thickness up to 400 m) (Ershova et al., 2011; Prokopiev et al., 2013). To the south, the coeval deposits (240 m) are mainly composed of mudstone and siltstone: in the lower part, with chert and siliceous shale, and in the upper part, with limestone and sandstone containing plant detritus (Yuferev, 1973). The Lower Carboniferous section is crowned by a thick mudstone unit (up to 900 m, upper Visean–Serpukhovian–lower Bashkirian (?)) with sparse siltstone and calcareous sandstone interlayers interpreted as distal fine-grained turbidites (Prokopiev et al., 2013). The top of the formation comprises interbeds of bioclastic limestones and carbonate conglomerates (Yuferev, 1973). The Ser-

pukhovian deposits near Lena delta share some similarities with the lower part of the Bel'kov Formation on the Tas-Ary Peninsula, although their thickness is lower by an order of magnitude there. The Tas-Ary Peninsula section is enriched in shales and also contains siliciclastic–carbonate turbidites, which, in particular, make up a thick unit approximately at the Lower–Middle Carboniferous boundary.

The Middle–Upper Carboniferous rocks in the Kharaulakh mountains are represented by delta (Prokopiev et al., 2013) sandstone and siltstone (400 m). The Permian section is composed of siltstone, mudstone, and sandstone with a total thickness of more than 1.5 km, with a regressive cyclicity and marine fossils (Abramov and Grigor'eva, 1988). More shallow water origin of the Middle Carboniferous–Permian deposits in comparison with the underlying ones can be explained by the eastward delta progradation. At the same time, hemipelagic sediments and turbidites have been accumulated away from the Siberian Platform (*Tektonika...*, 2001).

Hence, the predominantly terrigenous sedimentation in the present-day Northern Verkhoyansk fold belt began earlier (Visean) than in the neighboring areas discussed above. However, the carbonate sedimentation continued at that time to the west (Kutyungde graben) in the shallow-marine and lagoonal settings (Smetannikova et al., 2013).

CONCLUSIONS

The detailed study of the Upper Palaeozoic section on the Tas-Ary Peninsula allowed to clarify significantly the age and lithology of the stratigraphic subdivisions identified there. The lower part of the section (not less than 950 m) which corresponds to the Tas-Ary Formation includes shelf, mainly carbonate deposits of the Tournaisian and Visean. The overlying Bel'kov Formation (not less than 300 m) is dominated by deeper water mudstone and sandstone of the Serpukhovian–Middle (?) Permian. The most numerous fossil findings originate from the middle part of the Tas-Ary Formation (brachiopods, conodonts, and corals) and the lower part of the Bel'kov Formation (brachiopods, conodonts, and foraminifera). The proposed position of the lower boundary of the Tas-Ary Formation is not substantiated by fossils owing to their absence in the Devonian–Lower Carboniferous; however, it seems preferable relative to the previous variant (Kos'ko et al., 1985) for sedimentological reasons, at least in the Tas-Ary section. Visible tops of the Bel'kov Formation were formed not earlier than at the end of the Middle Permian, which is justified by detrital zircon dating.

We reconstructed a gradual evolution of the depositional settings from coastal-marine in the Famennian to open shelf: shallow water during the Tournaisian, slightly below the storm wave base at the end of this age and more deep-water in the Visean. The Serpukhovian was marked by a new stage in the basin deepening: its bottom profile changed likely due to active faulting, and the late Early Carboniferous–Middle Permian deposits were accumulated on a well-defined slope. In addition, a new source of immature siliciclastic material appeared in the Serpukhovian and became predominant in the second half of the Carboniferous. It supplied the basin with volcanic rock fragments of different composition as well as plagioclase, quartz, and microcline (throughout the underlying section up to the Famennian inclusively, the terrigenous admixture is represented only by quartz and chert).

Comparison of the studied section with the coeval formations exposed in other areas of the New Siberian Islands makes it possible to reconstruct the homoclinal (?) ramp in the western part of the archipelago for the Tournaisian–Visean time, which was dominated by carbonate sedimentation; this ramp was adjacent to the land (the recent central part of Kotel'ny Island) and passed into a deep-water shale basin to the west–southwest (Bel'kov Island). At the end of the Visean–Serpukhovian, some tectonic events caused changes in the configuration of the basin and depositional environments. This was likely related to growth of the Northern Taimyr orogen. During the Middle Carboniferous–Middle Permian, limestones were accumulated only in a narrow (?) shallow-water zone which occupied the present central areas of Kotel'ny Island and, in the pre-Artinskian time, the northwestern areas of this island. A complex of slope sediments with turbidites and black shales was formed to the southwest. The clastic material was supplied from the Northern Taimyr orogen, while carbonate sediments of the shallow-water zone were an additional source of clastics (mainly for Serpukhovian sandstones).

The significant similarity of the Lower Carboniferous part of the section exposed in the Tas-Ary Peninsula to the key section of the Lower Carboniferous of Taimyr, the synchronous shift from carbonate sedimentation to terrigenous one, and single clastic source for the Upper Carboniferous (?)–Permian sandstones of both regions indicate their belonging to the same sedimentary basin in the Late Palaeozoic. However, in the Southern Taimyr region, a shallow-water foreland basin is reconstructed which to the south (in modern coordinates) was replaced by coastal and continental facies of less downwarped areas of the Siberian Platform, while for the Carboniferous–Permian formations of the New Siberian Islands, it is more logical to assume a passive continental margin setting. This assumption can also be confirmed by the fact that the Upper Palaeozoic facies zoning of the archipelago inherits that of the Late Devonian. In other words, the deep-water basin in the western part of the New Siberian Islands existed at least from the beginning of the Frasnian Age to the Middle Permian inclusively (more than 100 m.y.). At first glance, the replacement of the

Upper Devonian–Permian shallow-water facies by deep-water ones in the southwestern direction (in the recent structure) points that the New Siberian Islands were separated from Siberia by a deep (oceanic (?)) basin. But if we take into consideration the two-polar rotational model of the Mesozoic Amerasian basin opening (Kuzmichev, 2009), in the pre-Late Jurassic, the area of the archipelago can be reconstructed as turned 90 degrees counterclockwise relative to its present position; in this case, the deep-water facies of Bel'kov Island occur on the strike of the Verkhoyansk margin of Siberia. Such an assumption certainly requires further studies; meanwhile, it is in good agreement with the above-mentioned similarity of the Carboniferous–Permian deposits of the New Siberian Islands and Taimyr, with common features in the sedimentation evolution and lithology between the Upper Palaeozoic section of Bel'kov and Kotel'ny islands and the Verkhoyansk belt, and with the occurrence of Siberian Permian–Triassic traps in the archipelago (Kuzmichev and Pease, 2007).

ACKNOWLEDGMENTS

We are grateful to B.B. Levochsky for his help in the field reconnaissance study of the Tas-Ary section, E.I. Kulagina for her advice in the identification of foraminifera, and J. Hourigan for providing the instrumentation base and instructions for zircon dating by LA-ICP-MS.

FUNDING

This work was supported by the Russian Science Foundation (project no. 17-77-10123). Isotopic dating of zircons was funded by the Russian Foundation for Basic Research (RFBR) (project no. 16-05-00176). Final processing of data was supported by the RFBR (project no. 19-05-00926). The investigations were carried out in accordance with the scientific research plans of the Geological Institute, Russian Academy of Sciences (M.K. Danukalova and A.B. Kuzmichev, project no. 0135-2019-0051; T.N. Isakova, project no. 0135-2019-0062; and V.G. Ganelin, project no. 0135-2019-0057). The work of O.L. Kossovaya was supported by the Program of Competitive Growth of Kazan Federal University among the World's Leading Academic Centers and has been performed following the research plans of the Karpinsky Russian Geological Research Institute (project no. 04900031-1600). The work of V.G. Ganelin was partially supported by the Program of the Presidium of the Russian Academy of Sciences "Evolution of the Organic World. Role and Effect of the Planetary Events."

SUPPLEMENTARY MATERIALS

Supplementary materials are available for this at doi 10.1134/S0869593819070013 and are accessible for authorized users.

Reviewer A.S. Byakov

REFERENCES

Abramov, B.S. and Grigor'eva, A.D., *Biostratigrafiya i brakhiopody permi Verkhoyan'ya* (Biostratigraphy and Brachiopods of the Permian of the Verkhoyansk Region), Moscow: Nauka, 1988 [in Russian].

Alekseev, A.S., Carboniferous System, in *Sostoyanie izuchennosti stratigrafii dokembriya i fanerozoya Rossii. Zadachi dal'neishikh issledovanii. Postanovleniya Mezhvedomstvennogo stratigraficheskogo komiteta i ego postoyannykh komissii. Vyp. 38* (State of Knowledge of the Precambrian and Phanerozoic Stratigraphy in Russia: Tasks for Further Investigations. Resolutions of the Interdepartmental Stratigraphic Committee and Its Permanent Stratigraphic Commissions. Vol. 38), St. Petersburg: Vseross. Nauchno-Issled. Geol. Inst., 2008, pp. 61–68.

Alekseev, A.S., Lebedev, O.A., Barskov, I.S., Kononova, L.I., and Chizhova, V.A., On the stratigraphic position of the Famennian and Tournaisian fossil vertebrate beds in Andreyevka, Tula Region, Central Russia, *Proc. Geol. Assoc.*, 1994, vol. 105, pp. 41–52.

Austin, R.L., Evidence from Great Britain and Ireland concerning West European Dinantian conodont palaeoecology, in *Conodont Palaeoecology*, Barnes, C.R., Ed., *Geol. Assoc. Canada Spec. Pap.*, 1976, vol. 15, pp. 201–224.

Austin, R.L., Husri, S., and Conil, R., *Correlation and age of the Dinantian rocks north and south of the Shannon*, Ireland, *Congr. Colloq. Univ. Liège*, 1970, vol. 55, pp. 179–192.

Baesemann, J.F. and Lane, H.R., Taxonomy and evolution of the genus *Rhachistognathus* Dunn (Conodonta: Late Mississippian to Early Middle Pennsylvanian), *Cour. Forsch.– Inst. Senckenberg*, 1985, vol. 74, pp. 93–136.

Bahrami, A., Corradini, C., and Yazdi, M., Upper Devonian–Lower Carboniferous conodont biostratigraphy in the Shotori Range, Tabas area, Central-East Iran Microplate, *Boll. Soc. Palaeontol. Italiana*, 2011, vol. 50, no. 1, pp. 35–53.

Barskov, I.S., Kononova, L.I., and Migdisova, A.V., Conodonts from Lower Turnesian deposits of the Moscow Basin, in *Palaeontologicheskaya kharakteristika stratotipicheskikh opornykh razrezov karbona Moskovskoi sineklizy* (Palaeontological Characteristic of Carboniferous Reference Sections in the Moscow Syneclise), Menner, V.V., Ed., Moscow: Mosk. Gos. Univ., 1984, pp. 3–33.

Bezzubtsev, V.V., Zalyaleev, R.Sh., and Sakovich, A.B., *Geologicheskaya karta Gornogo Taimyra. Masshtab 1 : 500000. Ob"yasnitel'naya zapiska* (The 1 : 500000 Geological Map of the Taimyr Mountains. Explanatory Note), Bezzubtsev, V.V., Ed., Krasnoyarssk, 1986 [in Russian].

Bischoff, G., Die conodonten-stratigraphie des rheno-herzynischen Unterkarbons mit Beriicksichtigung der Wocklumeria-Stufe und der Karbon/Devon – Grenze, *Abh. Hess. Landesamtes Bodenforsch.*, 1957, vol. 19, pp. 1–64.

Blanco-Ferrera, S., García-López, S., and Sanz-López, J., Conodontos carboníferos de la sección del río Cares (Unidad de Picos de Europa, Zona Cantábrica, N de España), *Geobios*, 2005, vol. 38, pp. 17–27.

Bogush, O.I. and Yuferev, O.V., The Carboniferous of the Omolon and the southwestern part of the Kolyma massifs, in *Tr. Inst. Geol. Geofiz. Sib. Otd. AN SSSR. Vyp. 60* (Trans.

Inst. Geol. Geophys. Sib. Branch USSR Acad. Sci. Vol. 60), Moscow: Nauka, 1970, pp. 68–73.

Boland, K., Étude des Tétracoralliaires des couches de transition de la limite Tournaisien/Viséen en Europe occidentale, in *Thèse Inéditée, Université de Liège, Faculté des Sciences, Service de Paléontologie Animale*, 2002, pp. I–XI, 1–390.

Bouckaert, J. and Groessens, E., *Polygnathus paprothae, Pseudopolygnathus conili, Pseudopolygnathus graulichi*: espèces nouvelles à la limite Dévonien–Carbonifère, *Ann. Soc. Géol. Belg.*, 1976, vol. 99, pp. 65–67.

Branson, E.B. and Mehl, M.G., New and little known Carboniferous conodont genera, *J. Palaeontol.*, 1941, vol. 15, no. 2, pp. 97–106.

Bromley, R.G., Uchman, A., Gregory, M.R., and Martin, A.J., Hillichnus lobosensis igen. et isp. nov., a complex trace fossil produced by tellinacean bivalves, Palaeocene, Monterey, California, USA, *Palaeogeogr., Palaeoclimatol., Palaeoecol.*, 2003, vol. 192, pp. 157–186.

Burchette, T.P. and Wright, V.P., Carbonate ramp depositional systems, *Sediment. Geol.*, 1992, vol. 79, pp. 3–57.

Bushmina, L.S. and Kononova, L.I., *Mikrofauna i biostratigrafiya pogranichnykh sloev devona i karbona (yug Zapadnoi Sibiri)* (Microfauna and Biostratigraphy of the Devonian–Carboniferous Boundary Beds (Southern Western Siberia)), Moscow: Nauka, 1981 [in Russian].

Tschernjak, G.E., Solov'eva, M.F., Rogozov, Yu.G., and Dedok, T.A., Biostratigraphy of the Lower Carboniferous reference section in the Eastern Taimyr, in *Sb. statei "Opornyi razrez nizhnekamennougol'nykh otlozhenii Vostochnogo Taimyra"* (Coll. Sci. Works "*The Reference Section of the Lower Carboniferous Deposits of the Eastern Taimyr*"), Cherkesov, S.V. and Tschernjak, G.E., Eds., Leningrad: Nauchno-Issled. Inst. Geol. Arktiki, 1972, pp. 11–37.

Clifton, E., *Hillichnus, A Feathery, Enigmatic Trace Fossil*, 2013. http://www.sjvgeology.org/geology/trace_fossils.html#hillichnus.

Danukalova, M.K. and Kuzmichev, A.B., Sandy intrusions in the Carboniferous deposits of Kotel'ny Island: composition, morphology, reasons and the formation mechanism, in *Mater. XLVIII Tekton. soveshch. "Tektonika, geodinamika i rudogenez skladchatykh poyasov i platform". T. 1* (Proc. XLVIII Tecton. Conf. "Tectonics, Geodynamics, and Ore Genesis of Folded Belts and Platforms." Vol. 1), Moscow: GEOS, 2016, pp. 133–136.

Denayer, J. and Hosŋgör, I., Lower Carboniferous rugose corals from the Arabian Plate: An insight from the Hakkari area (SE Turkey), *J. Asian Earth Sci.*, 2014, vol. 79, pp. 345–357.

Denayer, J., Poty, E., and Aretz, M., Atlas-Uppermost Devonian and Dinantian rugose corals from Southern Belgium and surrounding areas, in *Proc. 11th Symposium on Fossil Cnidaria and Porifera, Liege, 2011*, Aretz, M. and Poty, E., Eds., *Kölner Forum Geol. Paläont.*, 2011, vol. 20, pp. 151–201.

Dibner, A.F., Palynological substantiation of the stage subdivision of Carboniferous and Permian deposits in Soviet Arctic islands, in *Sb. nauchn. tr. "Mikrofossilii polyarnykh oblastei i ikh stratigraficheskoe znachenie"* (Coll. Sci. Works "Microfossils of Polar Regions and Their Stratigraphic Significance"), Leningrad: PGO "Sevmorgeologiya", 1982, pp. 63–73.

Dobrolyubova, T.A., Kabakovich, N.V., and Sayutina, T.A., The Lower Carboniferous corals from the Kuznetsk Depression, in *Tr. PIN. T. 111* (Trans. Palaeontol. Inst. Vol. 111), Moscow: Nauka, 1966.

Domeier, M. and Torsvik, T.H., Plate tectonics in the late Palaeozoic, *Geosci. Frontiers*, 2014, vol. 5, pp. 303–350.

Druce, E.C., Devonian and Carboniferous conodonts from the Bonaparte Gulf Basin, Northern Australia and their use in international correlation, *Bull. Austral. Bur. Min. Res., Geol. Geophys.*, 1969, vol. 98, pp. 1–243.

Dunn, D.L., Late Mississippian conodonts from the Bird Spring Formation in Nevada, *J. Palaeontol.*, 1965, vol. 39, pp. 1145–1150.

Durkina, A.V., *Foraminifery serpukhovskogo yarusa Timano-Pechorskoi provintsii* (Foraminifers of the Serpukhovian Stage from the Timan–Pechora Province), St. Petersburg: Vseross. Nauchno-Issled. Geol. Inst., 2002 [in Russian].

Dzik, J., Emergence and succession of Carboniferous conodont and ammonoid communities in the Polish part of the Variscan sea, *Acta Palaeontol. Polon.*, 1997, vol. 42, no. 1, pp. 57–170.

Ershova, V.B., Khudoley, A.K., Prokopiev, A.V., and Vasiliev, D.A., The sedimentation environments and facies of the Lower Visean deposits in the north of the Siberian Platform (the lower reaches of Lena River), in *Sovremennoe sostoyanie nauk o Zemle* (The Current State of the Earth Sciences), Moscow: Mosk. Gos. Univ., 2011, pp. 634–637.

Ershova, V.B., Prokopiev, A.V., Khudoley, A.K., Sobolev, N.N., and Petrov, E.O., U/Pb dating of detrital zircons from late Palaeozoic deposits of Bel'kovsky Island (New Siberian Islands): Critical testing of Arctic tectonic models, *Int. Geol. Rev.*, 2015, vol. 57, no. 2, pp. 199–210.

Ershova, V.B., Khudoley, A.K., Prokopiev, A.V., Tuchkova, M.I., Fedorov, P.V., Kazakova, G.G., Shishlov, S.B., and O'Sullivan, P., Trans-Siberian Permian rivers: A key to understanding Arctic sedimentary provenance, *Tectonophysics*, 2016, vol. 691, pp. 220–233.

Fedorowski, J., Some peculiar rugose coral taxa from Upper Serpukhovian strata of Czech Republic, *Acta Geol. Polon.*, 2010, vol. 60, no. 2, pp. 165–198.

Fedorowski, J., The new Upper Serpukhovian genus *Zaphrufimia* and homeomorphism in some rugose corals, *Palaeontographica, A*, 2012, vol. 296, pp. 109–161.

Fedorowski, J., Tournaisian and Viséan *Lophophyllum* of Gorskiy (1932) from the Kirghiz Steppe and a possible ancestor of a new Bashkirian rugose coral genus from the Donets Basin (Ukraine), *Geologos*, 2017, vol. 23, no. 3, pp. 215–221.

Fedorowski, J. and Kullmann, J., Voinovskytesidae – a new family of Mississippian Rugosa (Anthozoa), *Acta Geol. Polon.*, 2013, vol. 63, no. 4, pp. 657–679.

Filimonova, T.V., Ganelin, V.G., Danukalova, M.K., and Kuzmichev, A.B., The Artinskian assemblages of smaller foraminifers and brachiopods from Kotel'nyi Island (New

Siberian Islands, Russia), in *XVIII Int. Congr. on the Carboniferous and Permian. August 11–15, 2015, Kazan, Russia. Abstr. Vol.*, Nurgaliev, D.K., Alekseev, A.S., Della Porta, G., Kossovaya, O.L., Kotlyar, G.V., Nikolaeva, S.V., Silantiev, V.V., and Urazaeva, M.N., Eds., Kazan: Kazan Univ. Press, 2015.

Folk, R.L., Spectral subdivision of limestone types, in *Classification of carbonate Rocks – A Symposium*, Ham, W.E., Ed., *Am. Assoc. Petrol. Geol. Mem.*, 1962, no. 1, pp. 62–84.

Gagiev, M.Kh., *Konodonty iz pogranichnykh otlozhenii devona i karbona Omolonskogo massiva. Putevoditel' ekskursii po turu IX k 14-mu Tikhookeanskomu nauchnomu kongressu. Pril. 2* (Conodonts from the Devonian–Carboniferous Boundary Deposits of the Omolon massif. Guidebook for Scientific Excursion (Tour IX) XIV Pacific Sci. Congr., Suppl. IX), Magadan, 1979 [in Russian].

Gagiev, M.Kh., *Stratigrafiya devona i karbona Prikolymskogo podnyatiya (Severo-Vostok Azii)* (Devonian and Carboniferous Stratigraphy of the Prikolymian Uplift (Northeastern Asia)), Magadan: Severovost. Kompl. Nauchno-Issled. Inst. Dalnevost. Otd. Ross. Akad. Nauk, 2009 [in Russian].

Ganelin, V.G. and Tschernjak, G.E., Marine basins of Northeast Asia, in *The Carboniferous of the World. III, Madrid: Inst.* Tecnol. Geomin. Espana, 1996, pp. 207–234.

Gibshman, N.B., Foraminifers from the Serpukhovian Stage stratotype, the Zabor'e Quarry site (Moscow region), *Stratigr. Geol. Correl.*, 2003, vol. 11, no. 1, pp. 36–60.

Gorskii, I.I., Corals from the Lower Carboniferous deposits of the Kyrgyz steppe, in *Tr. GGU VSNKh SSSR*, Moscow–Leningrad: Geolizdat, 1932, vol. 51.

Gosudarstvennaya geologicheskaya karta Rossiiskoi Federatsii. Masshtab 1 : 1000000 (novaya seriya). List S-53-55 - Novosibirskie ostrova. Ob"yasnitel'naya zapiska (The 1 : 1000000 State Geological Map of the Russian Federation (New Ser.). Sheet S-53-55–New Siberian Islands. Explanatory Note), St. Petersburg: Vseross. Nauchno-Issled. Geol. Inst., 1999 [in Russian]. *Gosudarstvennaya geologicheskaya karta Rossiiskoi Federatsii. Masshtab 1 : 1000000 (tret'e pokolenie). Seriya Taimyrsko-Severozemel'skaya. List S-48 - oz. Taimyr (vostochnaya chast'). Ob"yasnitel'naya zapiska* (The 1 : 1000000 State Geological Map of the Russian Federation, 3rd ed. Taimyr–Severnaya Zemlya Ser. Sheet S-48-Lake Taimyr (Eastern Part). Explanatory Note), St. Petersburg: Kartfabrika Vseross. Nauchno-Issled. Geol. Inst., 2009 [in Russian].

Hance, L., Poty, E., and Devuyst, F.-X., Tournaisian, *Geologica Belgica*, 2006, vol. 9, nos. 1–2, pp. 47–53.

Higgins, A.C., *Conodont zonation of the late Viséan–early Westphalian strata of the south and central Pennines of northern England*, *Bull. Geol. Surv. Great Britain*, 1975, vol. 53.

Higgins, A.C. and Bouckaert, J., Conodont stratigraphy and palaeontology of the Namurian of Belgium, *Mém. Expl. Cartes Géol. Min. Belg.*, 1968, no. 10, pp. 1–64.

Hill, D., *A Monograph on the Carboniferous Rugose Corals of Scotland*, London: The Palaeontograph. Soc., 1938–1941, pp. 1–213.

Ivanovskii, A.B., *Etyudy o rannekamennougol'nykh rugozakh* (Essays on the Early Carboniferous Rugosa), Moscow: Nauka, 1967 [in Russian].

Johnston, I.S. and Higgins, A.C., Conodont faunas from the Lower Carboniferous rocks at Hook Head, County Wexford, *J. Earth Sci. (Dublin)*, 1981, vol. 4, pp. 83–96.

Kabanov, P.B., Gibshman, N.B., Barskov, I.S., Alekseev, A.S., and Goreva, N.V., Zaborie Section. Lectostratotype of Serpukhovian Stage, in *Type and Reference Carboniferous Sections in the South Part of the Moscow Basin. Field Trip Guidebook of Int. I.U.S.C. Field Meet., August 11–12, 2009*, Alekseev, A.S. and Goreva, N.V., Eds., Moscow: Borissiak Palaeontol. Inst. RAS, 2009, pp. 45–64.

Kislyakov, S.G. and Eikhvald, L.P., New evidence of the age of the Korelskaya and Lamskaya suites, Western Priokhotye, *Tikhookean. Geol.*, 2004, vol. 23, no. 3, pp. 94–97.

Konstantinov, A.G., First finds of the Permian ammonoids in the Kotel'nyi Island, *Stratigr. Geol. Correl.*, 2001, vol. 9, no. 1, pp. 20–25.

Kos'ko, M. and Korago, E., Review of geology of the New Siberian Islands between the Laptev and the East Siberian Seas, North East Russia, in *Geology, Geophysics and Tectonics of Northeastern Russia: A Tribute to Leonid Parfenov*, Stone, D.B., Fujita, K., Layer, P.W., Miller, E.L., Prokopiev, A.V., Toro, J., Eds., *Stephan Mueller Spec. Publ.*, 2009, Ser. 4, pp. 45–64.

Kos'ko, M.K., Bondarenko, N.S., and Nepomiluev, V.F., *Gosudarstvennaya geologicheskaya karta SSSR masshtaba 1 : 200000. Listy T-54-XXXI, XXXXII, XXXXIII; S-53-IV, V, VI, XI, XII; S-54-VII, VIII, IX, XIII, XIV, XV. Ob"yasnitel'naya zapiska (The 1 : 200000 State Geological Map of the USSR. Sheets T-54-XXXI, XXXXII, XXXXIII; S-53-IV, V, VI, XI, XII; S-54-VII, VIII, IX, XIII, XIV, XV. Explanatory Note)*, Ustritskii, V.I., Ed., Moscow: Min. Geol., 1985 [in Russian].

Kossovaya, O.L., Borisenkov, K.V., Goreva, N.V., Isakova, T.N., Konovalova, M.V., and Oshurkova, M.V., Carboniferous System, in *Zonal'naya stratigrafiya fanerozoya Rossii* (Zonal Stratigraphy of the Phanerozoic in Russia), Koren', T.N., Ed., St. Petersburg: Vseross. Nauchno-Issled. Geol. Inst., 2006.

Kozitskaya, R.I., Kosenko, Z.A., Lipnyagov, O.M., and Nemirovskaya, T.I., *Konodonty karbona Donetskogo basseina* (Carboniferous Conodonts from the Donetsk Basin), Kiev: Naukova Dumka, 1978 [in Russian].

Krumhardt, A.P., Harris, A.G., and Watts, K.F., Lithostratigraphy, microlithofacies, and conodont biostratigraphy and biofacies of the Wahoo Limestone (Carboniferous), Eastern Sadlerochit Mountains, Northeast Brooks Range, Alaska, *U. S. Geol. Surv. Prof. Pap.*, 1996, vol. 1568, pp. 1–70.

Kulagina, E.I. and Gibshman, N.B., Foraminifer-based zonal subdivision of the Serpukhovian Stage, in *Stratigrafiya i palaeogeografiya karbona Evrazii* (Carboniferous Stratigraphy and Palaeogeography of Eurasia), Ekaterinburg: Inst. Geol. Geokhim. Ural. Otd. RAN, 2002, pp. 183–191.

Kulagina, E.I., Pazukhin, V.N., Nikolaeva, S.V., and Kochetova, N.N., Biozonation of the Syuran Horizon of the Bashkirian Stage in the Southern Urals as indicated by am-

monoids, conodonts, foraminifers and ostracodes, *Stratigr. Geol. Correl.*, 2000, vol. 8, no. 2, pp. 137–156.

Kulagina, E.I., Pazukhin, V.N., Kochetkova, N.M., Sinitsina, Z.A., and Kochetova, N.N., *Stratotipicheskie i opornye razrezy bashkirskogo yarusa karbona Yuzhnogo Urala* (The Stratotype and Reference Sections of the Bashkirian Stage (Carboniferous) in the Southern Urals), Ufa: Gilem, 2001 [in Russian].

Kuzmichev, A.B., Where does the South Anyui suture go in the New Siberian islands and Laptev Sea?: Implications for the Amerasia basin origin, *Tectonophysics*, 2009, vol. 463, nos. 1–4, pp. 86–108.

Kuzmichev, A.B. and Pease, V.L., Siberian trap magmatism on the New Siberian Islands: constraints for Arctic Mesozoic plate tectonic reconstructions, *J. Geol. Soc. (London, U. K.)*, 2007, vol. 164, pp. 959–968.

Lane, H.R. and Straka, J.J., Late Mississippian and Early Pennsylvanian conodonts Arkansas and Oklahoma, *Spec. Pap.–Geol. Soc. Am.*, 1974, vol. 152, Lane, H.R., Sandberg, C.A., and Ziegler, W., Taxonomy and phylogeny of some Lower Carboniferous conodonts and preliminary standard post-Siphonodella zonation, *Geol. Palaeontol.*, 1980, vol. 14, pp. 117–164.

Litvinovich, N.V., *Beleutella* – a new genus of the Carboniferous productid brachiopods, *Palaeontol. Zh.*, 1967, no. 3, pp. 55–61.

Menning, M., Alekseev, A.S., Chuvashov, B.I., Davydov, V.I., et al., Global time scale and regional stratigraphic reference scales of Central and West Europe, East Europe, Tethys, South China, and North America as used in the Devonian–Carboniferous-Permian Correlation Chart 2003 (DCP 2003), *Palaeogeogr., Palaeoclimatol., Palaeoecol.*, 2006, vol. 240, pp. 318–372.

Mikhailov, Yu.A. and Tschernjak, G.E., The description of the reference section, in *Sb. statei "Opornyi razrez nizhnekamennougol'nykh otlozhenii Vostochnogo Taimyra"* (Coll. Sci. Works "*The Reference Section of the Lower Carboniferous Deposits of the Eastern Taimyr*"), Cherkesov, S.V. and Tschernjak, G.E., Eds., Leningrad: Nauchno-Issled. Inst. Geol. Arktiki, 1972, pp. 6–11.

Miklukho-Maclay, A.D., New Early Carboniferous asteroarchaediscids, in *Novye vidy rastenii i bespozvonochnykh SSSR* (New Species of Fossil Plants and Invertebrates of the USSR), Leningrad: Vseross. Nauchno-Issled. Geol. Inst., 1960. Pt. I.

Mitchell, M. and Somerville, I.D., A new species of Sychnoelasma (Rugosa) from the Dinantian of the British Isles: Its phylogeny and biostarigraphical significance, *Proc. Yorkshire Geol. Soc.*, 1988, vol. 47, no. 2, pp. 175–162.

Mull, C.G., Harris, A.G., and Carter, J.L., Lower Mississippian (Kinderhookian) biostratigraphy and lithostratigraphy of the western Endicott Mountains, Brooks Range, Alaska, in *Geologic Studies in Alaska by the U.S. Geological Survey.* 1995, Dumoulin, J.A. and Gray, J.E., Eds., *U. S. Geol. Serv. Prof. Pap.*, 1995, vol. 1574, pp. 221–242.

Nalivkin, D.V., *Brakhiopody turneiskogo yarusa Urala* (Brachiopods from the Tournaisian Stage of the Urals), Leningrad: Nauka, 1979 [in Russian].

Nemyrovska, T.I., Late Visean/early Serpukhovian conodont succession from the Triollo section, Palencia (Cantabrian Mountains, Spain), *Scr. Geol.*, 2005, vol. 129, pp. 13–89.

Nemirovskaya, T., Perret, M.-F., and Meischner, D., Lochriea ziegleri and Lochriea senckenbergica – new conodont species from the latest Viséan and Serpukhovian in Europe, *CFS, Cour. Forschungsinst. Senckenberg*, 1994, vol. 168, pp. 311–317.

Nemyrovska, T.I., Wagner, R.H., Winkler Prins, C.F., and Montanez, I., Conodont faunas across the mid-Carboniferous boundary from the Barcaliente Formation at La Lastra (Palentian Zone, Cantabrian Mountains, northwest Spain): Geological setting, sedimentological characters and faunal descriptions, *Scr. Geol.*, 2011, vol. 143, pp. 127–183.

Nikishin, A.M., Sobornov, K.O., Prokopiev, A.V., and Frolov, S.V., Tectonic evolution of the Siberian Platform during the Vendian and Phanerozoic, *Moscow Univ. Geol. Bull.*, 2010, vol. 65, no. 1, pp. 3–16.

Nizhnii karbon Moskovskoi sineklizy i Voronezhskoi anteklizy (The Lower Carboniferous of the Moscow Syneclise and Voronezh Anteclise), Moscow: Nauka, 1993 [in Russian].

Pazukhin, V.N., *Conodont zonation of the Lower Carboniferous in the Southern Urals and the eastern Russian Platform, in 200 let otechestvennoi palaeontologii* (The 200th Anniversary of Russian Palaeontology,), Barskov, I.S. and Nazarov, V.M., Eds., Moscow: Palaeontol. Inst. RAN, 2009, pp. 96-97.

Pazukhin, V.N., Diversity dynamics of Early Carboniferous conodonts in the Southern Urals and the eastern Russian Platform, in *Mater.LVI sess. Palaeontol. obshch. pri RAN "Evolyutsiya organicheskogo mira i bioticheskie krizisy" (5–9 aprelya 2010 g., Sankt-Peterburg)* (Proc. LVI Sess. Palaeontol. Soc. RAS "The Evolution of the Organic World and Biotic Crises" (April 5–9, 2010), Bogdanov, T.N., Krymgol'ts, N.G., Eds., St. Petersburg, 2010.

Pazukhin, V.N., Late Viséan and Serpukhovian conodonts of the Southern Urals, in *Geol. Sb.* IG UNTs RAN (Coll. Geol. Works Inst. Geol., Ufa Sci. Center, Russ. Acad. Sci., Anni. Iss. 9, 2011, no. 9, pp. 63–73.

Pease, V.L., Kuzmichev, A.B., and Danukalova, M.K., The New Siberian Islands and evidence for the continuation of the Uralides, Arctic Russia, *J. Geol. Soc.*, 2015, vol. 172, pp. 1–4.

Plotitsyn, A.N., Correlation levels in the Upper Famennian and Tournesian of the north of the Urals and the Chernyshev Swell, *Vestn. IG Komi NTs UrO RAN*, 2016, no. 7, pp. 46–53.

Pomar, L., Types of carbonate platforms: A genetic approach, *Basin Research*, 2001, vol. 13, pp. 313–334.

Poty, E., Recherches sur les Tétracoralliaires et les Hétérocoralliaires du Viséen de la Belgique, *Meded. Rijks Geol. Dienst.*, 1981, vol. 35, pp. 1–161.

Poty, E., Tourneur, F., and Javaux, E., The Uppermost Devonian and the Lower Carboniferous coral faunas of Belgium, in Excursion Guidebook. VI International Symposium on Fossil Cnidaria Including Archaeocyatha and Porifera. Münster/Westphalia, September 9–14, 1991.

Prokopiev, A.V., Ershova, V.B., Miller, E.L., and Khudoley, A.K., Early Carboniferous palaeogeography of the

northern Verkhoyansk passive margin as derived from U–Pb dating of detrital zircons: role of erosion products of the Central Asian and Taimyr–Severnaya Zemlya fold belts, *Russ. Geol. Geophys.*, 2013, vol. 54, no. 10, pp. 1195–1204.

Proskurnin, V.F., Gavrish, A.V., Mezhubovskii, V.V., Trofimov, V.R., et al., *Gosudarstvennaya geologicheskaya karta Rossiiskoi Federatsii. Masshtab 1 : 1000000 (tret'e pokolenie). Seriya Taimyrsko-Severozemel'skaya. List S-49 - Khatangskii zaliv. Ob"yasnitel'naya zapiska* (The 1 : 1000000 State Geological Map of the Russian Federation, 3rd ed. Ser. Taimyr–Severnaya Zemlya. Sheet S-49–Khatanga Bay), St. Petersburg: Kart. fabr. Vseross. Nauchno-Issled. Geol. Inst., 2013 [in Russian].

Rauzer-Chernousova, D.M., Some new foraminifer species from from Lower Carboniferous deposits of the Moscow Basin, in *Stratigrafiya i foraminifery nizhnego karbona Russkoi platformy i Priural'ya. Tr. IGN. Vyp. 62. Geol. Ser. no. 19* (Stratigraphy and Foraminifers of the Lower Carboniferous of the Russian Platform and Cis-Urals. Trans. Inst. Geol. Sci. Vol. 62. Geol. Ser. no. 19), 1948, pp. 227–238.

Rhodes, F.H.T. and Austin, R.L., Carboniferous conodont faunas of Europe, in *Proc. Symp. on Conodont Biostratigraphy*, Sweet, W.C. and Bergstrom, S., Eds., *Mem.–Geol. Soc. Am.,* 1971, vol. 127, pp. 317–352.

Rhodes, F.H.T., Austin, R.L., and Druce, E.C., British Avonian (Carboniferous) conodont faunas, and their value in local and intercontinental correlation, *Bull. Br. Mus. (Nat. Hist.), Geol.,* vol. 5, no. 1969, pp. 1–313.

Rogozov, Yu.G., Corals from the Lower Carboniferous of the Eastern Taimyr, in *Opornyi razrez nizhnekamennougol'nykh otlozhenii Vostochnogo Taimyra. Sbornik statei* (The Reference Section of the Lower Carboniferous Deposits of the Eastern Taimyr. Coll. Sci. Works), Cherkesov, S.V. and Tschernjak, G.E., Eds., Leningrad: Nauchno-Issled. Inst. Geol. Arktiki, 1972, pp. 38–56.

Sando, W.J. and Bamber, E.W., Coral zonation of the Mississippian System in the Western Interior Province of North America, *U.S. Geol. Surv. Prof. Pap.*, 1985, vol. 1334.

Sanz-Lopez, J., Blanco-Ferrera, S., Garcia-Lopez, S., and Sanchez de Posada, L.C., The Mid-Carboniferous boundary in northern Spain: Difficulties for correlation of the global stratotype section and point, *Riv. Ital. Palaeontol. Stratigr.*, 2006, vol. 112, no. 1, pp. 3–22.

Sarycheva, T.G. and Sokol'skaya, A.P., *Opredelitel' palaeozoiskikh brakhiopod Podmoskovnoi kotloviny* (A Key to Palaeozoic Brachiopods of the Moscow Syncline), Moscow: Izd. Akad. Nauk SSSR, 1952 [in Russian].

Sarycheva, T.G., Sokol'skaya, A.P., Beznosova, G.A., and Maksimova, S.V., *Brakhiopody i palaeogeografiya karbona Kuznetskoi kotloviny* (Brachiopods and Palaeogeography of the Carboniferous of the Kuznetsk Depression), Moscow: Izd. Akad. Nauk SSSR, 1963 [in Russian].

Sayutina, T.A., Lower Carboniferous corals of the Northern Urals. Sub-Order Acrophyllina, in *Tr. PIN. T. 140* (Trans. Palaeontol, Inst. Vol. 140), Moscow: Nauka, 1973.

Sayutina, T.A., On the genus *Sychnoelasma* from the Lower Carboniferous of the Northern Urals, *Byull. Mosk. O-va Ispyt. Prir., Otd. Geol.*, 1976, vol. 51, no. 1, pp. 111–122.

Scott, H.W., Conodont assemblages from the Heath Formation, Montana, *J. Palaeontol.*, 1942, vol. 16, no. 3, pp. 293–301.

Shilo, N.A., Bouckaert, J., Afanasjeva, G.A., Bless, M.J.M., Conil, R., et al., *Sedimentological and Palaeontological Atlas of the Late Famennian and Tournaisian deposits in the Omolon region (NE-USSR)*, *Ann. Soc. Geol. Belg.*, 1984, vol. 107, pp. 137–247.

Shtukenberg, A.A., Corals and bryozoans from the Carboniferous deposits of the Urals and Taimyr, in *Tr. Geol. Kom.* (Trans. Geol. Com.), St. Petersburg, 1895, Vol. 10, no. 3.

Smetannikova, L.I., Grinenko, V.S., Malanin, Yu.A., Prokopiev, A.V., et al., *Gosudarstvennaya geologicheskaya karta Rossiiskoi Federatsii. Masshtab 1 : 1000000 (tret'e pokolenie). Seriya Anabaro-Vilyuiskaya. List R-5–Dzhardzhan. Ob"yasnitel'naya zapiska* (The 1 : 1000000 State Geological Map of the Russian Federation, 3rd ed. Ser. Anabad–Vilyui. Sheet R-51–Dzhardzhan. Explanatory Note), St. Petersburg: Kart. fabr. Vseross. Nauchno-Issled. Geol. Inst., 2013 [in Russian].

Sobolev, N.N., Stratigraphy of Lower Carboniferous deposits of the Taimyr Mountains, in *Nedra Taimyra. Sb. nauch. trudov. Vyp. 3* (Coll. Sci. Works "Mineral Resources of Taimyr" Vol. 1), Norilsk, 1999, pp. 11–21.

Solov'eva, M.F., Formainiferal biostratigraphy of Lower–Middle Carboniferous deposits of Kotel'ny Island, Wrangel Island and Chukotka Peninsula, in *Verkhnii palaeozoi severovostoka SSSR. Sb. statei* (Coll. Sci. Works "*Upper Palaeozoic of the Northeastern USSR*"), Ustritskii, V.I., Ed., Leningrad: Nauchno-Issled. Inst. Geol. Arktiki, 1975, pp. 42–53.

Soshkina, E.D., Tournaisian Rugose corals and their relationships with the Devonian forms, in *Sbornik trudov po geologii i palaeontologii* (Coll. Sci. Works on Geology and Palaeontology), Syktyvkar: Komi Fil. Akad. Nauk SSSR, 1960, pp. 272–299.

Spravochnik po sistematike melkikh foraminifer palaeozoya (za isklyucheniem endotiroidei i permskikh mnogokamernykh lagenoidei) (The Reference Book on the Systematics of the Palaeozoic Smaller Foraminifera, Excluding Endothyroida and Permian Multilocular Lagenoida), Moscow: Nauka, 1993. [in Russian].

Stow, D.A.V., *Sedimentary Rocks in the Field: A Color Guide*, Acad. Press, 2012.

Stratigraphy of Carboniferous and Permian deposits of the Northern Verkhoyansk Region, in *Tr. NIIGA. T. 154* (Trans. Res. Inst. Arctic Geol. Vol. 154), 1970.

Sutherland, P.K., Carboniferous stratigraphy and Rugose coral faunas of Northeastern British Columbia, *Geol. Surv. Canada. Mem.*, 1958, vol. 295.

Tektonika, geodinamika i metallogeniya territorii Respubliki Sakha (Yakutiya) (Tectonics, geodynamics and metallogeny of the Re-public of Sakha (Yakutia)), Parfenov, L.M. and Kuzmin, M.I., Eds., Moscow: MAUK "Nauka/Interperiodika", 2001 [in Russian].

The Study of Trace Fossils, Frey, R.W., Ed., New York: Springer-Verlag, 1975.

Tynan, M.C., Conodont biostratigraphy of the Mississippian Chainman Formation, western Millard County, Utah, *J. Palaeontol.*, 1980, vol. 54, no. 6, pp. 1282–1309.

Ulitina, L.M., Rugoses, in *Fauna pogranichnykh otlozhenii devona i karbona Tsentral'nogo Kazakhstana. Materialy po geologii Tsentral'nogo Kazakhstana. Tom XVIII* (Materilas on the Geology of Central Kazakhstan. Vol. XVIII), Moscow: Nedra, 1975, pp. 36–41.

Ustritskii, V.I. and Tschernjak, G.E., Biostratigraphy and brachiopods from the Upper Palaeozoic of Taimyr, in *Tr. NIIGA. T. 134* (Trans. Res. Inst. Arctic Geol. Vol. 134), 1963.

Voinovskii-Kriger, V.G., Lower Carboniferous corals from the environs of the Arkahgelsk Plant (the western slope of the Southern Urals), *Tr. Vsesoyuz. Geol.-Razved. Ob"ed.*, 1934, vol. 107.

Vuillemin, C., Les Tétracoralliaires (Rugosa) du Carbonifère Inférieur du Massif Armoricain (France), in *Cah. Paléontol.*, Paris: Édition du Centre National de la Recherche Scientifique, 1990.

Wang, X.-D., Sugiyama, T., and Fang, Run Sen, Carboniferous and Permian coral faunas of West Yunnan, Southwest China: Implication for the Gondwana/Cathaysia divide, *Bull. Tohoku Univ.*, 2001, vol. 1, pp. 265–278.

Weyer, D., *Korallen aus dem Obertournai und Untervisé der Inseln Hiddensee and Rügen, Abh. Ber. Naturkd. (Magdeburg Mus.*), 1993, vol. 16, pp. 31–69.

Yancey, T.E., Controls on carbonate and siliciclastic sediment deposition on a mixed carbonate–siliciclastic shelf (Pennsylvanian Eastern Shelf of north Texas), in *Sedimentary Modeling: Computer Simulations and Methods for Improved Parameter Definition*, Franseen, E.K., Watney, W.L., Kendall, C.G.St.C., and Ross, W., Eds., *Kansas Geol. Surv. Bull.*, 1991, vol. 233, pp. 263–272.

Yuferev, O.V., The Carboniferous of the Siberian Biogeographic Belt, in *Tr. Inst. Geol. Geofiz. SO RAN. Vyp. 162* (Trans. Inst. Geol. Geophys. Sib. Branch Ross. Acad. Sci. Vol. 162), Novosibirsk: Nauka, 1973.

Zhuravlev, A.V., *Konodonty verkhnego devona-nizhnego karbona severo-vostoka Evropeiskoi Rossii* (The Upper Devonian–Lower Carboniferous conodonts from the Northeastern European Russia), St. Petersburg: Izd. Vseross. Nauchno-Issled. Geol. Inst., 2003 [in Russian].

Translated by E. Maslennikova